



Scan to know paper details and  
author's profile

# Advances in Cyclometalated Iridium (III) Complexes: Emerging Strategies and Applications in Anticancer Therapy

Irena Kostova

Medical University

## ABSTRACT

Recently, organometallic iridium(III) complexes have attracted considerable attention in the development of new metal-based antineoplastic drugs, and this area of research has been intensively explored. Their diverse mechanisms of antitumor action are distinct from those of classical metal complexes approved for clinical use, which makes them particularly worthy of detailed investigation. A typical organometallic anticancer Ir(III) complex consists of an iridium(III) center coordinated to two cyclometalated C<sup>N</sup> ligands and one N<sup>N</sup> ancillary ligand. Modification of the cyclometalated ligands plays a dominant role in controlling the photophysical properties, whereas alteration of the ancillary ligand allows functionalization for targeted imaging or therapeutic applications.

This review discusses and analyzes cyclometalated iridium complexes that exhibit significant anticancer activity and exceptional photophysical characteristics. Unlike platinum-based anticancer drugs, these iridium(III) complexes primarily act by damaging various intracellular organelles (such as mitochondria and lysosomes), although the reported results remain scattered and systematic structure–activity relationships are still underdeveloped.

**Keywords:** organometallic Ir(III) complexes, cyclometalated ligands, N<sup>N</sup> ancillary ligands, antitumor agents, photodynamic therapy, reactive oxygen species, theranostic agents, mitochondrial targeting, ligand modification, metal-based chemotherapy.

**Classification:** LCC Code: QD411, RS431.C45, RC271.C5

**Language:** English



Great Britain  
Journals Press

LJP Copyright ID: 925614

Print ISSN: 2631-8490

Online ISSN: 2631-8504

London Journal of Research in Science: Natural & Formal

Volume 25 | Issue 14 | Compilation 1.0





# Advances in Cyclometalated Iridium (III) Complexes: Emerging Strategies and Applications in Anticancer Therapy

Irena Kostova

## ABSTRACT

Recently, organometallic iridium(III) complexes have attracted considerable attention in the development of new metal-based antineoplastic drugs, and this area of research has been intensively explored. Their diverse mechanisms of antitumor action are distinct from those of classical metal complexes approved for clinical use, which makes them particularly worthy of detailed investigation. A typical organometallic anticancer Ir(III) complex consists of an iridium(III) center coordinated to two cyclometalated C<sup>N</sup> ligands and one N<sup>N</sup> ancillary ligand. Modification of the cyclometalated ligands plays a dominant role in controlling the photophysical properties, whereas alteration of the ancillary ligand allows functionalization for targeted imaging or therapeutic applications.

This review discusses and analyzes cyclometalated iridium complexes that exhibit significant anticancer activity and exceptional photophysical characteristics. Unlike platinum-based anticancer drugs, these iridium(III) complexes primarily act by damaging various intracellular organelles (such as mitochondria and lysosomes), although the reported results remain scattered and systematic structure–activity relationships are still underdeveloped.

Furthermore, organometallic Ir (III)-based complexes can overcome several limitations associated with Pt-based chemotherapeutic agents. Although they have only recently gained substantial attention, Ir(III) complexes display a range of properties that make them highly promising as prospective antineoplastic agents. Their chemical reactivity and binding behavior depend largely on their coordination geometry and the nature of the ligands employed.

The biological profiles and cellular uptake of metal-based antitumor agents are determined by the structure of the complex—specifically, the metal center, the biologically active auxiliary ligands, and their spatial arrangement. Among the various Ir(III) complexes evaluated for pharmacological activity, cyclometalated iridium complexes are particularly interesting due to their favorable photochemical and photophysical properties, including high stability under physiological conditions, luminescence across the visible to near-infrared (NIR) spectrum, and ability to participate in redox processes. Consequently, these highly luminescent organometallic complexes have been extensively investigated for various photophysical applications, especially as promising photosensitizers or phosphorescent agents in biosensing and biological imaging.

Overall, this review provides new insights into the development of cyclometalated iridium complexes and perspectives on enhancing their properties for improved therapeutic applications and synergy with existing treatment strategies.

**Keywords:** organometallic Ir(III) complexes, cyclometalated ligands, N<sup>N</sup> ancillary ligands, antitumor agents, photodynamic therapy, reactive oxygen species, theranostic agents, mitochondrial targeting, ligand modification, metal-based chemotherapy.

**Author:** Department of Chemistry, Faculty of Pharmacy, Medical University, 2 Dunav St., Sofia 1000, Bulgaria.  
email: irenakostova@yahoo.com

## I. INTRODUCTION

Over the past several decades, classical metal-based antitumor agents have represented an indispensable class of chemotherapeutic drugs; however, their clinical use remains constrained by significant functional and physiological limitations. Conventional platinum- and ruthenium-based compounds, such as cisplatin, carboplatin, and NAMI-A, while therapeutically effective, suffer from several drawbacks including severe systemic toxicity, poor selectivity toward malignant cells, the emergence of multidrug resistance, insufficient cellular uptake, and limited pharmacological efficacy [1–4]. These disadvantages collectively highlight the urgent necessity of designing and developing new generations of metal-containing antineoplastic agents that could overcome the limitations inherent to traditional metallodrugs.

The induction of cell death represents a fundamental strategy in anticancer therapy, whereby the successful accumulation of a cytotoxic agent within tumor cells triggers irreversible molecular and biochemical alterations leading to cellular demise. Cell death can proceed through several mechanistically distinct pathways, not all of which are therapeutically favorable. Among the best characterized are: (i) apoptosis, or programmed cell death, which is generally regarded as the most desirable anticancer mechanism; (ii) necrosis, an uncontrolled and often inflammatory form of cell death; and (iii) autophagy, a self-degradative process essential for cellular homeostasis. Other less common, yet biologically relevant, pathways include (iv) ferroptosis, (v) oncosis, (vi) paraptosis, and (vii) pyroptosis. The ability of metal-based agents to selectively modulate these death pathways constitutes a critical determinant of their pharmacological effectiveness and therapeutic index.

In recent years, non-platinum metal complexes have emerged as a diverse and promising class of antineoplastic agents exhibiting mechanisms of action distinct from those of classical Pt(II)-based drugs. The structural diversity and redox versatility of transition metals allow for unique modes of biomolecular interaction, including DNA intercalation, protein binding, enzyme inhibition, and the generation of reactive oxygen species (ROS). Advances in coordination and medicinal chemistry have facilitated the design of various metal-based scaffolds with notable biological activity, including complexes of Ru(III) [5], Pd(II) [6], Pt(II) and Pt(IV) [7,8], Rh(III) [9], and numerous other metallodrugs under active investigation.

Among these systems, iridium-based complexes have attracted growing attention due to their remarkable structural, chemical, and photophysical properties. Iridium exhibits a wide range of accessible coordination numbers and oxidation states under physiological conditions, a rich variety of coordination geometries, and exceptional photochemical stability [10,11]. In particular, Ir(III) complexes possess highly tunable photophysical and electrochemical characteristics, including strong spin-orbit coupling, long-lived excited states, and efficient phosphorescence—all of which contribute to their potential for both therapeutic and diagnostic (theranostic) applications. Chloroiridium(III) complexes have been reviewed elsewhere [12] and are therefore beyond the scope of this discussion.

Cyclometalated iridium(III) complexes, in particular, have demonstrated distinctive intracellular localization patterns, including accumulation within the cytoplasm, nucleus, lysosomes, endosomes, mitochondria, and endoplasmic reticulum [10–13]. In contrast to conventional platinum-based drugs, which primarily target nuclear DNA, iridium complexes often preferentially accumulate in mitochondria or lysosomes, where they can actively participate in intracellular redox processes, induce oxidative stress through ROS generation, and ultimately promote apoptotic cell death [13]. This subcellular targeting confers additional advantages such as enhanced selectivity and reduced off-target toxicity.

Cyclometalated Ir(III) species also represent promising analogues to their isoelectronic ruthenium(II) counterparts, offering a broader range of tunable photophysical characteristics and higher ligand-field stabilization energies. The versatile photochemical behavior of Ir(III) complexes has led to their application across multiple therapeutic modalities, including photothermal therapy (PTT), photoactivated chemotherapy (PACT), and sonodynamic therapy (SDT). Of particular note is their utilization in photodynamic therapy (PDT)—a minimally invasive therapeutic strategy that leverages light-activated photosensitizers to generate cytotoxic singlet oxygen and other reactive species [13,14]. These unique photoresponsive properties render iridium(III) complexes valuable platforms for the development of multifunctional agents capable of simultaneous imaging and targeted therapy.

Structurally, cyclometalated compounds are organometallic complexes containing metallacycles characterized by a D–M–C  $\sigma$ -bond framework, where D denotes a donor atom (typically from group VA or VIA elements), M represents the metal center, and C is a carbon atom in either  $sp^2$  or  $sp^3$  hybridization. A prototypical organometallic Ir(III) complex can be represented by the general formula  $[Ir(C^N_2(N^N)]^+$ , where  $C^N$  denotes a bidentate cyclometalating ligand and  $N^N$  represents an ancillary diimine ligand. Typical examples include 2-phenylpyridinate (ppy) as the  $C^N$  ligand and 2,2'-bipyridine (bpy) as the  $N^N$  ligand. Although most complexes are monocationic and stabilized by counterions such as  $Cl^-$  or  $PF_6^-$ , variations incorporating monodentate ligands are also well documented.

Over the past decade, a substantial number of polypyridyl Ir(III) complexes have been synthesised and systematically investigated, revealing pronounced biological activity, particularly in the context of anticancer activity [15–17]. The inherent modularity of these complexes—stemming from their chemically modifiable ligand frameworks—enables fine-tuning of key physicochemical parameters, including lipophilicity, solubility, redox potential, and photochemical responsiveness. This molecular flexibility facilitates the rational optimization of pharmacological and optical properties, establishing cyclometalated Ir(III) complexes as one of the most promising classes of next-generation metallodrugs for targeted and multifunctional cancer therapy.

Investigating the ligands (monodentate or bidentate) and the leaving groups can effectively modulate the activity of the resulting complexes. Currently, the activity regulations are primarily focusing on the study of different bidentate ligands, including  $N^N$  ligands (bipyridine, phenanthroline, etc.),  $N^C$  ligands (phenylpyridine,  $\beta$ -carboline, etc.), in some cases  $N^O$  ligands (hydrazone derivatives, picolinic acid, amino acids),  $N^S$  (thiocarbazones),  $O^O$  ( $\beta$ -diketonato derivatives), which have been proven to display improved activity. Among all these ligands, the most studied for the ascertainment of their anticancer mode of action were  $N^N$  and  $N^C$  ligands, presented in detail in the current review. The design of the  $C^N$  ligands is critical to regulate the extension of emission wavelengths of Ir(III) complexes. While the alteration of the ancillary  $N^N$  ligand largely determines the strength and functionalization with biological targets for imaging or therapy purposes [18–20]. Given the versatility of the ligands employed, it is unsurprising that numerous iridium(III) complexes have been extensively investigated for a variety of applications [21–23].

The current broad overview, based on recently published reports, focuses on the anticancer activity of this interesting class of organometallic compounds, which offers advantages in the development of new metallodrugs. The reported work, which presents results from cytotoxicity screenings against various cancer cell lines as well as studies on cellular internalization mechanisms, will be reviewed and discussed.

## II. CYCLOMETALATED Ir(III) COMPLEXES WITH 2-PHENYL PYRIDINE (PPY) AS A C<sup>N</sup> LIGAND

2-Phenylpyridine (ppy) is the prototypical and most widely used cyclometalating ligand. The cyclometalated iridium complexes with 2-phenylpyridine as a C<sup>N</sup> ligand have been widely investigated for their potential application as anticancer therapeutic agents. They have exhibited notable antiproliferative activity against various cancer cell lines [24] and demonstrated good selectivity, making them promising candidates for inhibiting the invasion of malignant cells into surrounding tissues. Cyclometalated Ir(III) complexes bearing 2-phenylpyridine derivatives can efficiently sensitize ground-state oxygen <sup>3</sup>O<sub>2</sub> to generate cytotoxic singlet oxygen <sup>1</sup>O<sub>2</sub>, thus serving as highly promising photosensitizers. Moreover, numerous cyclometalated iridium(III) complexes have exhibited desirable two-photon absorption (TPA) features [25]. The general formula of the complexes can be expressed as [Ir(ppy)<sub>2</sub>(biPy)]PF<sub>6</sub>, where ppy is 2-phenylpyridine or its derivatives, and with easy adjustment of ligands, the luminescence and pharmacological properties of these complexes can also be readily modified [26]. 2-Phenylpyridine is a C<sup>N</sup> chelating ligand and bipyridine or its derivatives (biPy) is a N<sup>N</sup> chelating ligand. The combination of potential antineoplastic activity and luminescent properties of cyclometalated Ir(III) complexes makes them promising candidates for the development of novel theranostic systems. These complexes exhibit unique biologically favorable photophysical characteristics, including high quantum yields, excellent resistance to photobleaching and cell bleaching, which render them effective bioimaging agents [27]. Their large ligand-field splitting energy and strong spin-orbit coupling arise from the pronounced  $\sigma$ -donating nature of the cyclometalating ligands, the high positive charge of the Ir(III) center, and the extensive spatial distribution of the 5d orbitals. In addition, they possess long luminescence lifetimes, large Stokes shifts [28], tunable energy levels [29], as well as good cell permeability and photostability [30]. Cyclometalated iridium complexes are primarily investigated as potential anticancer agents [31]. In addition, phosphorescent cyclometalated Ir(III) complexes serve as excellent biosensing probes due to their high photostability and resistance to photobleaching. These properties enable them to selectively target various subcellular organelles and inhibit specific protein activities [32].

### 2.1. Tris-Cyclometalated Iridium Complexes with 2-Phenylpyridine

The tris-cyclometalated iridium complexes holding three cyclometalating C<sup>N</sup> ligands are neutral. These complexes have been used far less extensively in cellular imaging compared to iridium(III) bis-cyclometalated complexes. Meksawangwong *et al.* reported a photoactive tris-cyclometalated Ir(III) complex bearing a quaternary ammonium moiety and investigated its photophysical properties as a potential probe for cellular imaging, Fig. 1, [28]. The complex has possessed outstanding features, enabling it to be used as a cellular stain in fluorescence microscopy. Cytotoxicity was assessed using mouse skin fibroblasts (NIH-3T3) and human prostate adenocarcinoma (PC3) cell lines by fluorescence and laser scanning confocal microscopy. Studies have demonstrated that the complex was less toxic than its precursor amine complex and had lysosomal localisation [28].

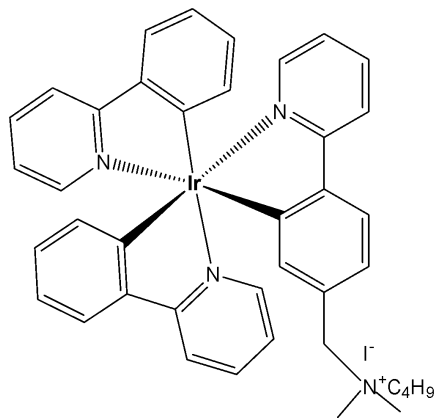


*Fig. (1):* Structure of  $[\text{Ir}(\text{ppy})_2(\text{ppy}-\text{Me}_2\text{N}^+\text{C}_4\text{H}_9)\text{I}^-]$ .

Similarly, a series of iridium(III) mono-, bis, and tris-amino acid complexes, Fig. 2, exhibited varying degrees of cellular uptake [33]. The authors have synthesised a series of nine neutral luminescent cyclometalated octahedral iridium(III) tris(2-phenylpyridine) complexes, functionalized with three different amino acids (glycine, alanine, and lysine), on one, two, or all three of the 2-phenylpyridine ligands. It has been revealed that the monosubstituted complexes in this series exhibit significantly higher cellular uptake compared to the bis- and tris-substituted compounds, with the lysine complexes showing greater uptake than their glycine and alanine analogues [33]. All compounds were comprehensively characterized using one- and two-dimensional NMR spectroscopy, and photophysical data were collected for the mono-, bis-, and tris-substituted Ir(III) complexes. Cellular uptake and localisation have been studied with flow cytometry and confocal microscopy, respectively. Confocal experiments have demonstrated that all nine substituted Ir(III) complexes showed variable uptake in the cancer cells. Among the tested compounds, the monosubstituted complexes demonstrated the highest levels of cellular uptake, whereas the lysine derivatives displayed the highest cytotoxicity. This systematic study of amino acid-functionalized  $\text{Ir}(\text{ppy})_3$  complexes provides guidelines for further functionalization and possible implementation of luminescent iridium complexes, for example, in (automated) peptide synthesis or biomarker specific targeting [33].

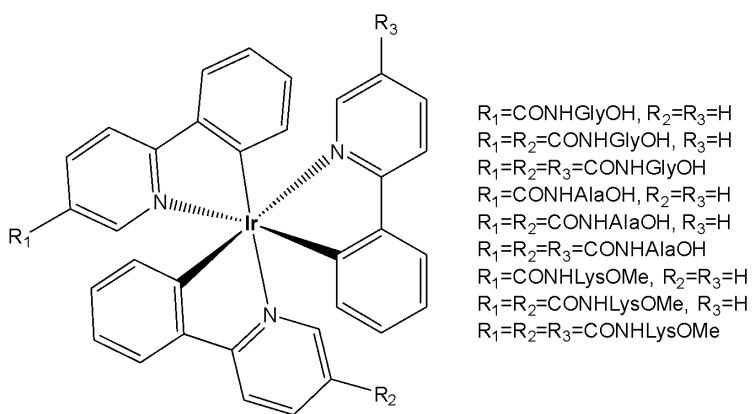


*Fig. (2):* Ir(III) tris(2-phenylpyridine) complexes, functionalized with amino acids.

Berkers *et al.* established methods using fluorescent reporters to profile proteasome activity across different mouse tissues while carefully avoiding post-lysis artefacts, demonstrating that proteasome subunit activity is regulated in an organ-specific manner [34]. The techniques described could be used to study the pharmacological properties of proteasome inhibitors *in vivo*. The monosubstituted complexes exhibited a remarkable 20-fold increase in cellular uptake in 4T1 cells (at 10  $\mu\text{M}$

concentration for one h incubation), which was attributed to the higher lipophilicity of the probes. This result has been supported by the theoretical lipophilicity (ClogP), which showed a distribution coefficient between 2.05 and 3.18, in comparison to the negative values of ClogP for the di- and trisubstituted complexes. Flow cytometry analysis revealed a significant reduction in cell viability following treatment with the lysine derivatives, indicating increased toxicity. The cellular distribution of the studied complexes varied depending on the number of residues, showing nuclear localisation for mono-compounds, endosomal localisation for bis-compounds, and lysosomal localisation for tris-compounds [33].

Moromizato *et al.* developed a neutral iridium(III) probe, Fig. 3, that functions as both a luminescent pH sensor and a pH-dependent photosensitizer in live cells [35]. In this study, the design and synthesis of a new pH-sensitive cyclometalated Ir(III) complex *fac*-Ir(deatpy)<sub>3</sub>, containing 2-(5'-N,N-diethylamino-4'-tolyl)pyridine (deatpy) ligand with three amino groups at the 5'-positions, Fig. 3a, have been reported. The complex has exhibited a considerable change in emission intensity between neutral and slightly acidic pH (pH 6.5–7.4). Luminescence microscopic studies using HeLa-S3 cells have indicated that the complex could be used to selectively stain lysosomes. Moreover, this complex was capable of generating singlet oxygen in a pH-dependent manner, inducing the death of HeLa-S3 cells upon photoirradiation at 377 or 470 nm. As predicted, the complex localised within the lysosomes of HeLa-S3 cells through a passive transport mechanism. Additionally, photoirradiation of the complex induced necrosis-like death in HeLa-S3 cells, demonstrating the ability of the probe to generate <sup>1</sup>O<sub>2</sub> in a pH-dependent manner.

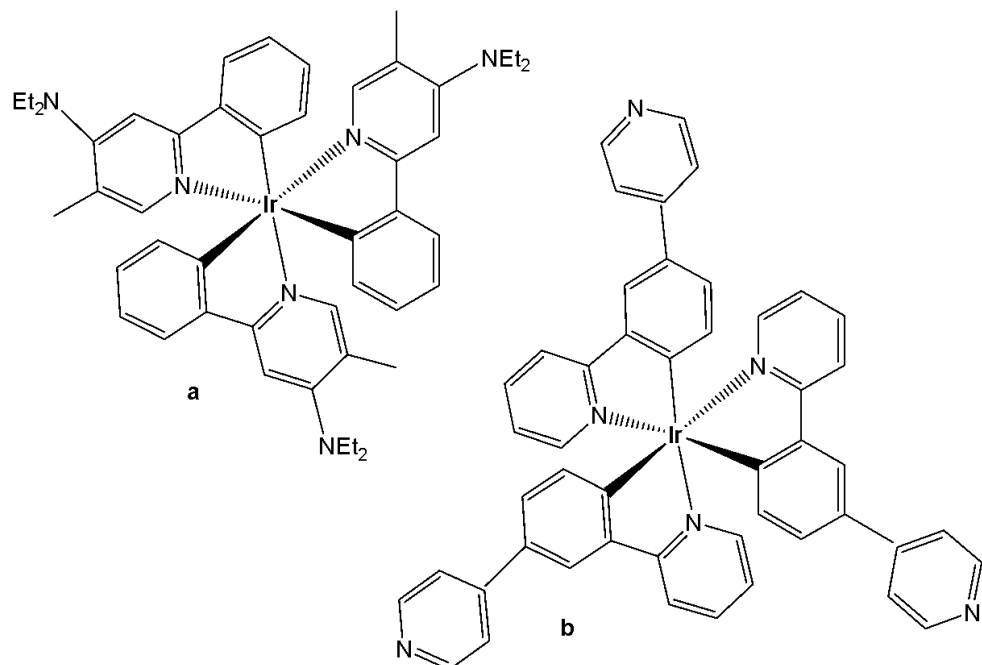


*Fig. (3):* Ir(III) complexes *fac*-Ir(deatpy)<sub>3</sub> and *fac*-Ir(4pyppy)<sub>3</sub>.

Following their previous publication on pH-responsive probes [35], Aoki and co-workers synthesised another neutral iridium(III) analogue, *fac*-Ir(4pyppy)<sub>3</sub>, which contains three pyridyl groups at the 4'-position of the phenylpyridine ligands, (Fig. 3b), [36]. The introduction of three pyridyl groups resulted in strong emission (at 500 nm) in dimethylsulfoxide (DMSO). The reversible pH-dependent emission profile of the complex, resulting from the protonation and deprotonation of the pyridine rings, has also been discussed. The generation of singlet oxygen (<sup>1</sup>O<sub>2</sub>) by the photoirradiation of the Ir(III) complex was evidenced by the decomposition of 1,3-diphenylisobenzofuran (DPBF), the

oxidation of thioanisole, and the oxidation of 2,2,5,5-tetramethyl-3-pyrroline-3-carboxamide (TPC). The induction of necrosis-like cell death of HeLa-S3 cells upon photoirradiation was also reported. Upon incubation in HeLa-S3 cells, the complex (Fig. 3b) has exhibited accumulation within mitochondria, potentially through a passive transport mechanism. Additionally, after photoirradiation at 465 nm for 10 min, the complex in Fig. 3b has generated much more  ${}^1\text{O}_2$  in comparison to the Ir(III) complex  $\text{fac-}\text{Ir}(\text{deatpy})_3$  [35], thus inducing necrosis-like cell death.

Qiu *et al.* designed a neutral iridium(III) probe (Fig. 4) for long-term lysosome tracking [37]. The water-soluble tris-cyclometalated iridium(III) complex has been functionalized by morpholine moieties, which could be protonated inside the lysosomes and work as a “locker”, allowing the accumulation of the complex, Fig. 4, in these acidic organelles. Additionally, the electron-rich morpholine moiety quenched the iridium(III) phosphorescence via photoinduced electron transfer (PET) under basic conditions. Upon protonation, this process was inhibited, resulting in enhanced emission intensity in acidic lysosomes. The uptake of the complex shown in Fig. 4 occurred via an energy-dependent pathway, and the probe exhibited no toxicity toward HeLa cell lines (at a concentration of 10  $\mu\text{M}$  after 48 h of incubation). Furthermore, the complex in Fig. 4 successfully tracked lysosomes for up to 4 days, enabling imaging and monitoring of various physiological activities of lysosomes during cell migration and apoptosis. The ability to achieve long-term lysosomal tracking is crucial for elucidating lysosomal functions and for evaluating drug and gene delivery systems.

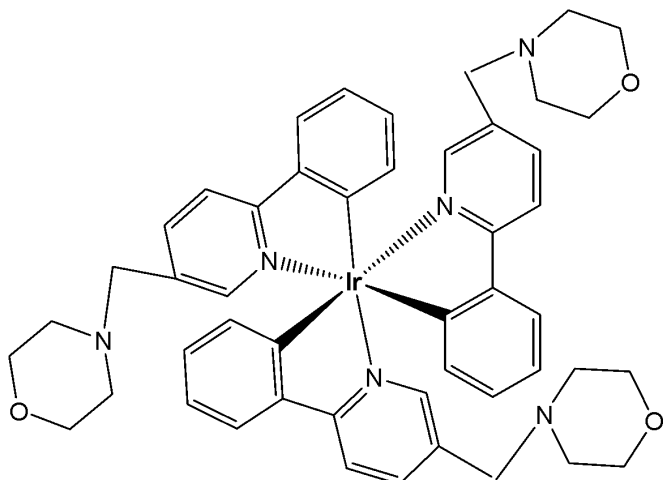


*Fig. (4):* Tris-cyclometalated iridium(III) complex, functionalized by morpholine moieties.

## 2.2. Biscyclometalated Iridium(III) Complexes with 2-Phenylpyridine

Biscyclometalated complexes of the type  $[\text{Ir}(\text{C}^{\text{N}})^2(\text{N}^{\text{N}})]^+$  present a wide variety of cellular targets depending on the ancillary ligands. Indeed, mitochondria [38-41], lysosomes [42-44], endoplasmic reticulum [45,46], endosomes or nucleus [47,48] have all been recognized as common target organelles for a range of Ir(III) biscyclometalated derivatives.

### 2.2.1. Biscyclometalated Iridium(III) Complexes of 2-Phenylpyridine with Two Monodentate Ligands

N-monodentate ligands have not been extensively explored in biscyclometalated iridium(III) complexes and limited examples have been reported. The -NH moiety on the ancillary ligands can modulate the overall charge of the complex through acid–base equilibrium, thereby influencing its photophysical properties, cellular uptake, and localisation.

Wu *et al.* have reported three cyclometalated Ir(III) complexes containing monodentate five-membered heterocyclic ligands, shown in Fig. 5(a-c) [49]. These complexes displayed intense absorption bands at approximately 250–300 nm attributed to  $\pi-\pi^*$  transitions and relatively weaker bands at 350–450 nm assigned to metal-to-ligand charge transfer absorption. These iridium(III) complexes have been found to generate  $^1\text{O}_2$  efficiently. Cytotoxicity studies were conducted using lung cancer using lung cancer (A549, A549R), prostate cancer (PC3), hepatocellular carcinoma (HepG2), and normal liver (LO2) cell lines to evaluate the effects of the compounds. In the dark, the  $\text{IC}_{50}$  values of these complexes ranged from 8.91 to 38.9  $\mu\text{M}$ ; however, upon light irradiation, the  $\text{IC}_{50}$  values decreased to below 0.94  $\mu\text{M}$ . Additionally, these complexes have exhibited selectivity towards human cancer cells over non-cancerous cells. The complex, shown in Fig. 5(b), has demonstrated five times lower cytotoxicity against LO2 cells. The complexes in Fig. 5(a–c) not only formed covalent bonds upon light irradiation but were also efficiently internalized by tumor cells, where they were further retained within the cytoplasm. They can be activated by light via dual modes to induce tumor cell death [49]. Upon visible light (425 nm) irradiation, the five-membered heterocyclic ligands would dissociate from the metal centre. Moreover, the complexes in Fig. 5(a–c) could also act as effective singlet oxygen photosensitizers. Thus, the complexes shown in Fig. 5(a–c) may exert their light-mediated anticancer effects through dual mechanisms: ligand exchange reactions and the generation of singlet oxygen ( $^1\text{O}_2$ ) under visible light irradiation. Notably, the complex in Fig. 5(a) has displayed a high phototoxicity index of 61.7 against human cancer cells. Additional studies have demonstrated that the light-mediated antineoplastic effects exerted by the complexes shown in Fig. 5(a–c) occur through the generation of reactive oxygen species (ROS), activation of caspases, and subsequent induction of apoptosis. This study has demonstrated that these complexes can act as novel dual-mode light-mediated antitumor agents.

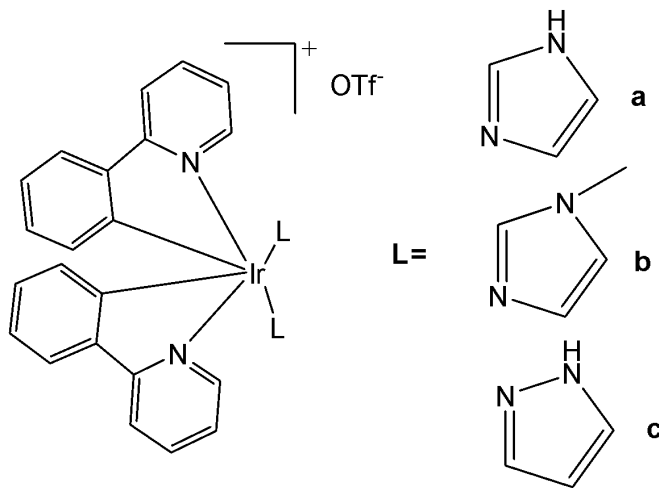


*Fig. (5):* Cyclometalated Ir(III) complexes with monodentate five-membered heterocyclic ligands.

## 2.2.2. Biscyclometalated Iridium(III) Complexes of 2-Phenylpyridine with One Bidentate N<sup>+</sup>N Ligand

Liu *et al.* synthesised and characterized four triphenylamine (TPA)-appended cyclometalated iridium complexes of the type  $[\text{Ir}(\text{ppy})_2(\text{N}^+\text{N})]\text{PF}_6$ , featuring TPA-functionalized bipyridine chelating ligands ( $\text{N}^+\text{N}$ ) and phenylpyridine (ppy) ligands, Fig. 6(a-d), [26]. The introduction of TPA units helped to adjust the lipid solubility of complexes and also improved their anticancer and bactericidal activity. The complexes presented in Fig. 6(a, b, d) demonstrated comparable antineoplastic activity. All the complexes have exhibited improved antitumor properties compared to cisplatin against A549 cells. The complex shown in Fig. 6(a) ( $\text{IC}_{50} = 4.34 \mu\text{M}$ ) was nearly five times more potent than cisplatin,

while the complex in Fig. 6(d) exhibited some selectivity toward cancer cells over normal cells. Meanwhile, complexes could effectively prevent the metastasis of cancer cells. These complexes could be transported via serum proteins, followed by a binding mechanism consistent with static quenching. They were observed to disturb the cell cycle at the G<sub>0</sub>/G<sub>1</sub> phase and induce apoptosis. The complexes exhibited largely similar photophysical properties, displaying a strong interligand absorption band ( $\pi-\pi^*$ ) at 280 nm and a relatively weaker metal-to-ligand charge transfer (MLCT) transition band in the 350–500 nm range. Cellular uptake occurred via a non-energy-dependent pathway, with effective accumulation in lysosomes. This induced lysosomal damage, which affected mitochondrial membrane potential, ultimately triggering apoptosis and leading to cell death [26]. The study has demonstrated that these complexes could be regarded as potential antitumor agents with dual functions, including metastasis inhibition and lysosomal damage.

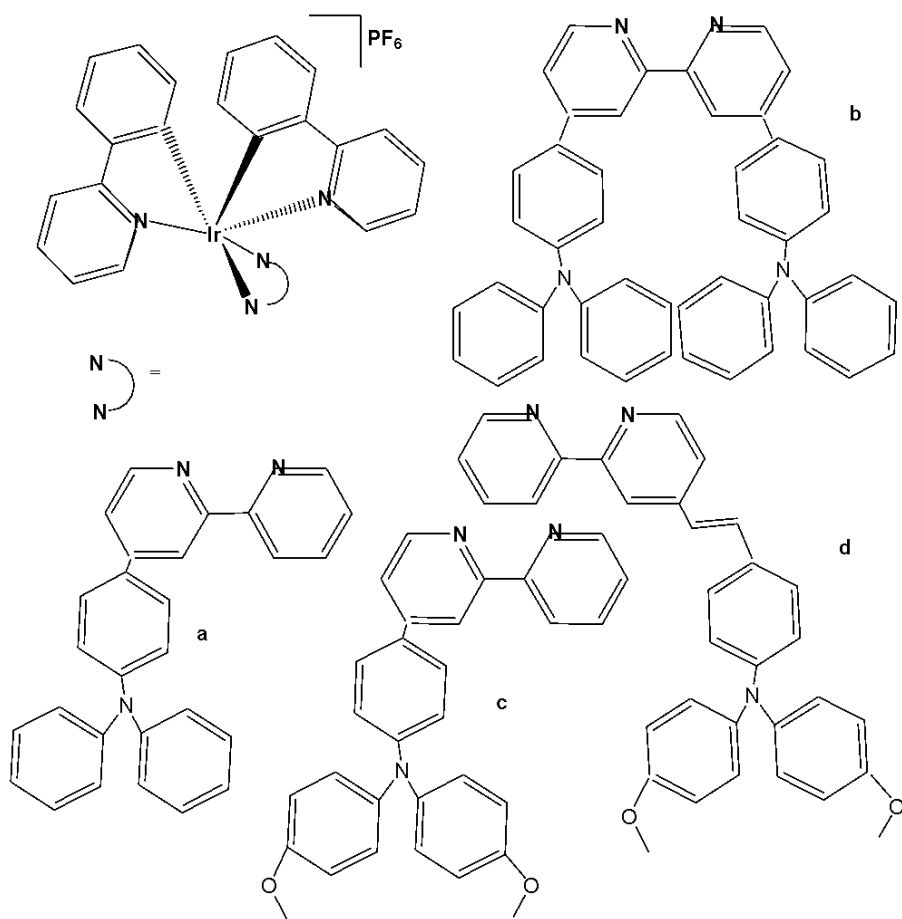


*Fig. (6):* Iridium(III) complexes with general formula  $\text{Ir}(\text{ppy})_2(\text{N}^{\wedge}\text{N})\text{PF}_6$ .

Wu *et al.* have synthesised and reported four phosphorescent Ir(III) complexes, Fig. 7(a-d), with the general formula  $[\text{Ir}(\text{N}^{\wedge}\text{C})_2(\text{N}^{\wedge}\text{N})](\text{PF}_6)$ , where  $\text{N}^{\wedge}\text{N} = (2,2'\text{-bipyridine})\text{-}4,4'\text{-diyl dimethanol}$ ,  $4,4'\text{-bis}(\text{chloro-methyl})\text{-}2,2'\text{-bipyridine}$ ;  $\text{N}^{\wedge}\text{C} = 2\text{-phenylpyridine}$  or  $2\text{-}(2,4\text{-difluorophenyl})\text{pyridine}$ , examined for anticancer activity by MTT assay [50]. The complexes shown in Fig. 7(b) and Fig. 7(d) exhibited high cytotoxicity against cisplatin-resistant A549, MDA-MB-231, human prostate carcinoma PC3, and HeLa cells. Notably, the complex in Fig. 7(b) demonstrated strong selectivity for cancer cells, effectively reduced intracellular ATP levels, and exerted anticancer effects by repressing metabolism and activating multiple cell death signalling pathways. All the complexes tended to accumulate in the mitochondria, likely due to their lipophilic nature. Owing to the substitution of two reactive chloromethyl units on the  $\text{N}^{\wedge}\text{N}$  chelate, complexes in Fig. 7(b) and Fig. 7(d) behaved significantly differently from the other two after subcellular uptake. Complexes in Fig. 7(b) and Fig. 7(d) have

shown much highest cytotoxic activity compared to those in Fig. 7(a) and Fig. 7(c) and these complexes induced cell death by nuclear fragmentation [50]. They were fixed within the mitochondria following nucleophilic substitution with the thiol moieties located in various mitochondrial proteins. The highest cytotoxicity was observed with the most active complexes, which induced caspase-dependent apoptosis. Moreover, mitochondrial damage, ROS elevation and cell cycle arrest for the most potent complexes have been investigated in detail.

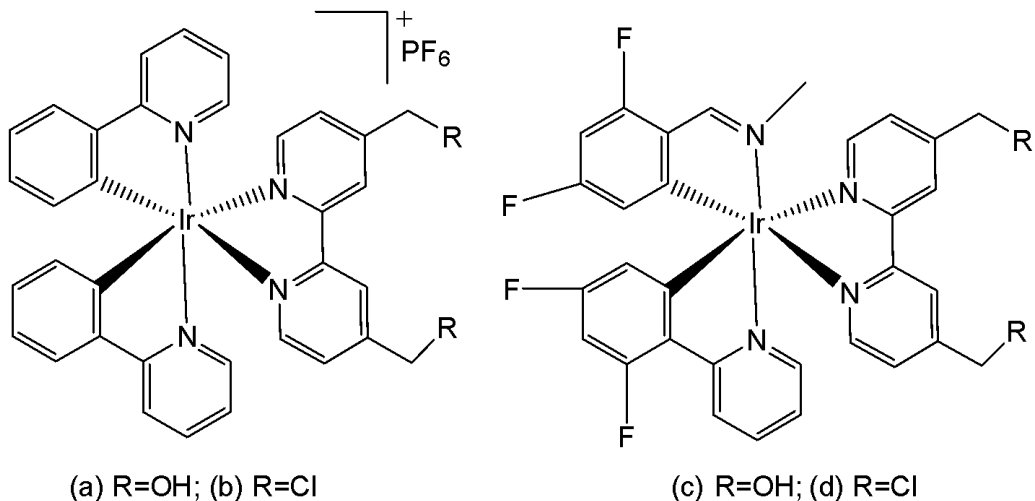


*Fig. (7):* Structures of Ir(III) complex with the general formula  $[\text{Ir}(\text{N}^{\text{C}})(\text{N}^{\text{N}})](\text{PF}_6)$ .

Zhang *et al.* reported the synthesis and anticancer evaluation of a series of iridium(III)–polypyridyl complexes with the formulas  $\text{Ir}(\text{ppy})_2(\text{BHPIP})$  ( $\text{BHPIP} = 2\text{-}(3\text{-bromo-4-hydroxy) phenylimidazo[4,5-f][1,10]phenanthroline}$ ; Fig. 8a) and  $\text{Ir}(\text{ppy})_2(\text{HPIP})$  ( $\text{ppy} = 2\text{-phenylpyridine}$ ;  $\text{HPIP} = 2\text{-}(4\text{-hydroxy) phenylimidazo[4,5-f][1,10]phenanthroline}$ ; Fig. 8b), along with their corresponding liposomal derivatives, Fig. 8(a)-Lipo and Fig. 8(b)-Lipo [51]. The complexes were fully characterized by elemental analysis, IR, ESI-MS,  $^1\text{H}$  NMR, and  $^{13}\text{C}$  NMR spectroscopy, and their *in vitro* and *in vivo* anticancer activities were systematically evaluated.

The complexes shown in Fig. 8(a) and Fig. 8(b) were tested against several cancer cell lines (MCF-7, HeLa, B16, and SGC-7901) and normal cells using MTT assays. Both complexes exhibited  $\text{IC}_{50}$  values above 200  $\mu\text{M}$  against HeLa, A549, B16, MCF-7, SGC-7901, BEL-7402, and LO2 cells, indicating negligible cytotoxic activity. However, their liposomal formulations—prepared via the reverse-phase evaporation method—showed a significant enhancement in cytotoxicity. The  $\text{IC}_{50}$  values of Fig. 8(a)-Lipo and Fig. 8(b)-Lipo against HeLa and B16 cells demonstrated markedly higher anticancer potency compared with the free complexes. Further mechanistic studies revealed that the liposome-encapsulated complexes induced apoptosis through reactive oxygen species (ROS)-mediated lysosomal–mitochondrial dysfunction and caused cell-cycle arrest at the S phase. DNA fragmentation analyses provided additional evidence of apoptosis [51]. The *in vivo* antitumor efficacy of the complexes in Fig. 8(b) and Fig. 8(b)-Lipo was also evaluated in B16 tumor-bearing mice, focusing on apoptosis induction, ROS generation, mitochondrial membrane potential changes, intracellular  $\text{Ca}^{2+}$  levels, and cytochrome  $\text{c}$  release.

The observed enhancement in cytotoxic activity upon liposomal encapsulation is a notable finding, although the precise mechanism of improvement has not been fully elucidated. It is likely attributed to enhanced cellular uptake, protection from degradation, and improved bioavailability conferred by liposomal delivery. Overall, the study demonstrated that liposome-encapsulated complexes induced apoptosis in B16 cells via two primary pathways: (1) DNA damage leading to microtubule

polymerization inhibition, cell-cycle arrest at the S phase, and apoptosis; and (2) ROS overproduction resulting in lysosomal–mitochondrial dysfunction, cytochrome *c* release, caspase-3 activation, PARP cleavage, and ultimately apoptosis. The observed ROS levels were within physiologically relevant ranges and comparable to those induced by standard chemotherapeutic agents.

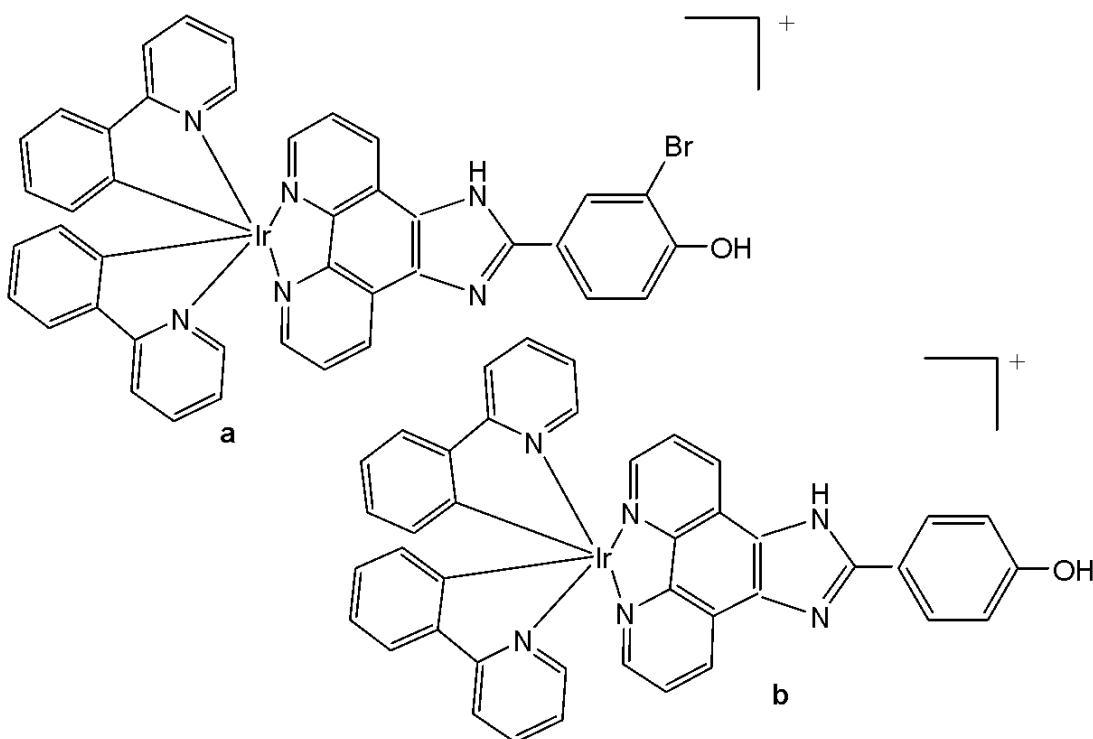


*Fig. (8):* Structures of iridium-polyppyridyl complexes.

Venkatesh *et al.* reported the preparation of two highly luminescent octahedral cationic Ir(III) complexes (Fig. 9a and Fig. 9b) featuring one or two 4-hydroxy- or amino-2,2,6,6-tetramethylpiperidine-N-oxyl (TEMPO) motif, and their anticancer potency investigation [52]. The antiproliferative activity of the ligands (TEMPO) and their Ir(III) complexes was mainly due to the induction of apoptosis through activation of multiple caspases, and their activity has been demonstrated in various cancer and non-cancer cell lines. Correspondingly, the *in vitro* cytotoxic activities of novel mono- and bis-TEMPO-substituted cyclometalated iridium(III) complexes, along with cisplatin, were evaluated against human prostate cancer cells (A2780, A2780cisR, A549, and PC3) and the human lung fibroblast MRC5 cell line. The results indicated that the presence of the TEMPO radical unit significantly enhanced antiproliferative activity. Notably, the complex shown in Fig. 9b demonstrated a fivefold higher cytotoxicity than cisplatin against A2780cisR cells and an eightfold greater cytotoxicity than cisplatin against PC3 cells. Both the complexes (Fig. 9a and Fig. 9b) were relatively inactive in inhibiting the growth of non-cancerous MRC5 cells, as compared to the tested cancer cell lines. The treatment of both the complexes (Fig. 9a and Fig. 9b) did not display an elevated ROS level in A2780 cells, possibly due to the presence of antioxidant TEMPO unit(s). The luminescence of the complexes allowed studying their subcellular localisation by confocal microscopy. When the complexes (Fig. 9a and Fig. 9b) were expected to preferentially localise in mitochondria, their effects on the mitochondrial membrane potential of drug-treated PC3 cells were examined using flow cytometry with the mitochondria-specific dye JC-10. The color change of JC-10 staining induced by the complexes (Fig. 9a and Fig. 9b) indicated mitochondrial membrane depolarization and a loss of membrane potential in the treated cancer cells. Moreover, these complexes were not cross-resistant with cisplatin in ovarian cancer cells, and the complex (Fig. 9b) was 7 times more active than CDDP

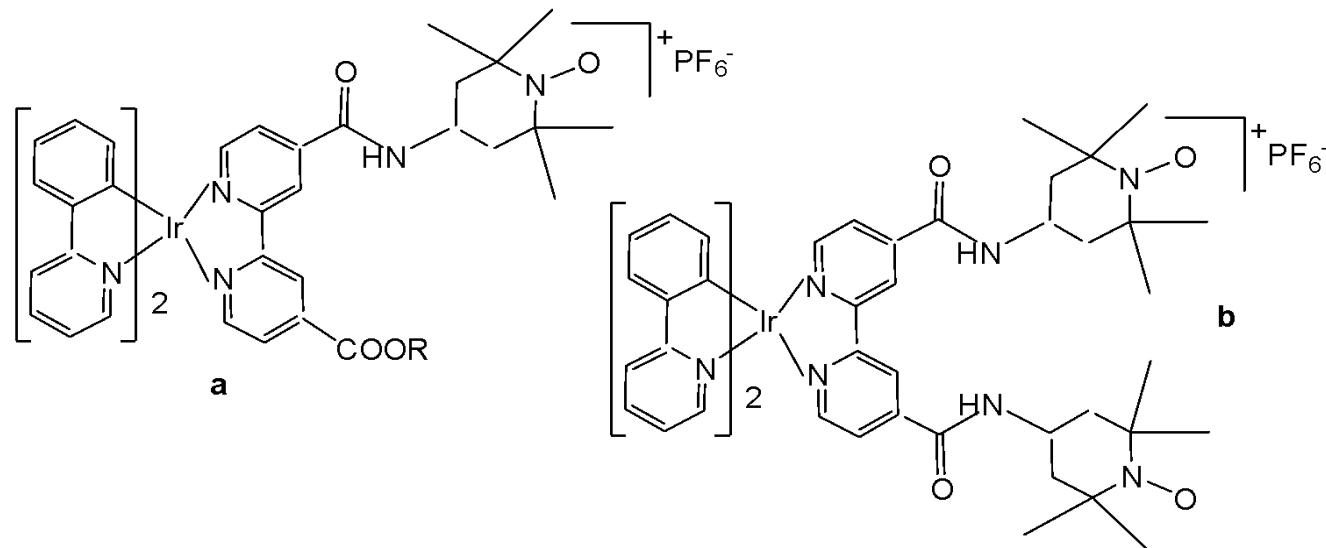


*Fig. (9):* Ir(III) complexes featuring one or two 4-hydroxy- or amino-2,2,6,6-tetramethylpiperidine-N-oxyl (TEMPO) motif(s).

The use of luminescent Ir(III) compounds in the area of cancer diagnosis and treatment has been recently reported, including modulators in protein–protein interactions, membrane-disruptors or mitochondria-targeted agents [53]. Iridium(III) anticancer agents have acted via targeting non-nucleic acid biomolecules, thereby perturbing cell function, which could be visualised owing to the intrinsic luminescence of the compounds, many of them being located in mitochondria. Photodynamic therapy (PDT) employs photosensitizers (PS) that become cytotoxic only upon light irradiation. Transition-metal complexes are highly promising PS due to long excited-state lifetimes and high photo-stabilities. However, these complexes usually absorb higher-energy UV/Vis light, whereas the optimal tissue transparency is in the lower-energy NIR region. One limitation to the clinical use of metal complexes investigated for PDT has been their absorption of light in the UV/Vis region, as the optimal tissue penetration window is 700–900 nm. Lipophilic cationic Ir(III) species have been reported to have a high affinity to mitochondria, and cyclometalated Ir(III) compounds have been demonstrated to be excellent PDT agents [53], causing dual-mode (oxygen-independent and oxygen-dependent) photodynamic damage in mitochondria and killing cancer cells effectively even under hypoxic conditions.

Iridium(III) organometal compounds absorb high-energy UV/vis light, while the optimal tissue transparency is located in the low-energy NIR spectrum region. Most of the metal complexes applied for PDT utilise UV/Vis light with limited penetration depth. McKenzie *et al.* have reported two photo-stable Ir(III) complexes (Fig. 10) with long-lived triplet excited states as photosensitizers that could be excited under both one- and two-photon light in a number of cancerous cell lines [54]. The new low-molecular-weight, long-lived, and cell-permeable iridium complexes of the  $[\text{Ir}(\text{N}^{\text{C}})^2(\text{N}^{\text{N}})]^+$  family, which exhibit strong two-photon absorption, were shown to localize to mitochondria and lysosomal structures in live cells. The compounds feature bisbenzimidazole and

its N, N-dimethylated derivative, respectively, as the N<sup>+</sup>N ligand. The studied Ir(III) biscyclometalated octahedral complexes based on the N-functionalized 2,2'-bibenzo[d]imidazole (Fig. 10) were efficient photosensitizers under 1-photon irradiation (405 nm) with photo-indices greater than 555 [54]. The obtained complexes have been studied against HeLa cells. The non-substituted derivative (R = H) has shown lower cytotoxic activity in the dark, whereas the substituted one (R = Me) has exhibited better cytotoxicity in the dark with a low LD<sub>50</sub> value. The reason for the superior cytotoxicity of this compound was the presence of N-CH<sub>3</sub> groups, which greatly affected the interaction with cells, reducing the number of H-bonds. The non-substituted derivative has displayed a photosensitizing effect against A-375, HCT-116, and U2-OS tumour cells, indicating its potential as a photodynamic therapy (PDT) agent. Both the complexes in Fig. 10 were cell-permeable, and the substituted one (R = Me) showed higher dark cytotoxicity, while the non-substituted derivative (R = H) possessed more potent PDT activity. Targeting different subcellular organelles can achieve different antitumour effects and mechanisms. The non-substituted derivative (R = H) sequentially localises in mitochondria and lysosomes over the course of incubation and can disrupt the functions of both organelles, inducing apoptosis upon light irradiation. Additionally, this complex maintained high PDT activity under NIR TPE (760 nm) at low concentrations and light doses [54].

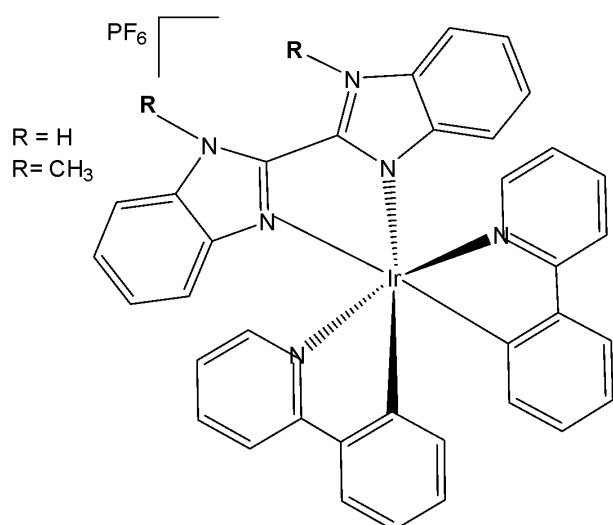


*Fig. (10):* Ir(III) complexes derived from the N-functionalized 2,2'-bibenzo[d]imidazole.

Murphy *et al.* have published the cyclometalated iridium(III) complex Ir(ppy)<sub>2</sub>(pybz) (pybzH = 2-pyridyl-benzimidazole), carrying a 2-pyridylbenzimidazole ligand, and its protonated analogue, Fig. 11, [55]. Photophysical data in dichloromethane solution have shown a structured emission profile in the green region of the spectrum for the non-protonated complex, and an expected red shift for the protonated complex with emission centred around 590 nm. Nevertheless, the emission profiles from CHO cells incubated with the probes at a concentration of 10  $\mu$ M for 5 min were essentially identical. In fact, the protonation equilibrium between the two complexes depended on the local pH, with the non-protonated complex predominating in cellular environments maintained at approximately pH 7.4. A shift was observed in acidic lysosomes, as the protonation equilibrium formed the cationic protonated complex. The MTT assay has demonstrated low cytotoxicity of these complexes, with IC<sub>50</sub> values >200  $\mu$ M for 24 h incubation for both the complexes [55].

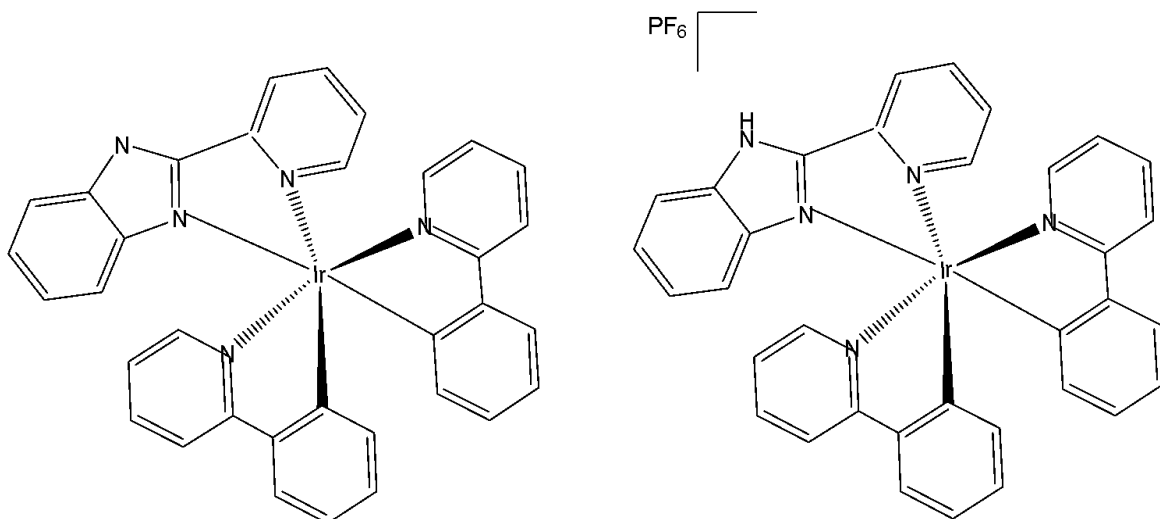


*Fig. (11):* Iridium(III) non-protonated and protonated complexes  $\text{Ir}(\text{ppy})_2(\text{pybz})$ .

Wang *et al.* have synthesised and reported anticancer Ir(III) complexes with half-sandwich and cyclometalated (Fig. 12) structures of the functionalized  $\alpha$ -lipoic acid ( $\text{N}^{\wedge}\text{N-LA}$ ) as a  $\text{N}^{\wedge}\text{N}$  ligand, which is a 2,2-bipyridine derivative [56]. The cyclometalated complex, shown in Fig. 12, possessed the formula  $[\text{Ir}(\text{C}^{\wedge}\text{N})_2(\text{N}^{\wedge}\text{N-LA})]\text{PF}_6$ , where  $\text{C}^{\wedge}\text{N}$  is 2-phenylpyridine. The half-sandwich and cyclometalated complexes were treated with various cancer cell lines. Their antiproliferative activity was determined against human lung carcinoma A549, cisplatin-resistant A549R, human breast carcinoma MCF-7, epithelial ovarian carcinoma A2780, human cervical carcinoma HeLa, and human normal liver LO2 cell lines by MTT assay after 48 h treatment. The iridium(III) half-sandwich complex exhibited no cytotoxicity ( $\text{IC}_{50} > 200 \mu\text{M}$ ), likely due to its poor stability, low lipophilicity limiting cellular uptake, and its susceptibility to hydrolysis and reaction with GSH. The cyclometalated complex (Fig. 12) exhibited excellent cytotoxicity, compared to cisplatin, with  $\text{IC}_{50}$  values ranging from 3.4 to 6.7  $\mu\text{M}$ . The complex, formed by combining the  $\text{N}^{\wedge}\text{N-LA}$  ligand with tripyridine, has shown a positive synergic effect. It also displayed an ability to overcome the cisplatin-resistance in A549R cells. The cyclometalated complex was stable in aqueous solution and had no reaction with GSH, guaranteeing its bioactivity. Furthermore, the excellent photophysical property of the cyclometalated complex provided a more convenient way to study its anticancer mechanism of action through confocal spectroscopy, especially the subcellular localisation. The complex localised and accumulated in the lysosomes of A549 cells, induced the production of a significant amount of ROS, and arrested the cell cycle at the  $\text{G}_0/\text{G}_1$  phase, which differs from the apoptosis induced by the clinical drug  $\alpha$ -lipoic acid itself. The complex (Fig. 12) was hydrophobic in nature, thus having an effect on the cellular uptake due to the lipid bilayer of the cell membrane and the cell death by autophagy [56]. The study has demonstrated the relationship between the anticancer activity and the affiliated structure. This work has also provided insights to clarify the subtle structure-property relationship between the half-sandwich and cyclometalated iridium complexes, and highlighted the importance of the tailored design of metallodrugs according to their future functions.

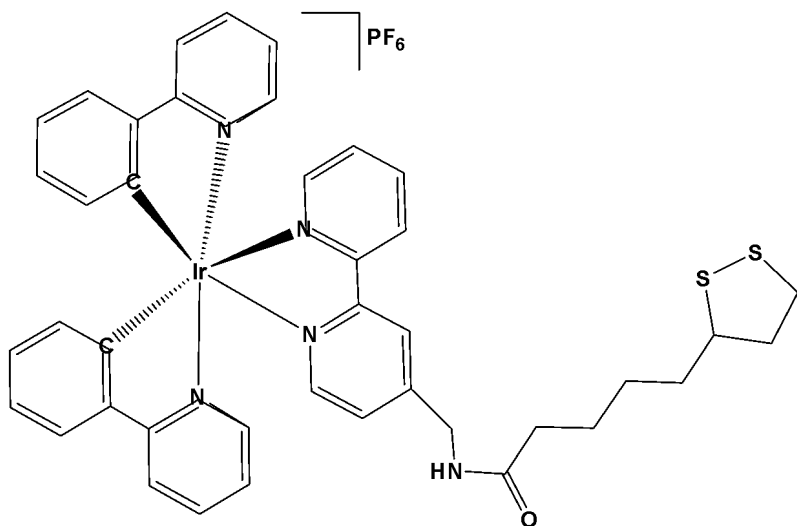


*Fig. (12):* Structure of  $(\text{Ir}[\text{C}^{\text{N}}]_2(\text{N}^{\text{N}}\text{-LA}))\text{PF}_6$  ( $\text{C}^{\text{N}} = 2\text{-phenylpyridine}$ ).

The biscyclometalated cationic complexes of the type  $[\text{Ir}(\text{III})(\text{C}^{\text{N}})_2(-\text{N}^{\text{N}})]\text{Cl}$  (Fig. 13), incorporating thiabendazole and N-benzyl-thiabendazole, have been designed and synthesised to investigate the photophysical and biological effects associated with modifications of the ancillary ligand [57]. These complexes exhibit a diverse range of cellular targets, largely influenced by the nature of the auxiliary ligands, including the nucleus, endosomes, lysosomes, endoplasmic reticulum, mitochondria, and others. In this viewpoint, arylazoles of the  $\text{N}^{\text{N}}$  type are admirable ancillary ligands, because of their structural and biochemical variety. Precisely, the imidazole or benzimidazole ligands can be readily functionalized through the amine bond. In this series of biscyclometalated Ir(III) complexes, the amine (N-H) group of 4-(1H-benzo [d]imidazol-2-yl)thiazole ligand has been functionalized with a lipophilic benzyl (N-Bnz) group [57]. The complexes have been tested against human colon SW480 and human lung A549 adenocarcinoma cell lines. In the dark, the Ir(III) complex with benzyl group ( $\text{R} = \text{Bnz}$ ) was one order more cytotoxic than cisplatin against the tested cell lines. The biological properties were studied further to determine their mechanism of action. These Ir(III) complexes have interfered with mitochondrial functions, leading to cell apoptosis. In addition, improvement of their effects has been observed after irradiation with visible blue light via photocatalyzing the oxidation of S-containing L-amino acids. It has been demonstrated that the complex with thiabendazole was more active than the complex with N-benzyl-thiabendazole, which provided a reasonable mechanism for their biological action (oxidative stress could be selectively promoted through a photocatalytic action) upon irradiation. This different PDT behaviour depending on the ancillary substituent might be helpful for future rational design of new metal-based photosensitizers.

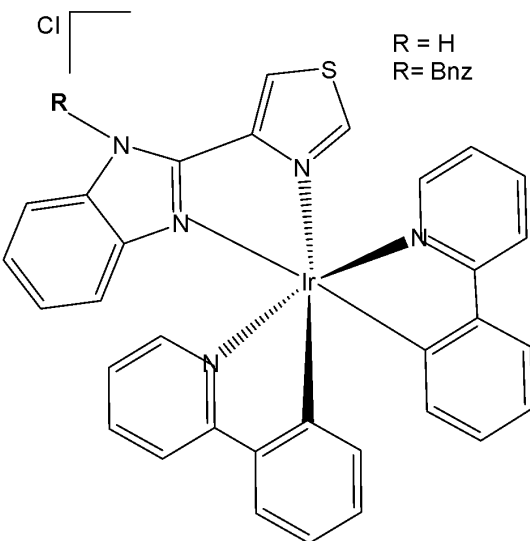


*Fig. (13):* Iridium compounds with substituted 4-(1H-benzo [d]imidazol-2-yl)thiazole ligand.

The derivatives of guanidine and thiourea are multifunctional compounds widely utilised in medicine. Guanidine derivatives are found in arginine and guanine, whereas thiourea is located in 2-thiouridine of tRNA. As their applications continue to expand across fields such as cancer therapy, sensors, and electronics, their toxicity becomes an important consideration. Iridium(III) complexes with guanidine and thiourea substituents (Fig. 14) have recently been systematically developed [58]. The cytotoxicity of these compounds has been evaluated against three human ovarian cancer (EFO-21, EFO-27 and COLO-704) cell lines and their cisplatin-resistant sub-lines (EFO-21<sup>r</sup>CDDP<sup>2000</sup>, EFO-27<sup>r</sup>CDDP<sup>2000</sup> and COLO-704<sup>r</sup>CDDP<sup>1000</sup>). The derivative of guanidine ( $IC_{50} = 1.4 \mu M$ ) was ten times more cytotoxic than the derivative of thiourea ( $IC_{50} = 13.5 \mu M$ ). The cisplatin-resistant sublines are more tolerant to both complexes. The results have confirmed that the guanidine derivative showed cytotoxic activity in the nM range against the tested cell lines. The compounds displayed toxicity trends that were strongly dependent upon S/NH substitution. The patterns of toxicity were illuminated by using the intrinsic luminescence of the complexes as a handle for cellular imaging.

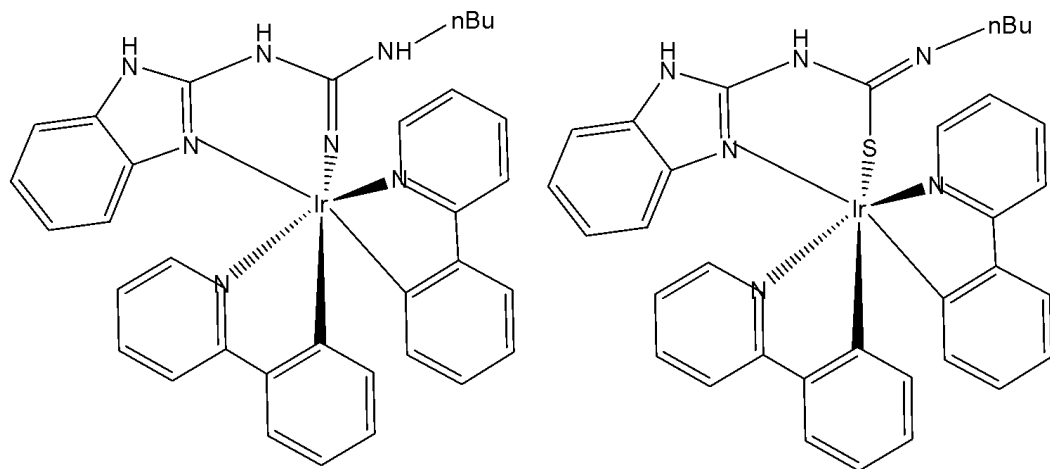


*Fig. (14):* Iridium(III) complexes with guanidine and thiourea substituents.

The incorporation of Ir(III) complexes with guanidine ligands might improve the efficacy in cancer therapy. Song *et al.* have synthesised three new cyclometalated iridium(III) complexes (Fig. 15), containing guanidine-modified ligands, which were found to exert excellent cytotoxic effects on

different types of cancer cells upon light irradiation at 425 nm [29]. Iridium(III) complexes containing guanidine ligands, Fig. 15(a-c), used in PDT, represented promising non-invasive therapeutic systems with no cumulative toxic effects [29]. Complex in Fig. 15(a) exhibited the lowest cytotoxicity towards cancer cell lines (HeLa, MCF-7, and Hep-G2) while showing the highest phototoxicity index. Complex in Fig. 15(b) demonstrated moderate cytotoxic effects on cancer cell lines with  $IC_{50}$  values ranging between 20 and 60  $\mu$ M. The mechanisms underlying the antitumour effects of the complex shown in Fig. 15(a), including subcellular localisation, mitochondrial dysfunction, ROS production, cell cycle arrest, and mitochondria-associated apoptotic signalling pathways, have been elucidated. Mechanistic investigations revealed that the complex in Fig. 15(a) could induce apoptosis via the activation of ROS-mediated mitochondria-associated caspase-independent signalling pathways, both in the presence and absence of light irradiation, and also promoted cell cycle arrest at the G<sub>2</sub>/M phase. Studies have shown that the complex in Fig. 15(a) induced tumour cell death *in vivo* in HepG2 xenograft-bearing mice under light irradiation and exerted no severe side effects on surrounding organs [29].

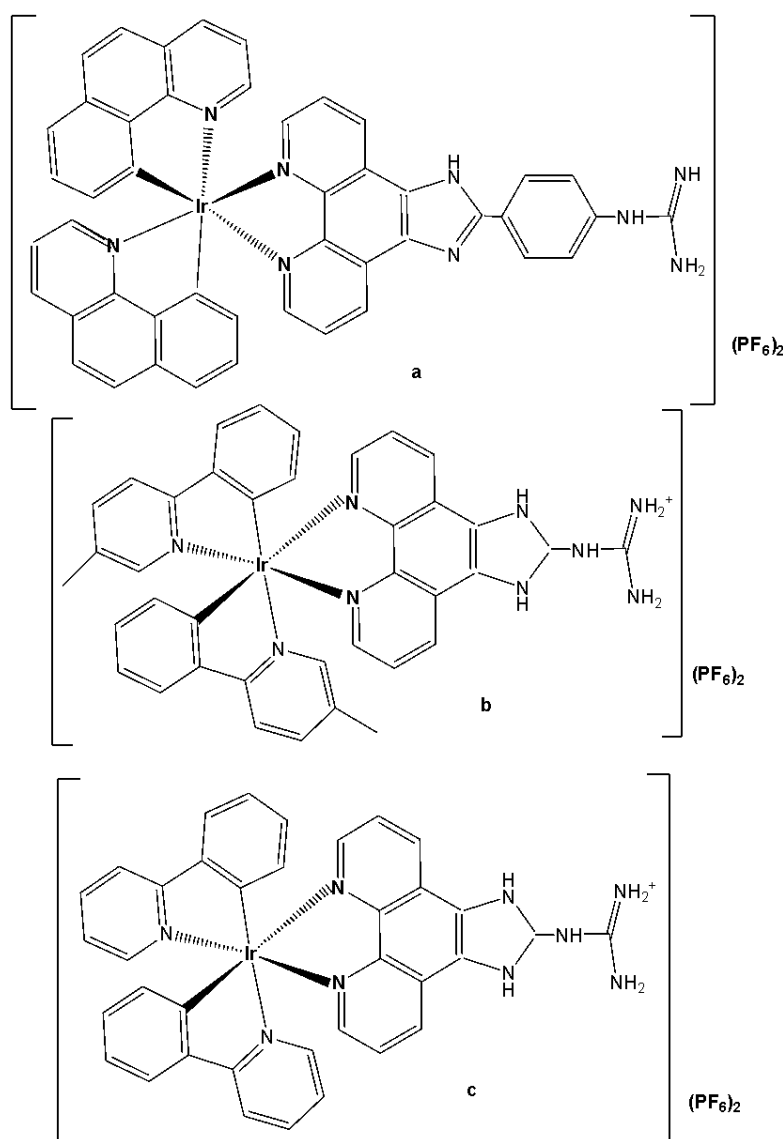


*Fig. (15):* Structures of Ir(III) complexes with guanidine-modified ligands.

Iridium-based photosensitizers are of great interest in photodynamic therapy (PDT) due to their tunable photophysical and photochemical characteristics and structural flexibility. Zhao et al. synthesised and

reported iridium(III) complexes, as shown in Fig. 16(a–b), highlighting the potential of a nanoplatform based on a long-lived iridium(III)-based photosensitizer for tumor therapy [59]. The iridium-naphthalimide photosensitizer in Fig. 16(a), featuring a long-lived intra-ligand excited state, was specifically designed to achieve significantly enhanced singlet oxygen ( ${}^1\text{O}_2$ ) generation efficiency, approximately 45 fold higher than that of the model iridium(III) complex shown in Fig. 16(b) under 460 nm irradiation. To achieve deep tissue penetration, the iridium-naphthalimide complex in Fig. 16(a) was further covalently bonded to the up-conversion nanoparticles (UCNPs). Besides, 1-benzyl-3-(5'-hydroxymethyl-2'-furyl)indazole (YC-1), an effective HIF-1 $\alpha$  inhibitor, was physically adsorbed into the hydrophobic layer at the surface of UCNPs. Upon near-infrared (NIR) irradiation iridium(III)-naphthalimide complex in Fig. 16(a), mediated the toxic  ${}^1\text{O}_2$ , which was generated for PDT, whose efficient conversion of oxygen to  ${}^1\text{O}_2$  during the PDT would exacerbate the hypoxic condition of tumour tissue and lead to the upregulation of HIF-1 $\alpha$  for the following HIF-1 targeting tumour therapy. All of this transforms PDT-induced tumor hypoxia into a therapeutic advantage, thereby opening up new strategies to overcome hypoxia in PDT therapy. These complexes showed slight cytotoxicity in normoxic and hypoxic cells, displaying their low dark toxicity and good biocompatibility [59].

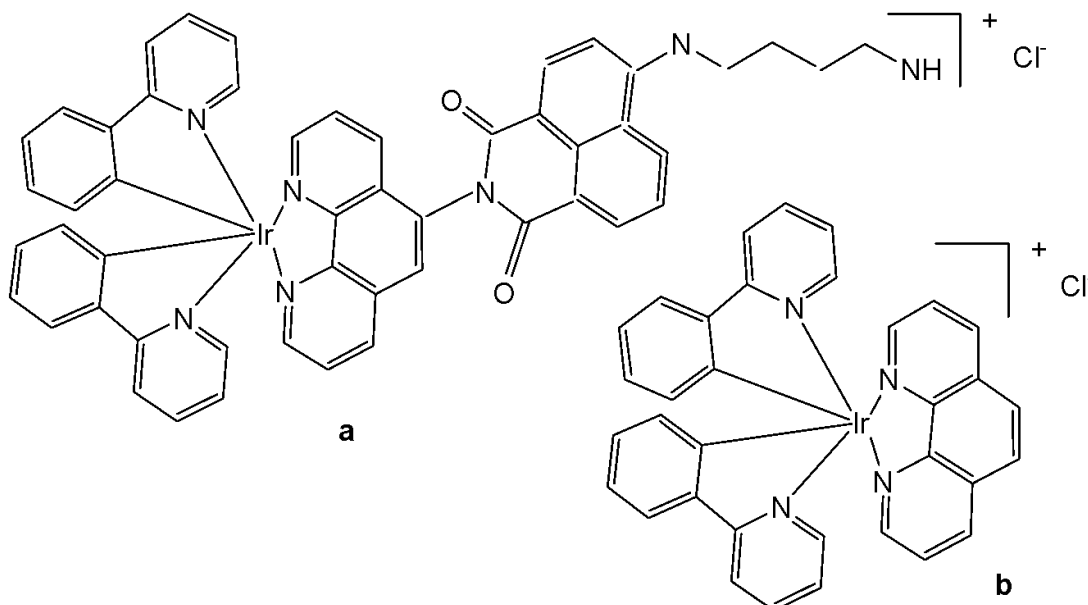


*Fig. (16):* The iridium-naphthalimide photosensitizer and its model iridium(III) complex.

The combination of the ease of synthesis and the excellent photophysical and biochemical properties makes the biscyclometalated Ir(III) complexes with a formula of  $[\text{Ir}(\text{C}^{\wedge}\text{N})_2(\text{N}^{\wedge}\text{N})]^+$  more suitable to be developed as non-platinum antineoplastic drugs. In many papers, phenanthroline and its derivatives as  $\text{N}^{\wedge}\text{N}$  chelating ligands have been applied to cyclometalated Ir (III) complexes and acted as effective phototherapy drugs towards different tumour cells. Xue *et al.* have synthesised and characterized phosphorescent cationic iridium complexes using phenanthroline derivatives as  $\text{N}^{\wedge}\text{N}$  ligands and 2-phenylpyridine as the  $\text{C}^{\wedge}\text{N}$  ligand [60]. Importantly, effective induction of the generation of singlet oxygen  ${}^1\text{O}_2$  after irradiation, leading to apoptosis, was observed. The photodynamic therapy effect was further assessed by histological examination and immunohistochemistry.

Hong *et al.* have reported the synthesis of iridium (III) complex with the general formula  $[\text{Ir}(\text{ppy})_2(\text{paip})]\text{PF}_6$  (Fig. 17), where ppy and paip are 2-phenylpyridine and 2-(4-aminophenyl) imidazo [4,5-f] [1,10] phenanthroline, respectively. The cytotoxicity studies were carried out by MTT

assay on Bel-740, HeLa, HepG-2 and PC-12 cell lines. The complex showed higher cytotoxic activity than cisplatin towards PC12 cells with  $IC_{50}=10.2\text{ }\mu\text{M}$ . The intracellular ROS generation and mitochondrial membrane potential (MMP) changes were determined by a fluorescent microscope and flow cytometry. Complex in Fig. 17 demonstrated efficient cellular uptake, accumulating in both the nucleus and mitochondria. It induced apoptosis by elevating ROS levels and decreasing mitochondrial membrane potential, thereby inhibiting cell growth in PC-12 cells at the  $G_0/G_1$  phase [61]. Cell invasion assay has shown that the complex could effectively inhibit the cell invasion and activate caspase 3 and procaspase 7, down-regulated the expression of Bcl-2 and Bcl-x, and up-regulated the expression levels of Bak.

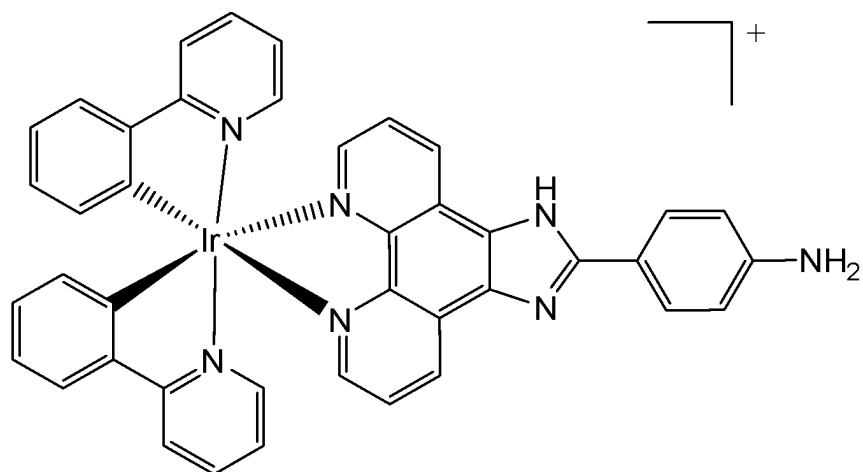


*Fig. (17):* Iridium(III) complex  $[\text{Ir}(\text{ppy})_2(\text{paip})]\text{PF}_6$  of 2-(4-aminophenyl) imidazo[4,5-f][1,10]phenanthroline.

Liang *et al.* have synthesised and reported the complex  $[\text{Ir}(\text{ppy})_2(\text{MHPIP})]\text{PF}_6$  (Fig. 18), where ppy = 2-phenylpyridine and MHPIP = 2-(1-methyl-1-H-Pyrazol-3yL)-1H-imidazo[4,5f][1,10]phenanthroline [62]. The *in vitro* cytotoxic activity of the free proligand MHPIP and its complex was evaluated using the MTT assay. The free ligand MHPIP exhibited no cytotoxicity against the tested cell lines. In contrast, the complex showed selective toxicity toward HepG2 cells ( $IC_{50} = 39.5\text{ }\mu\text{M}$ ) while exhibiting no cytotoxic effects on other cancer cell lines, including SGC-7901, HeLa, BEL-7402, A549, or on normal LO2 cells. The level of reactive oxygen species, mitochondrial membrane potential, autophagy, intracellular  $\text{Ca}^{2+}$  levels and cell invasion were investigated by fluorescence microscopy, and the cell cycle arrest was studied by flow cytometry. These studies demonstrated that the complex effectively induced apoptosis and autophagy in HepG2 cells by causing DNA damage and ROS-mediated mitochondrial dysfunction, as well as by inhibiting the PI3K/AKT/mTOR pathways, thereby promoting autophagy and significantly suppressing cell growth at the  $G_0/G_1$  phase [62].

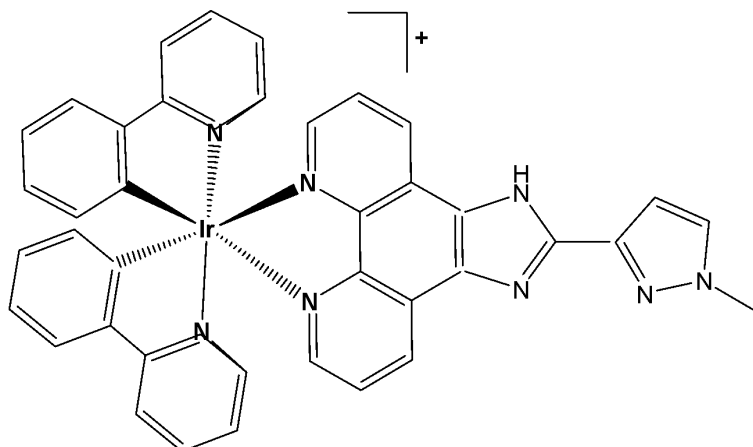


*Fig. (18):* Structure of Iridium (III) complex with formula  $[\text{Ir}(\text{ppy})_2(\text{MHPIP})]\text{PF}_6$ .

A charged iridium(III) complex carrying a phenanthroline-based ligand, functionalized with an isothiocyanate group, has been developed to target specific mitochondrial proteins [63]. The cellular properties of the studied luminescent cyclometalated iridium(III) complex  $[\text{Ir}(\text{pq})_2(\text{phen-ITC})](\text{PF}_6)$  ( $\text{Hpq}$ =2-phenylquinoline, phen-ITC=5-isothiocyanato-1,10-phenanthroline), that efficiently and specifically labels mitochondria in living mammalian cells, have been investigated. The isothiocyanate unit allowed the probe to covalently bind to amine-containing biomolecules such as lysine and the N-terminal of proteins, yielding luminescent bioconjugates. The studied complex accumulated only in the mitochondria of living 3T3, HeLa and RPE cells, while a diffuse staining was present with prefixed 3T3 cells, indicating that the process required active cellular metabolism. The binding of the complex to mitochondrial proteins interfered with the function and the morphology of this organelle, as shown by the MTT assay. The viability of 3T3 cells decreased to 60% with a concentration higher than  $10 \mu\text{M}$  and an incubation time of 12 h [63]. A family of three luminescent cyclometalated iridium(III) diimine complexes  $[\text{Ir}(\text{bsn})_2(\text{N}^{\wedge}\text{N})](\text{PF}_6)$ , bound to functionalized 1,10-phenanthroline ligands, where  $\text{Hbsn}$  = 2-(1-naphthyl)benzothiazole,  $\text{N}^{\wedge}\text{N}$  = 5-amino-1, 10-phenanthroline, 5-isothiocyanato-1, 10-phenanthroline, and N-butyl-N'-1, 10-phenanthroline-5-yl thiourea, has been studied by the group of Lo [64]. The photophysical and electrochemical properties of these complexes have been examined. The cytotoxic effects and cellular internalization of the complexes in HeLa cells have been investigated through multiple approaches. The intracellular distribution of the complexes in HeLa cells was the same, with the formation of a luminescent ring surrounding the nucleus. Additionally, cytotoxicity data have shown similar  $\text{IC}_{50}$  values in the range of  $1.0\text{--}4.2 \mu\text{M}$ , revealing the high toxicity of these probes. All the complexes have exhibited very efficient cellular uptake properties in a relatively short incubation time, indicating that they represented attractive candidates for developing novel cellular imaging reagents.

Kuang *et al.* have reported iron(III)-activated iridium(III) compounds as pro-drugs for gastric cancer theranostics that were firstly localised in lysosomes and subsequently transferred to mitochondria [65]. The Ir(III) complexes (Fig. 19) have not been toxic to normal LO2 and MCF-10A cell lines; however, they have shown considerable cytotoxicity and selectivity against AGS and MKN-28 gastric cancer cells with low  $\text{IC}_{50}$  values. When activated by  $\text{Fe}^{3+}$ , the complexes are hydrolyzed in lysosomes to yield an amino-bipyridyl Ir(III) complex and 2-hydroxybenzochinone, a ROS generator. In addition to exhibiting high cytotoxicity against various tumor cells, the complexes display an intense phosphorescence, making them advantageous for diagnostic applications. Additionally, in the xenograft AGS tumor model, these compounds demonstrated greater activity than the reference drug fluorouracil while exhibiting fewer side effects in murine models. The same research group has also reported a series of iridium(III) complexes with benzothiazole-substituted ligands [66]. Notably, the

compound bearing benzothiazole substituents,  $[\text{Ir}(\text{ppy})_2(\text{bbtb})]^+$  (Fig. 19), specifically targeted mitochondria and activated oncosis-related proteins, including porimin and calpain [66]. Ir(III) complexes, shown in Fig. 19, have exhibited high cytotoxic activity against various tumour cell lines, together with cisplatin-resistant cells, showing low  $\text{IC}_{50}$  values ( $\text{IC}_{50} < 10 \mu\text{m}$  for AGS cells) and lower cytotoxicity against normal hepatocytes ( $\text{IC}_{50} > 200 \mu\text{m}$  for LO2 cells) [65,66]. An increase in phosphorescence and cytotoxicity, along with the shift of subcellular localisation from lysosomes to mitochondria, can be monitored using confocal microscopy.

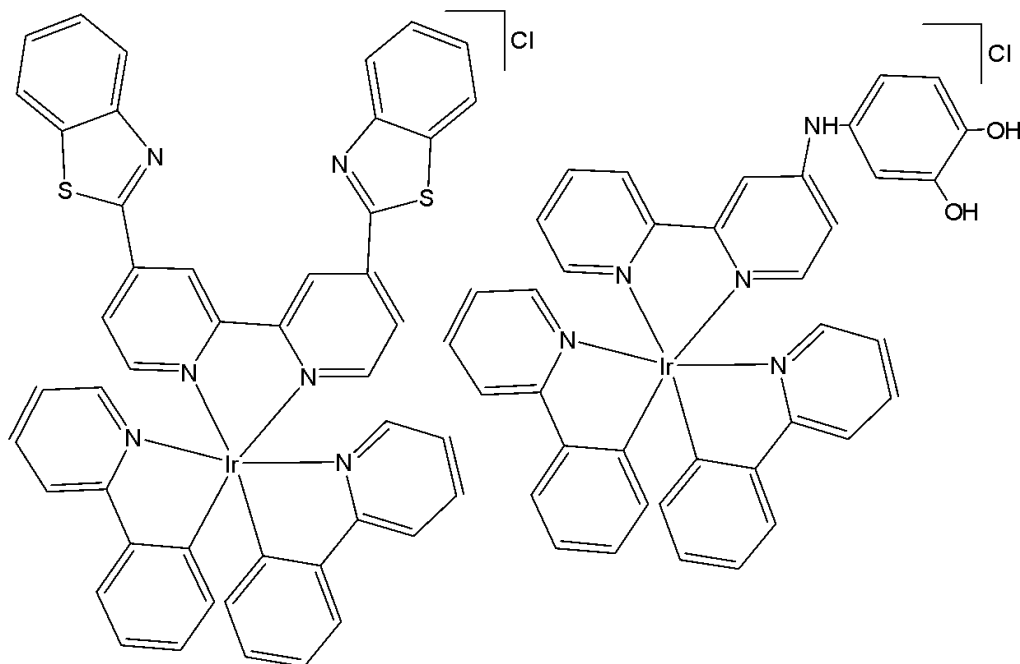


*Fig. (19):* Oncosis-inducing cyclometalated Ir (III) complexes.

### 2.3. Biscyclometalated Ir(III) Complexes with Substituted 2-Phenylpyridines as Modified C<sup>N</sup> Ligands

The development of multifunctional theranostic agents, which combine tumour targeting, imaging, and therapeutic capabilities, has significantly advanced the clinical diagnostics and treatment of tumours. However, the integration of imaging and therapy functionalities into a unimolecular framework remains a great challenge. Yi *et al.* have synthesised and reported a family of amphiphilic gemini Ir(III) complexes, presented in Fig. 20(a-f) [67]. These complexes contain quaternary ammonium groups (QA) which were employed as hydrophilic functional groups to modify both the C<sup>N</sup> ligands and the auxiliary N<sup>N</sup> ligands of the hydrophobic iridium(III) complex. This structure gives the complexes adjustable water solubility and excellent self-assembly properties. These complexes can spontaneously form vesicles in aqueous media through self-assembly due to their amphiphilic nature, exhibiting two distinct molecular arrangements in the aggregated vesicles depending on the position of the quaternary ammonium groups.

Spectroscopic and computational results have revealed that introducing quaternary ammonium groups into cyclometalating ligands (C<sup>N</sup> ligands), Fig. 20(a-c), endows gemini iridium(III) complexes with adjustable water solubility, excellent self-assembly properties, and the opportunity to overcome the drawback of aggregation-caused emission quenching, ensuring high emission intensity and excellent singlet oxygen  ${}^1\text{O}_2$  generation ability of the complexes in aqueous media due to the dipyridyl groups arranged by an edge-to-edge configuration. The efficacy of  ${}^1\text{O}_2$  generation of the complexes followed the

order Fig. 20(c) > 20(b) > 20(a) > 20(f) > 20(e) > 20(d), which was consistent with their increasing emission lifetimes.

The potential application of the studied gemini iridium(III) complexes for photodynamic therapy has been assessed toward HepG2 and MCF-7 cells via a MTT assay under dark and irradiation conditions. Under dark condition, the complexes exhibited slight cytotoxicity toward the tested cells ( $IC_{50} > 300 \mu M$ ), which is an important characteristic for the PDT agent. The possible reason is that the heavy atom iridium is wrapped by the aggregated vesicles, which avoid interacting nonspecifically with the proteins. In comparison, the complex in Fig. 20(c), due to its appropriate lipophilicity, became highly phototoxic to HepG2 and MCF-7 cells with  $IC_{50}$  values as low as  $1.2 \mu M$  (PI = 250.0) and  $1.3 \mu M$  (PI = 230.7), where PI is the ratio between the  $IC_{50}$  values in the dark upon light irradiation.

With appropriate water solubility and positive charge, the complex in Fig. 20(c) showed higher cellular uptake efficiency by an energy-dependent endocytosis pathway. This complex localized specifically in the mitochondria, exhibited outstanding photostability, low dark cytotoxicity, and an impressive phototoxicity index with satisfactory performance in mitochondria-targeted imaging and photodynamic therapy (PDT) of tumour cells. Due to its excellent photostability the complex in Fig. 20(c) could be used as mitochondria targeted imaging agent.

Furthermore, *in vivo* studies have proven that the complex in Fig. 20(c) was nontoxic to normal organs and possessed exceptional antitumor activity and remarkably inhibited the growth of the HepG2 tumour cells under PDT treatment. Therefore, this work represents a promising strategy for designing potential clinically applicable multifunctional iridium(III) complexes as theranostic agents for mitochondria-targeted imaging and PDT in a single molecular framework [67].

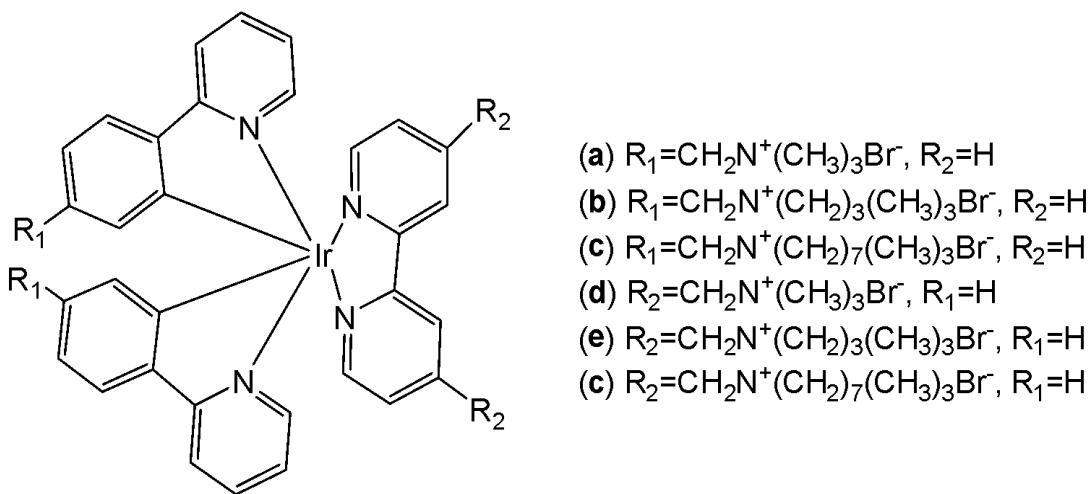


*Fig. (20):* Ir(III) complexes with quaternary ammonium groups in  $C^N$  and  $N^N$  ligands.

Cao *et al.* have synthesised six cyclometalated iridium(III) complexes, presented in Fig. 21(a-f), each incorporating a series of extended planar diimine ligands [11]. All complexes exhibited higher cytotoxic activity ( $IC_{50}$  varying between  $0.1$  and  $8.4 \mu M$ ) compared to cisplatin against different cancer cells (A549, A549R, HepG2, PC3 and HLF). The order of cytotoxicity was as follows: Fig. 21(c) > 21(d) > 21(e) > 21(f) > 21(a) > 21(b), and the most active of them, with an  $IC_{50}$  around  $0.1 \mu M$ , were found to be 100-fold times greater than cisplatin against HeLa cells. These complexes were likely to overcome the acquired and intrinsic drug resistance of cisplatin. Among the studied compounds, the complexes with dipyrdo[3,2-*a*:2',3'-*c*]phenazine ligands could bind to DNA tightly *in vitro*, intercalate to mtDNA *in situ*, and induce mtDNA damage. These compounds exhibited a drop in the mitochondrial

membrane potential, disability of adenosine triphosphate generation, disruption of mitochondrial energetic and metabolic status, which subsequently caused protective mitophagy, G<sub>0</sub>/G<sub>1</sub> phase cell cycle arrest, and apoptosis (Fig. 21) [11].

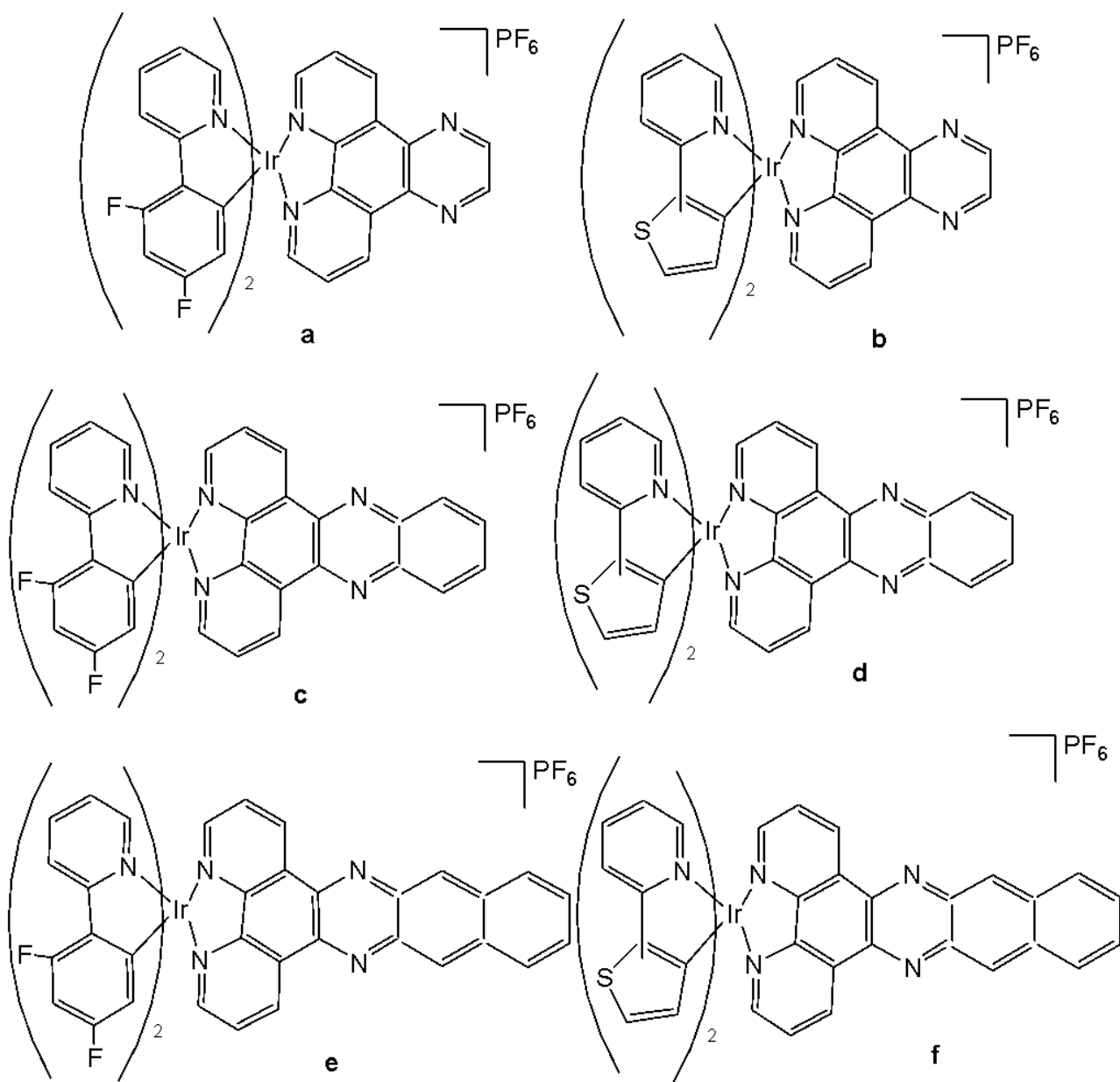
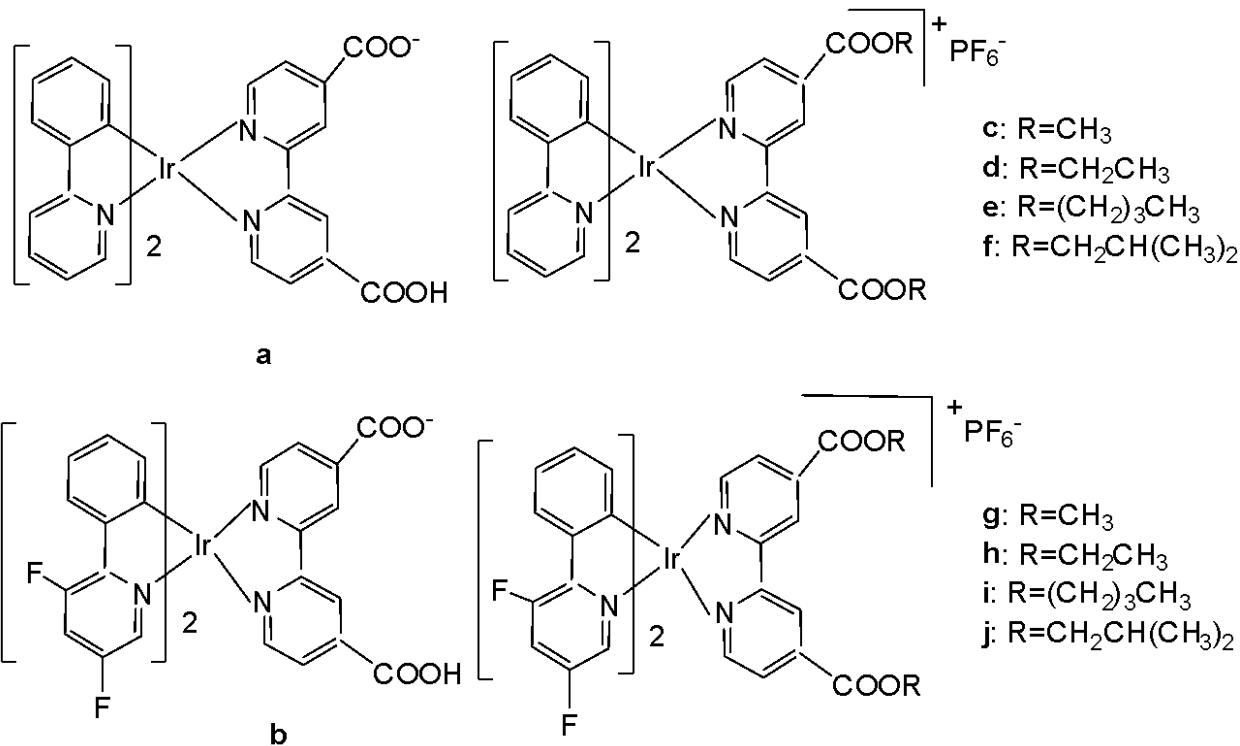


Fig. (21): Structures of cyclometalated Ir (III) complexes with extended planar ligands.

Wang and co-workers have reported the synthesis of a series of phosphorescent cyclometalated Ir (III) complexes containing 2,2'-bipyridine-4,4'-dicarboxylic acid and its diester derivatives as ligands (Fig. 22 a-j), along with studies on their chemotherapeutic properties, focusing on their antineoplastic potency [68]. The authors have prepared structurally diverse ester-appending moieties with different alkyl chain lengths (CH<sub>3</sub>, C<sub>2</sub>H<sub>5</sub>, n-C<sub>4</sub>H<sub>9</sub>, CH<sub>2</sub>CH(CH<sub>3</sub>)<sub>2</sub>) on the 2,2'-bipyridine N<sup>+</sup>N ligand, and compared these complexes with the analogues featuring dicarboxylic acid-functionalized 2,2'-bipyridine N<sup>+</sup>N ligand. Esterification is an efficient and convenient optimisation method for carboxylic acid-containing compounds, which can markedly improve their cellular uptake efficacy. In this study, the effects of ester modifications on the photophysical properties, lipophilicity, cellular uptake, and anticancer activity of cyclometalated iridium(III) complexes were investigated in detail. A

clear correlation between the alkyl chain length of the esters and cytotoxicity was observed. Notably, the complexes shown in Fig. 22e and Fig. 22i exhibited the highest antiproliferative activity across a panel of cancer cell lines, including HeLa, A549, A549R, MCF-7, and HepG2, as well as cisplatin-resistant tumor cells.

On the other hand, the ester-functionalized complexes in Fig. 22e and Fig. 22i would be expected to be hydrolyzed by esterase, and their intracellular staining experiment has shown that these luminescent complexes would be localised in the mitochondria in A549 cells with the validation of red MitroTracker (MTDR). In this regard, the cell-death mechanism has been investigated in several key aspects, including the cell cycle arrest, ROS level, autophagy and apoptosis. It has been found that both complexes in Fig. 22e and Fig. 22i would lead to mitochondrial dysfunctions, related to the intracellular ROS level, and would induce concentration-dependent cell cycle arrest, pro-death autophagy and caspase-dependent apoptosis simultaneously in A549 cells. The study has demonstrated that ester modification was a practical, feasible and straightforward strategy for structural optimisation of antineoplastic cyclometalated Ir(III) complexes [68].



*Fig. (22):* Ir (III) complexes, containing 2,2'-bipyridine-4,4'-dicarboxylic acid and its diesters.

New series of anticancer and photophysical neutral Ir (III) biscyclometalated complexes with auxiliary  $N^{\wedge}O$  ligands of the type  $[Ir(III)(C^{\wedge}N)_2(N^{\wedge}O)]$ , Fig. 23, where  $N^{\wedge}O = 2\text{-}(benzimidazolyl)\ phenolate-N,O$  and  $2\text{-}(benzothiazolyl)\ phenolate-N,O$ , and  $C^{\wedge}N = 2\text{-}\ (phenyl)pyridinate$  or its derivatives, have been described as PDT agents [69]. Complexes of the two series have exhibited dissimilar photophysical and biological properties. The proliferation effects of Ir(III) complexes against the colon adenocarcinoma SW-840 cell line have been studied by MTT in the dark and with UV irradiation. In the dark, the complexes with benzimidazole derivatives ( $X = NH$ ) were not cytotoxic, whereas the benzothiazole-substituted compounds ( $X = S$ ) were more cytotoxic than cisplatin. Consequently, the ancillary  $N^{\wedge}O$  ligand is the key factor in terms of cytotoxic activity both in the dark and upon irradiation. However, the  $C^{\wedge}N$  ligands play a central role concerning the metal accumulation in cells. The benzothiazole complexes preferred to be located in the nucleus, while the benzimidazole

complexes remained outside the cell nucleus. Notably, the complex of 2-(4,6-difluorophenyl) pyridinate has been identified as both an efficient photosensitizer for  ${}^1\text{O}_2$  generation and a potential agent for photodynamic therapy. Both categories of complexes have exhibited notable catalytic activity in the photooxidation of thioanisole and S-containing amino acids with full selectivity.

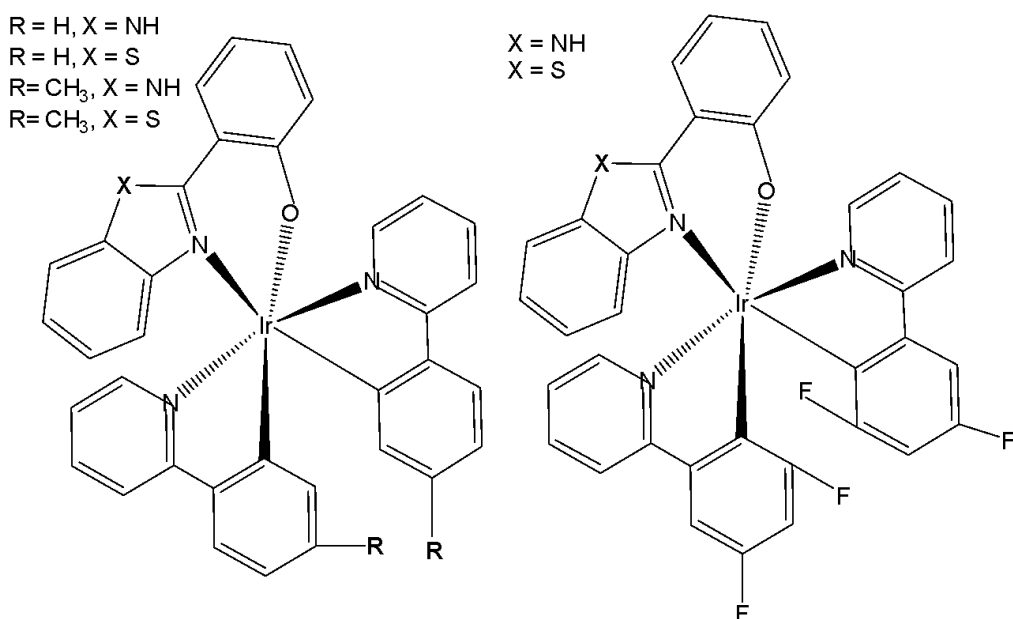


Fig. (23): Ir (III) complexes with different bidentate benzimidazole ligands and  $\text{N}^{\wedge}\text{C}$  co-ligands.

### III. CYCLOMETALATED Ir(III) COMPLEXES WITH MODIFIED AROMATIC $\text{C}^{\wedge}\text{N}$ LIGANDS

Many researchers have tried to replace the  $\text{C}^{\wedge}\text{N}$  ligand of widely studied 2-phenylpyridine iridium complexes by different bidentate  $\text{C}^{\wedge}\text{N}$  ligands to improve their biological activity [70].

Wu *et al.* have synthesised iridium(III) complexes, shown in Fig. 24(a-l), and evaluated them for potency against malignant melanoma metastasis [71]. The authors first obtained three Ir(III) complexes (Fig. 24a-c) with a general structure  $[\text{Ir}(\text{C}^{\wedge}\text{N})_2(\text{N}^{\wedge}\text{N})]^+$  bearing either methyl, t-butyl, and/or nonyl aliphatic groups attached to their  $\text{C}^{\wedge}\text{N}$  and  $\text{N}^{\wedge}\text{N}$  ligands (Fig. 24). To investigate the effects of the aliphatic groups in these Ir(III) complexes on S100B inhibitory activity, the authors further designed Ir(III) complexes (Fig. 24d-f), each containing two fewer aliphatic groups (Fig. 24) than their corresponding congeners (Fig. 24a-c), which were replaced with either bromine or hydrogen. For the most active compound (Fig. 24a), replacing the two t-butyl groups on the  $\text{N}^{\wedge}\text{N}$  ligands with bromine groups (Fig. 24d) led to a significant decrease in inhibition activity, suggesting the importance of the aliphatic group in S100B inhibitor. It should be noted that the higher activities of the complexes (Fig. 24 - a, c, and f) compared to the complexes (Fig. 24 - b and e) suggested that the t-butyl group was superior to the nonyl group in conferring S100B/p53 inhibitory activity. Based on these results, a subsequent series of Ir(III) complexes (Fig. 24g-i) has been synthesised, which contained the 4,4'-ditert-butyl-2,2'-bipyridyl (NN3) ligand identified as being the best  $\text{N}^{\wedge}\text{N}$  ligand in the first round of screening but varied in their  $\text{C}^{\wedge}\text{N}$  ligands (Fig. 24). Among these complexes, the complex in Fig. 24-g bearing the 1-phenylisoquinoline (CN4)  $\text{C}^{\wedge}\text{N}$  ligand emerged as the most potent complex, with 96% inhibitory potency against S100B/p53 at 10  $\mu\text{M}$ . To test whether the potency of the compounds could be further improved by pairing the CN4  $\text{C}^{\wedge}\text{N}$  ligand with different  $\text{N}^{\wedge}\text{N}$  ligands, Ir(III) complexes (Fig. 24j-l) have been designed and synthesised (Fig. 24). However, none of the final rounds of complexes

showed higher activity than the complex (Fig. 24g), indicating the superiority of the NN3 moiety in conferring S100B/p53 inhibitory activity.

The complex in Fig. 24-g has shown desirable photophysical properties including long lifetime, large Stokes shift, and high quantum yield with high photostability *in vitro*. This complex demonstrated a strong co-localization with S100B protein in melanoma cells along with the suppressing tumor growth. It blocked S100B dependent signal transduction and inhibited the migration of melanoma cells. The complex in Fig. 24-g has exhibited strong antiproliferative activity against cancerous A375 cells ( $IC_{50} = 0.14$ ) and showed comparatively lower cytotoxicity against normal LO2 cells ( $IC_{50} = 1.07$ ) [71]. In two separate melanoma mouse models, the complex (Fig. 24-g) suppressed tumor growth and restrained lung metastases with only slight toxicity to mice. Preliminary SAR analysis revealed that the nature of both the N<sup>+</sup>N and C<sup>+</sup>N ligands as well as the identity of the Ir(III) centre are important determinants for biological activity. The complex in Fig. 24-g was identified as a potent first reported theranostic agent with nanomolar potency and selectivity for simultaneously monitoring S100B and suppressing malignant melanoma metastasis *in vitro* and *in vivo* via targeting S100B protein.

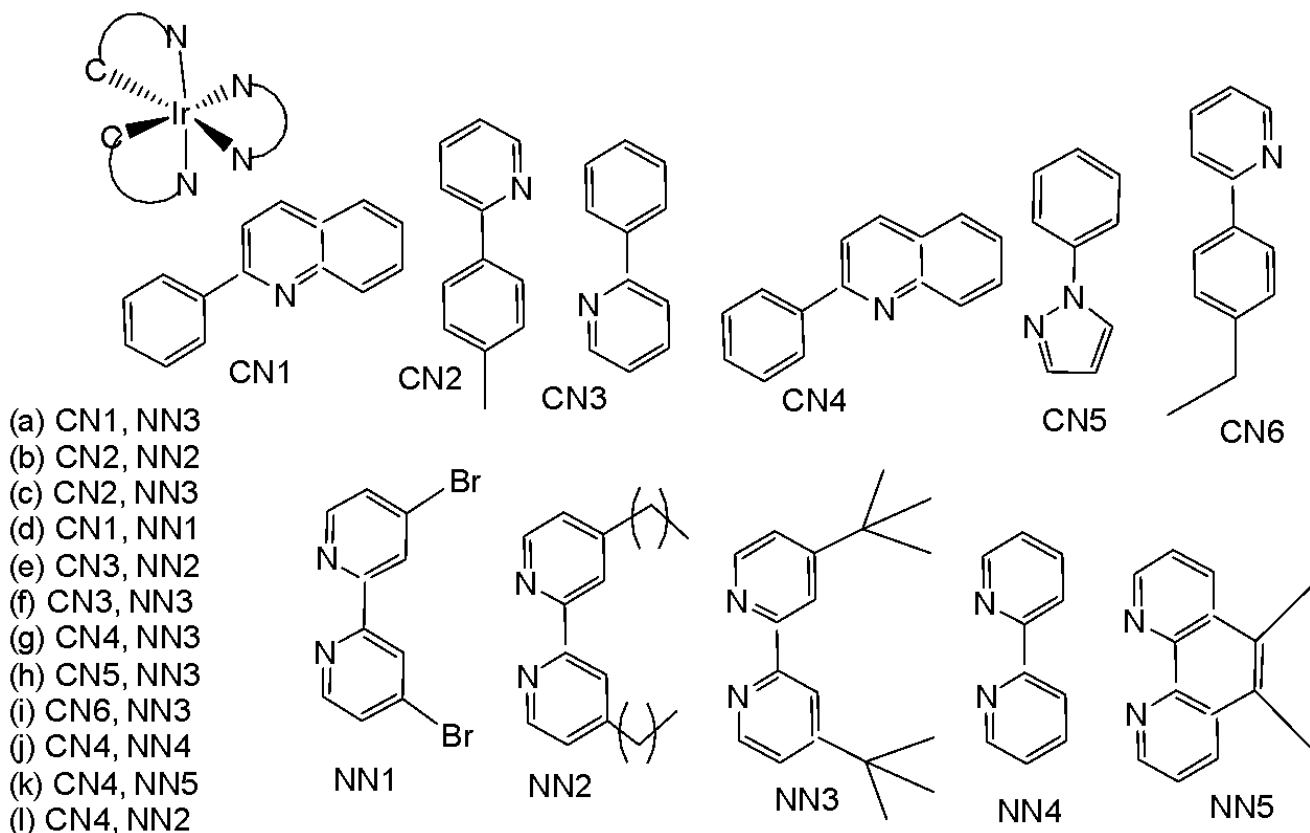


*Fig. (24):* Structures of iridium (III) complexes used for screening against S100B.

Xiang *et al.* have reported cyclometalated iridium(III) complexes for glutathione (GSH) activated targeted chemotherapy and photodynamic therapy (PDT) [27]. The complexes of the types  $Ir(ppy)_2(bpy\text{-CPT})^+$ ,  $Ir(ppy)_2(bpy)^+$ ,  $Ir(pq)_2(bpy\text{-CPT})^+$ ,  $Ir(pq)_2(bpy)^+$ , where CPT = camptothecin, Fig. 25(a-d), have been synthesised and characterized [27]. The cyclometalated Ir(III) complexes were prepared by conjugating phosphorescent iridium(III) compounds with the chemotherapeutic drug CPT via GSH-responsive disulfide bond linkages. Cytotoxicity was evaluated using the MTT assay on HeLa cells under both dark and visible light conditions. The results indicated that the complexes exhibited negligible cytotoxicity toward HeLa cells. These complexes exhibited remarkable imaging capabilities, which were attributed to their inherent fluorescence. It was observed that the disulfide

bond could be cleaved by the high glutathione concentrations present in tumour cells, thereby releasing the free chemotherapeutic drug camptothecin for targeted chemotherapy [27].

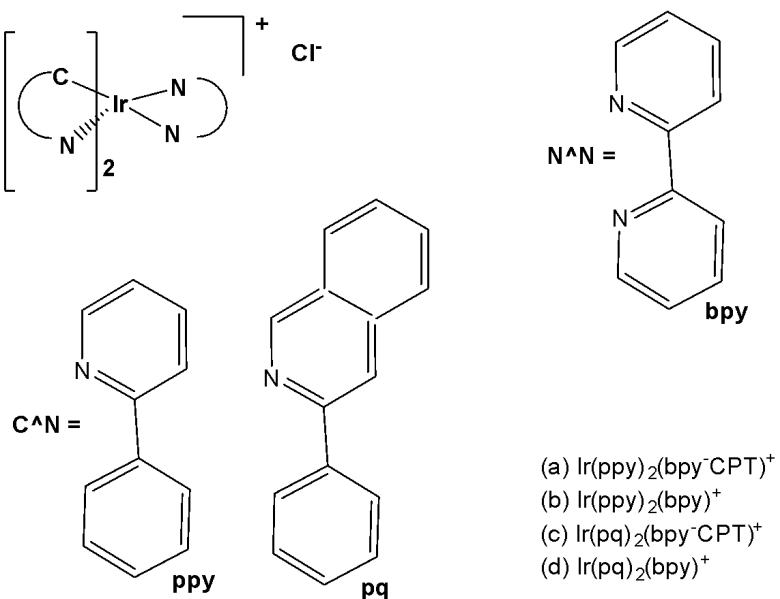


*Fig. (25):* Structures of complexes  $\text{Ir}(\text{ppy})_2(\text{bpy-CPT})^+$ ,  $\text{Ir}(\text{ppy})_2(\text{bpy})^+$ ,  $\text{Ir}(\text{pq})_2(\text{bpy-CPT})^+$ ,  $\text{Ir}(\text{pq})_2(\text{bpy})^+$ .

Sun *et al.* have developed four iridium(III) anthraquinone complexes (Fig. 26) that can be excited *via* two-photon absorption, as hypoxia-sensitive imaging probes [72]. The four mitochondria-specific and two-photon phosphorescence iridium(III) complexes have been prepared by coordinating bridge splitting reactions of the binuclear precursor  $[\text{Ir}(\text{C}^{\text{N}})_2\text{Cl}]_2$ , where the  $\text{C}^{\text{N}}$  ligand was 2-(benzo[d]thiazol-2-yl)anthracene-9,10-dione (AqSN) and the  $\text{N}^{\text{N}}$  ligands (2,2'-bipyridine (Fig. 26a), 1,10-phenanthroline (Fig. 26b), 1,10-phenanthrolinethiazole (Fig. 26c), 1,10-phenanthrolineselenazole (Fig. 26d).

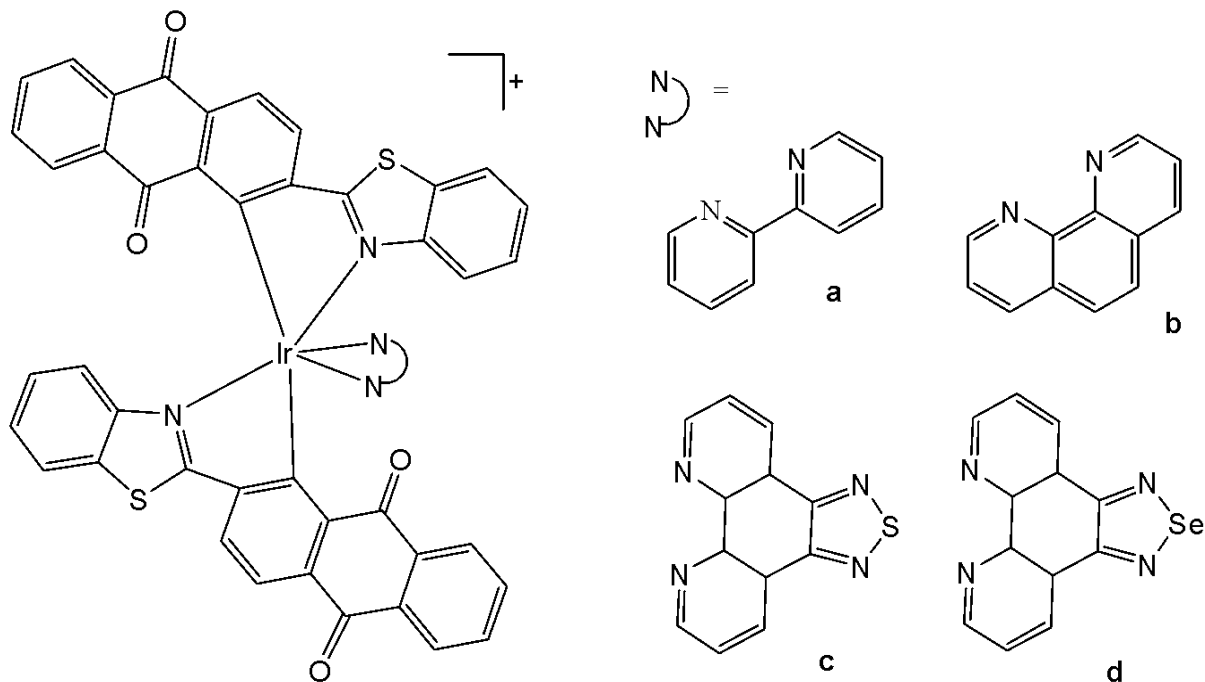


Fig. (26): Iridium(III) anthraquinone complexes.

The iridium(III) complexes (Fig. 26) have two anthraquinone groups as ancillary ligands that are hypoxia-sensitive moieties [72]. The anthraquinone units, as good electron acceptors, are efficient quenchers of the iridium luminescence. However, in hypoxic conditions, it can be converted into the hydroquinone form, thus restoring the emission of the probe [73]. In cells, the ligand could be reduced by the coenzyme nicotinamide adenine reductase phosphate (NAD(P)H) in the presence of cellular reductase [74]. It has been shown that the emission intensity of the complexes (Fig. 26) internalized within A549 cells, rapidly increased following enzymatic reactions with NAD(P)H under hypoxic conditions, without interference from other biological reductants. Moreover, the probes display different sensitivity toward oxygen. All the probes possessed excellent specificity for mitochondria of A549 cells, which allowed imaging and tracking of the mitochondrial morphological changes in a hypoxic environment over a long period of time. They have shown relatively low cytotoxicity with viability values greater than 80 % under both normoxic and hypoxic conditions, after 12 h incubation at a concentration of 10  $\mu$ M. Complexes, shown in Fig. 26, have potential applications for real-time tracking of mitochondrial changes, which offers a new method to recognise mitochondria-related physiological and pathological changes, and possibly offers novel medical strategies for diagnosis.

Du *et al.* have synthesised and reported three Ir(III) complexes  $[\text{Ir}(\text{ppy})_2(\text{adppz})](\text{PF}_6)$  ( $\text{adppz} = 7\text{-aminodipyrdo}[3,2-a:2',3'-c]\text{phenazine}$  and  $\text{ppy} = 2\text{-phenylpyridine}$ ) Fig. 27(a),  $[\text{Ir}(\text{bzq})_2(\text{adppz})](\text{PF}_6)$  ( $\text{bzq} = \text{benzo}[h]\text{quinolone}$ ) Fig. 27(b),  $[\text{Ir}(\text{piq})_2(\text{adppz})](\text{PF}_6)$  ( $\text{piq} = 1\text{-phenylisoquinoline}$ ) Fig. 27(c) [75]. The complexes have shown effective inhibition of the cell colonies. The cytotoxicity *in vitro* of the complexes against A549, HepG2, SGC-7901, BEL-7402 and normal NIH3T3 cells was evaluated by MTT method. The intracellular reactive oxygen species (ROS) levels, mitochondrial membrane potential, intracellular  $\text{Ca}^{2+}$  levels, the release of cytochrome c, the expression of B-cell lymphoma/leukemia-2 (Bcl-2) family protein and apoptosis induced by the complexes have been investigated under fluorescence microscopy. All complexes showed strong inhibitory effect towards selected cancer cells. Their  $\text{IC}_{50}$  values ranged from 1.2  $\mu\text{M}$  – 17.3  $\mu\text{M}$ . The data revealed that these complexes, Fig. 27(a–c) have high ability to inhibit cell growth in A549 cells with very low  $\text{IC}_{50}$  value of

3.2  $\mu$ M, 4.8  $\mu$ M and 1.2  $\mu$ M, respectively. The antitumor *in vivo* trial showed that the complex in Fig. 27(c) can inhibit tumour growth with an inhibitory rate of 76.34 %. The studies on the mechanism of action have indicated that these complexes caused apoptosis in A549 cell via a ROS-mediated lysosomal-mitochondrial dysfunction pathway. In addition, the interaction of the complexes with BSA, was explored. The complexes could also cause DNA damage and inhibit cell growth at G<sub>0</sub>/G<sub>1</sub> phase [75].

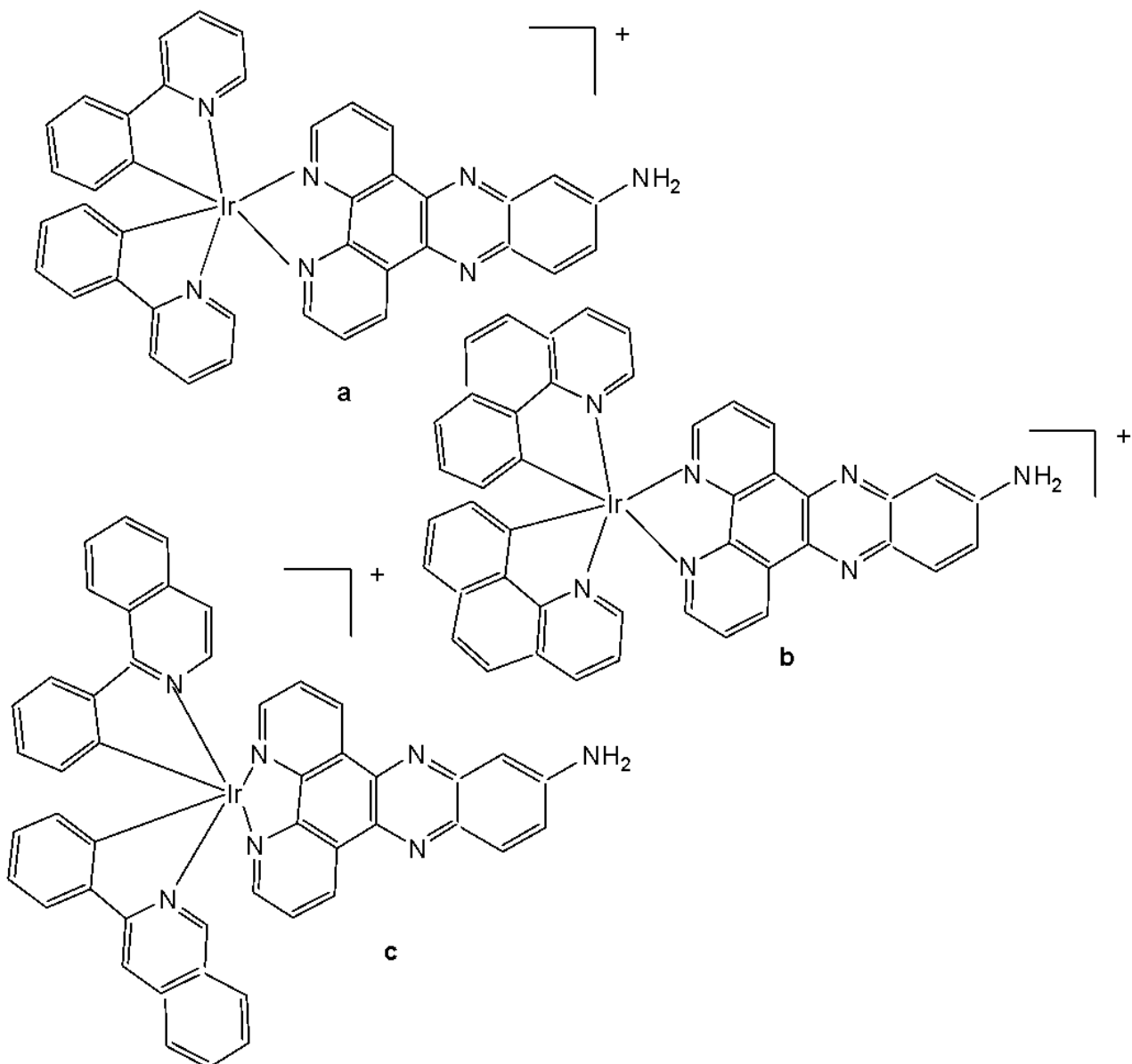


Fig. (27): Ir(III) complexes  $[\text{Ir}(\text{ppy})_2(\text{adppz})](\text{PF}_6)$ ,  $[\text{Ir}(\text{bzq})_2(\text{adppz})](\text{PF}_6)$  and  $[\text{Ir}(\text{piq})_2(\text{adppz})](\text{PF}_6)$ .

Other examples of substitutionally inert Ir(III) anticancer compounds have been reported by Lo and co-workers [76-78]. The authors have prepared a series of biological probes containing inert cyclometalated Ir(III) centers such as those depicted for a biotinyl reagent [76-78]. Luminescent tris(chelate) Ir(III) fragments were connected to substrates (indole, biotin) for biological target molecules via long alkyl chains attached to a polypyridyl ligand (bpy-dppz). Cytotoxicity similar to that of cisplatin was established towards the human cervix epithelial carcinoma HeLa cells and found to correlate with the compounds' lipophilicity. A series of organoiridium(III) polypyridine complexes  $[\text{Ir}(\text{N}^{\text{C}}\text{N})_2](\text{PF}_6)$  of  $\text{HN}^{\text{C}} = 2\text{-phenylpyridine}$ , 1-phenylpyrazole and 2-phenylquinoline with

$N^{\wedge}N$  ligands bearing an alkyl pendant: 4-*n*-octadecylaminocarbonyl-4'-methyl-2,2'-bipyridine, 4-*n*-decylaminocarbonyl-4'-methyl-2,2'-bipyridine and 4-ethylaminocarbonyl-4'-methyl-2,2'-bipyridine, shown in Fig. 28, have been synthesised and characterized [76]. The lipophilicity of the polypyridine complexes  $[\text{Ir}(\text{N}^{\wedge}\text{C})_2(\text{bpy}-\text{C}_n\text{H}_{2n+1})]^+$  ( $n = 18, 10, 2$ ) (Fig. 28) bearing an aliphatic alkyl chain ranged from  $-0.34$  to  $9.89$  [76]. Although efficient internalization of the complexes was supposed to be assisted by high lipophilicity, the most lipophilic complex of this family  $[\text{Ir}(\text{pq})_2(\text{bpy}-\text{C}_{18}\text{H}_{37})]^+$  was taken up the least efficiently by cells. This could be a consequence of it having the largest molecular size and/or undergoing a higher degree of self-aggregation in aqueous solution [76].

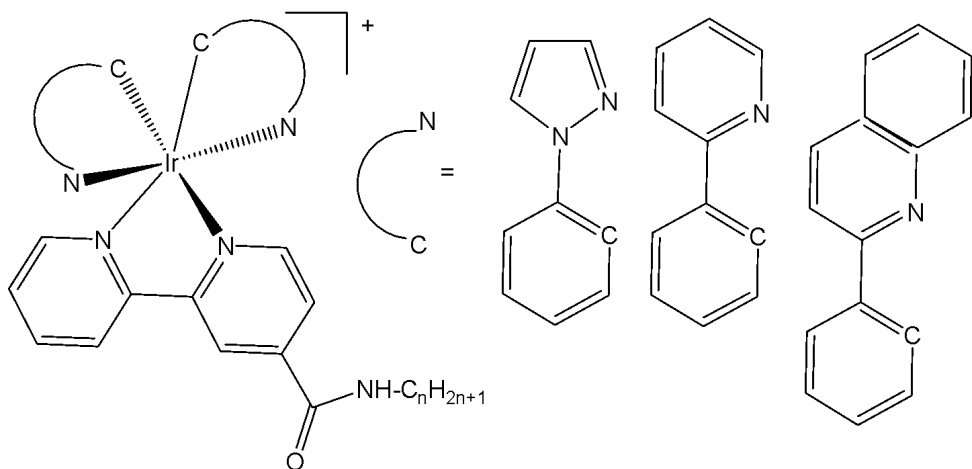
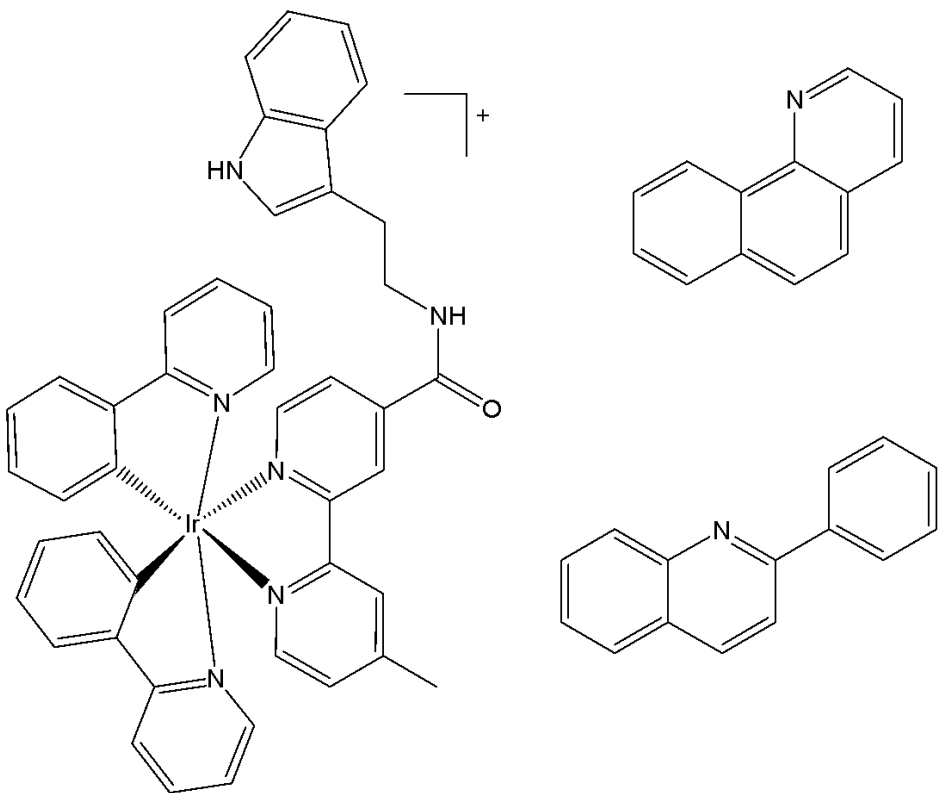


Fig. (28): Structure of the complexes  $[\text{Ir}(\text{N}^{\wedge}\text{C})_2(\text{bpy}-\text{C}_n\text{H}_{2n+1})]^+$ .

A series of luminescent cyclometalated Ir(III) polypyridine indole complexes with the general formula  $[\text{Ir}(\text{N}^{\wedge}\text{C})_2(\text{N}^{\wedge}\text{N})](\text{PF}_6)$ , where  $\text{HN}^{\wedge}\text{C} = 2\text{-phenylpyridine, 7,8-benzoquinoline, 2-phenylquinoline}$  (Fig. 29) and  $\text{N}^{\wedge}\text{N} =$  derivatives of 4-((2-(indol-3-yl)ethyl)aminocarbonyl)-4'-methyl-2,2'-bipyridine have been synthesised, characterized, and their photophysical and electrochemical properties and lipophilicity investigated [77]. Indole is known to bind to bovine serum albumin (BSA). The interactions of the Ir(III) complexes with BSA, have been studied. In addition, the cytotoxic activity of Ir(III) complexes against human cervix epithelioid carcinoma HeLa cell line has been tested. The  $\text{IC}_{50}$  values of Ir(III) complexes, ranging from  $1.1$  to  $6.3 \mu\text{M}$ , were significantly lower than that of cisplatin against HeLa cells [77]. Furthermore, the cellular uptake of the complexes has been investigated by flow cytometry and laser-scanning confocal microscopy [78].



*Fig. (29):* Structure of  $[\text{Ir}(\text{N}^{\wedge}\text{C})_2(\text{N}^{\wedge}\text{N})](\text{PF}_6)$  with  $\text{N}^{\wedge}\text{C}$  = 2-phenylpyridine, 7,8-benzoquinoline, 2-phenylquinoline ligands.

Chen *et al.* have synthesised and reported Ir(III) complexes, shown in Fig. 30(a-d), for tracking mitochondrial dysfunction. These complexes were designed to function by controlling the protonation of the benzimidazole and carboxyl groups. The complexes were tested for cytotoxicity on A549, A549R and Hep-G2 cells and all complexes were found to be non-cytotoxic in the dark, but highly toxic to cells after light radiation [79]. It has been found that the complexes in Fig. 30(b), Fig. 30(c) and Fig. 30(d) could be used in efficient cancer photodynamic therapy. The phototoxicity followed the order: Fig. 30(d) > 30(c) > 30(b) > 30(a). These pH-responsive probes can be used to monitor changes in mitochondrial pH and detect mitochondrial damage during photodynamic therapy (PDT), providing a convenient method for *in situ* assessment of therapeutic effects and treatment outcomes. The studied complexes also generated abundant intracellular ROS, such as  ${}^1\text{O}_2$  and exhibited high phototoxicity against cancer cells (Fig. 30) [79].

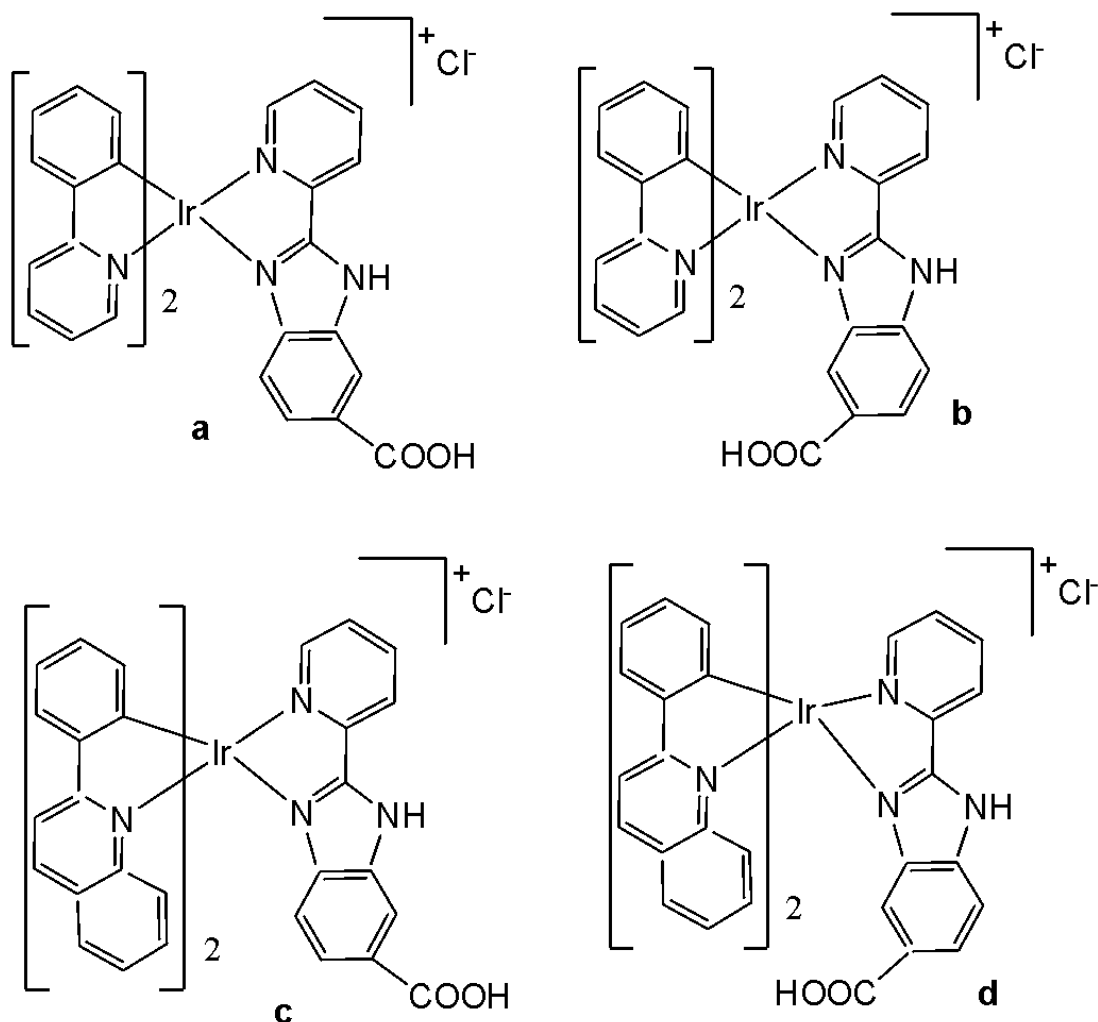
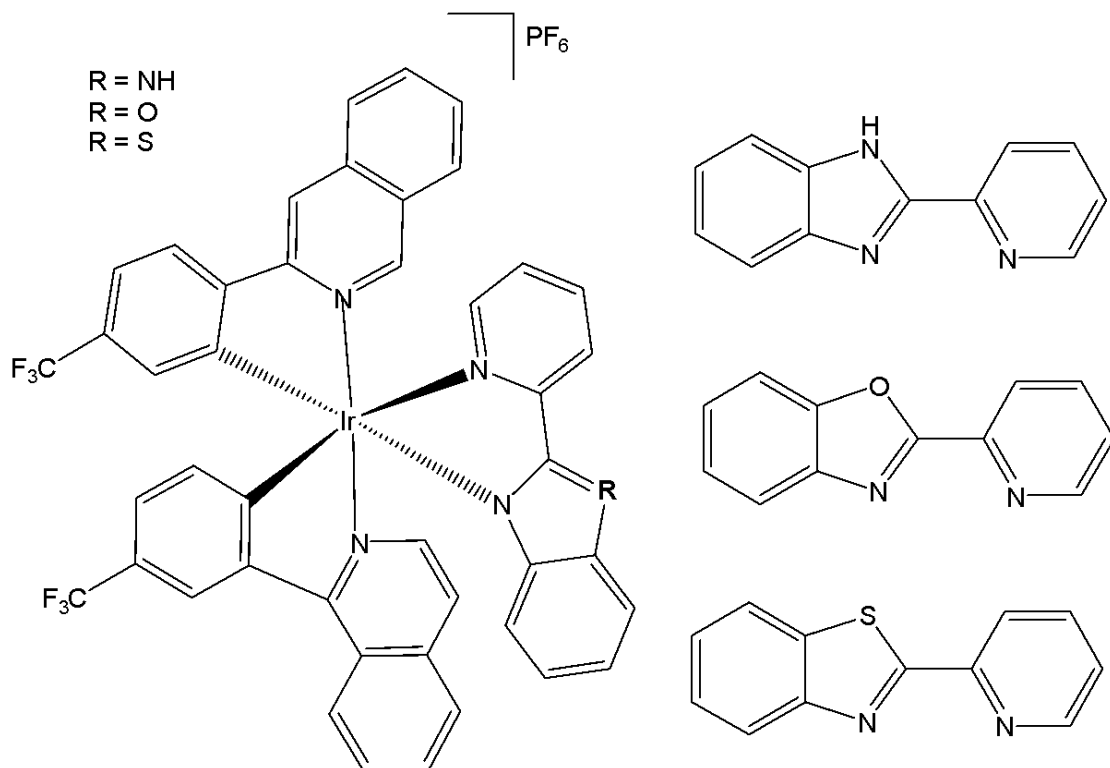


Fig. (30): Isomeric phosphorescent Ir(III) complexes.

Apart from benzimidazole, other ligands of the benzoxazole and benzothiazole type have been studied in the synthesis of new iridium(III) complexes. Novel bicyclometalated octahedral Ir(III) compounds  $[(cf_3piq)_2Ir(N^N)][PF_6]$ , based on two different heterocyclic ligands, have recently been designed [80]. The used C<sup>N</sup> ligand is 1-(4-(trifluoromethyl)phenyl)isoquinoline ((cf<sub>3</sub>piq)), and the variable auxiliary N<sup>N</sup> ligands are 2-(pyridine-2-yl)-1H-benzo[d]imidazole, 2-(pyridine-2-yl) benzo[d]oxazole and 2-(pyridine-2-yl)benzo[d]thiazole (Fig. 31). The structure-property relationships of these complexes have been discussed by spectroscopic, computational, and electrochemical studies. The cytotoxicity of the complexes against A-431, HeLa and SGC-7901 tumour cell lines has been evaluated using the MTT method. The complexes with 2-(pyridine-2-yl) benzo[d]oxazole and 2-(pyridine-2-yl)benzo[d]thiazole have shown better inhibition with respect to 2-(pyridine-2-yl)-1H-benzo[d]imidazole derivative and cisplatin. The introduction of O and S atoms into the secondary ligands has induced increased antineoplastic activity. Microscopic study has shown that 2-(pyridine-2-yl) benzo[d]oxazole and 2-(pyridine-2-yl)benzo[d]thiazole derivatives could enter cells, causing changes in cell morphology, which indicated biocompatibility for bioimaging applications [80].



*Fig. (31):* Ir(III) compounds with 1-(4-(trifluoromethyl)phenyl)isoquinoline ligand and N<sup>N</sup> co-ligands.

Zhang *et al.* have synthesised three Ir(III) complexes with formulas [Ir(ppy)<sub>2</sub>(ipbc)](PF<sub>6</sub>) Fig. 32(a), [Ir(bzq)<sub>2</sub>(ipbc)](PF<sub>6</sub>) Fig. 32(b), [Ir(piq)<sub>2</sub>(ipbc)](PF<sub>6</sub>) Fig. 32(c), containing aldehyde groups, where ppy = 2-phenylpyridine, bzq = benzo [h]quinolone, piq = 1-phenylisoquinoline, ipbc = 4'-(1H-imidazo [4,5-f][1,10]phenanthrolin-2-yl)-(1,10 -biphenyl)-4-carbaldehyde. The antineoplastic activity was investigated by cytotoxicity, apoptosis, cellular uptake, reactive oxygen species, mitochondrial membrane potential, autophagy, cell invasion, cell cycle arrest, intracellular Ca<sup>2+</sup> levels, release of cytochrome c, tubules and western blot analysis [81]. The cytotoxicity studies were carried out by MTT assay with Bel 7402, A549, HeLa and Hep G2 cells in both the dark and light. These complexes have shown no cytotoxicity in dark. However, upon irradiation with white light they showed cytotoxicity towards Bel 7402 and HeLa cells. The complex in Fig. 32(c) showed inhibitory effects on cell growth against all the tested cells. The order of cytotoxicity towards Bel 7402 cells was Fig. 32(a) > 32(b) > 32(c), and was observed that the complex in Fig. 32(b) showed higher cytotoxicity than cisplatin. The IC<sub>50</sub> values of the complexes in Fig. 32(a) and Fig. 32(b) were 5.5 and 7.3 μM. The effect of complexes on mitochondrial membrane potential (MMP) followed the order Fig. 32(c) > 32(b) > 32(a). These complexes increased intracellular ROS and Ca<sup>2+</sup> levels and entered into mitochondria causing decrease in MMP, thus inducing the release of cytochrome c. They inhibited cell invasion and cell growth at S phase, causing apoptosis (Fig. 32).

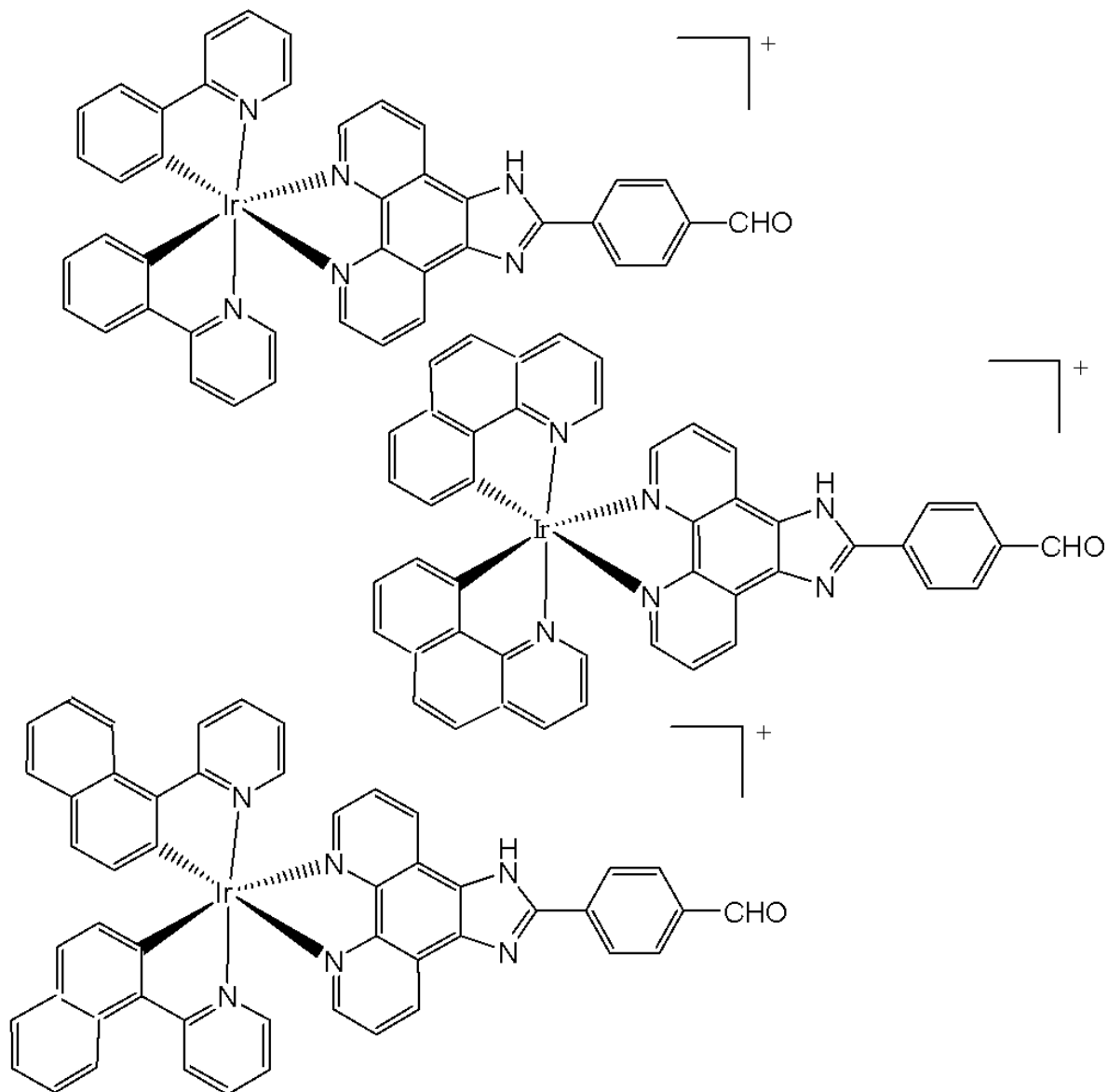
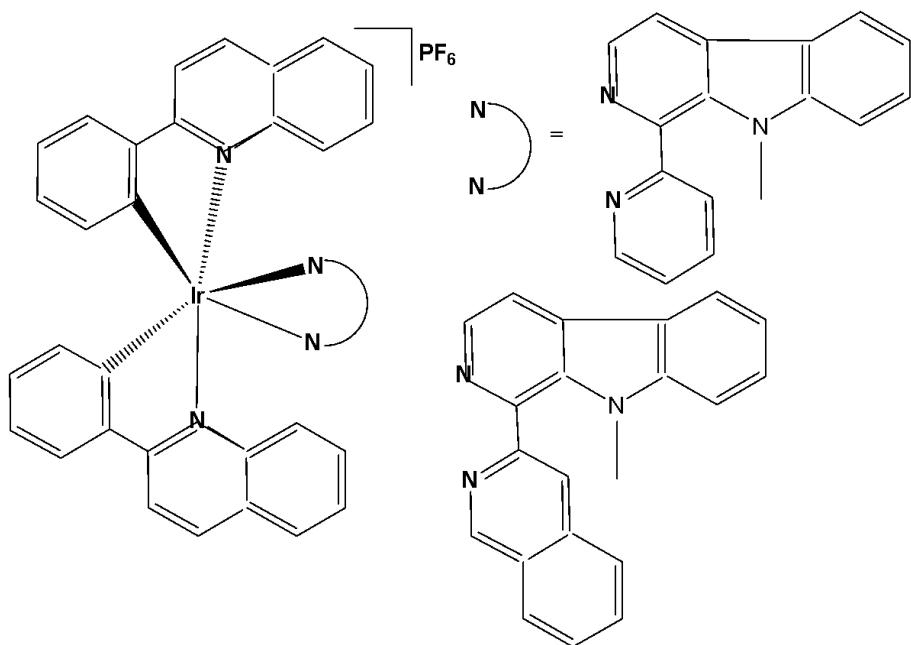


Fig. (32): Structures of  $[\text{Ir}(\text{ppy})_2(\text{ipbc})](\text{PF}_6)$ ,  $[\text{Ir}(\text{bzq})_2(\text{ipbc})](\text{PF}_6)$  and  $[\text{Ir}(\text{piq})_2(\text{ipbc})](\text{PF}_6)$  complexes.

Qin *et al.* have obtained two iridium(III) complexes, Fig. 33(a and b), with  $\beta$ -carboline alkaloid ligands. These complexes showed high potency towards cell lines tested with  $\text{IC}_{50}$  ranging between  $0.52 \mu\text{M}$  and  $1.3 \mu\text{M}$  [25]. The complex in Fig. 33(a) was 97 times more active than cisplatin in lung cancer A549 cells. The complexes were 10 times less cytotoxic towards HLF cells, suggesting selectivity of these complexes towards cancer cells. Both these complexes were effective singlet oxygen photosensitizers (PSs). Studies have shown that they exhibit excellent anticancer activity in the dark, with their antineoplastic effects further enhanced in the presence of light. The complex in Fig. 33(a) could induce intercellular reactive oxygen species levels to overproduce and ATP to fall under dark conditions. In the presence of light, it could specifically be enriched in the mitochondria to damage mitochondrial DNA, increase lipid peroxidation levels and inhibit proteasome activity in cells. The complex in Fig. 33(a) is self-medicated PDT. The photophysical properties of complexes were studied at room temperature in  $\text{CH}_2\text{Cl}_2$ ,  $\text{CH}_3\text{CN}$ , and phosphate-buffered saline. The complexes exhibited two leading absorption bands at  $250\text{--}360 \text{ nm}$  and  $370\text{--}450 \text{ nm}$ , corresponding to inter-ligand transitions and singlet and triplet metal-to-ligand charge transfer transitions, respectively [25]. Overall, it has been demonstrated that these iridium complexes have dual activities of chemotherapy and

photodynamic therapy, which may help to design new metal-based anticancer agents for combined chemo-photodynamic therapy.



*Fig. (33):* Iridium(III) complexes with  $\beta$ -carboline alkaloid ligands.

He *et al.* developed iridium(III)– $\beta$ -carboline complexes that not only caused an increase in ROS in the cell but also triggered the destruction of the cell by an autophagy mechanism. The authors reported the synthesis and anticancer investigations of two red-emitting Ir(III) complexes, shown in Fig. 34a and Fig. 34b, with an N<sup>+</sup>N ligand based on  $\beta$ -carboline [82]. The antineoplastic properties of the two complexes and their ligands were tested against A549, A549cisR, HepG2, HeLa, and Lo2 cell lines by MTT assay. As a result, the complexes outperformed cisplatin in terms of antiproliferative activity against the tested malignant cell lines, and the complex in Fig. 34b was more active than cisplatin in A549cisR cells. A similar study on HepG2 and Lo2 cells revealed that both complexes were more potent in malignant cells. TEM images of A549 cells treated with the complexes in Fig. 34a and Fig. 34b demonstrated the initiation of the autophagic process with the production of autophagic vacuoles and autolysosomes. The interactions between autophagy and the complex in Fig. 34b were investigated using 3-methyladenine, an autophagy inhibitor, to examine the autophagy-inducing mechanism of the complex in Fig. 34b. These findings showed that the complex in Fig. 34b functioned as an autophagy promoter in cancer cells. The complex in Fig. 34b increased ROS levels in A549 cells, and it has been proposed that intracellular ROS play a crucial role in triggering autophagy. Additionally, apoptosis assays showed that the complex in Fig. 34b only induced caspase-independent autophagic cell death, whereas cisplatin-induced cell death was through both apoptotic and caspase-dependent pathways.

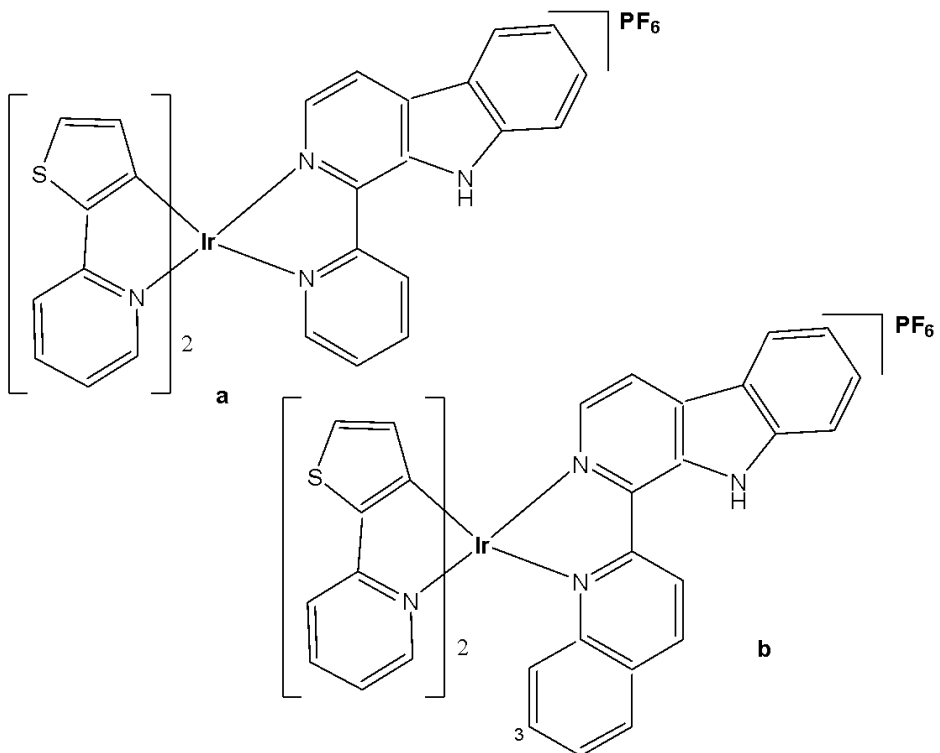
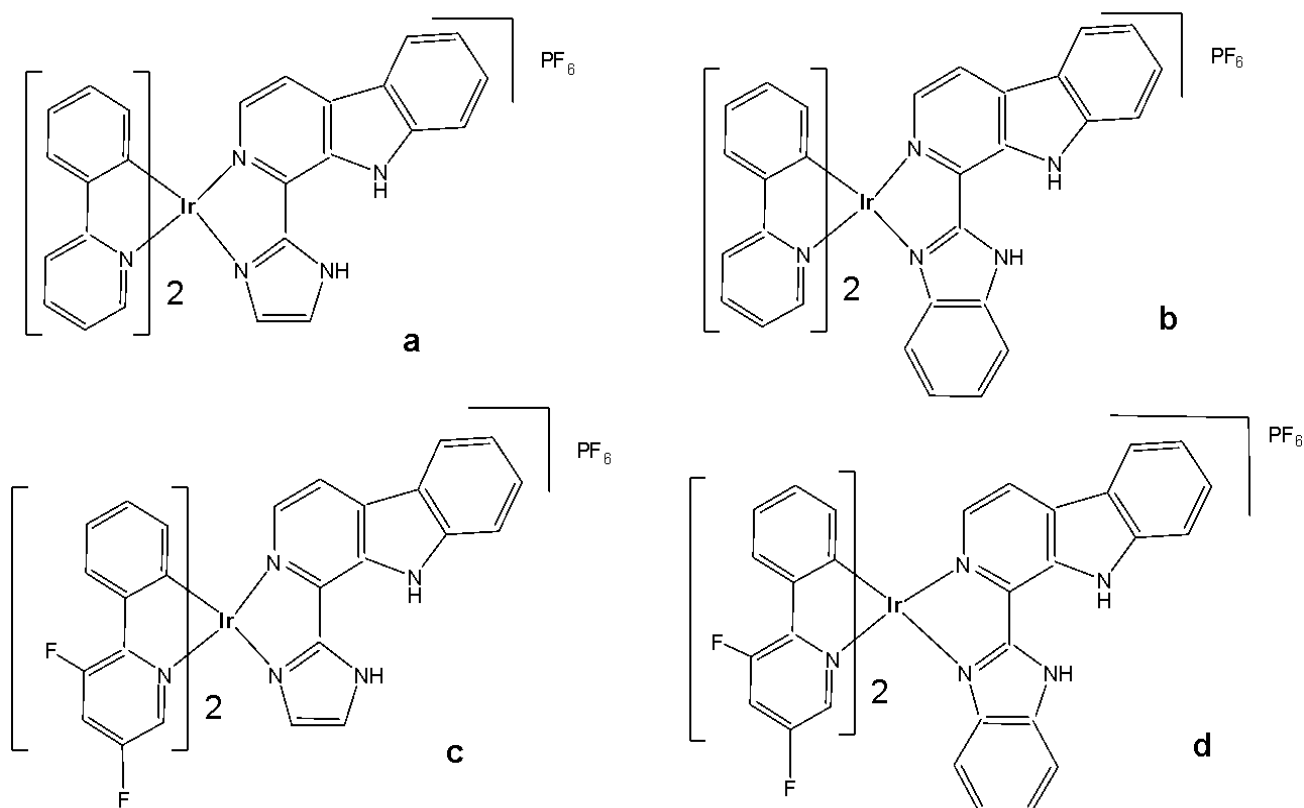


Fig. (34): Iridium(III)- $\beta$ -carboline complexes.

Based on the previous work [42], He *et al.* have reported iridium(III) complexes with  $\beta$ -carboline ligands as pH-responsive tumor/lysosome-targeted PDT agents. Lysosomes (pH 4.5–5.5) contain a variety of hydrolytic enzymes that are capable of degrading almost all kinds of biomolecules. Imidazole and benzimidazole groups, which are known to be important pharmacophores and pH-responsive groups, were introduced to the  $\beta$ -carboline ligands to enhance their selectivity toward cancer cells and sensitivity to acidic environments. Since tumour microenvironments and lysosomes are typically acidic (pH  $\approx$  5–6), this can lead to protonation-driven activation or localization of the studied complexes. Additionally, the dual role of the  $\beta$ -carboline moiety, as both a biological targeting unit and an extended  $\pi$ -conjugated chromophore for light absorption, could be elaborated to emphasize its multifunctional contribution. Ir(III) complexes with the general formula  $[\text{Ir}(\text{N}^{\wedge}\text{C})_2(\text{N}^{\wedge}\text{N})](\text{PF}_6)$  (the complexes in Fig. 35(a-d), where  $\text{N}^{\wedge}\text{C}$  = ppy (2-phenylpyridine) or dfppy (2-(2,4-difluorophenyl)pyridine);  $\text{N}^{\wedge}\text{N}$  = (1-(2-imidazolyl)- $\beta$ -carboline or (1-(2-benzimidazolyl)- $\beta$ -carboline), have been synthesised [43]. The pH-response could be achieved with the introduction of the protonation sites on the imidazole and benzimidazole groups. On the other hand, the selectivity toward acidic environment could be enhanced by the presence of the  $\beta$ -carboline ligand.

The cytotoxicity in the dark and PDT activity of the complexes, Fig. 35(a-d),  $\beta$ -carboline  $\text{N}^{\wedge}\text{N}$  ligands, the dimeric iridium(III) precursors and cisplatin were assessed against human lung carcinoma A549 cells, cisplatin-resistant A549cisR cells, breast cancer MCF-7 cells and human normal liver LO2 cells. The complexes bearing (1-(2-imidazolyl)- $\beta$ -carboline as  $\text{N}^{\wedge}\text{N}$  ligand displayed moderate cytotoxicity in the dark in A549 cells, whereas the  $\text{IC}_{50}$  values determined for the complexes in Fig. 35(a) and Fig. 35(c) were 19.5 and 29.9  $\mu\text{M}$ , respectively. Negligible cytotoxicity in the dark in A549 cells was observed for complexes Fig. 35(b) ( $\text{IC}_{50} \geq 100 \mu\text{M}$ ) and Fig. 35(d) ( $\text{IC}_{50} = 55.6 \mu\text{M}$ ) that incorporated (1-(2-benzimidazolyl)- $\beta$ -carboline ligand. Similar results were also observed in A549cisR, MCF-7 and LO2 cells. The complexes showed similar lipophilicity values (1.97–2.12), with a greater cell penetration for the smaller imidazole-derivatives. In terms of the mechanism of action, it should be noted that the

imidazole-containing complexes (Figs. 35a and 35c) displayed higher cytotoxicity than their benzimidazole analogues (Figs. 35b and 35d), which may correlate with their smaller steric bulk effect and better cellular uptake.



*Fig. (35):* Iridium(III) complexes with 1-(2-imidazolyl)- $\beta$ -carboline or (1-(2-benzimidazolyl)- $\beta$ -carboline ligands.

These complexes showed enhanced phosphorescent emission and ROS generation ( ${}^1\text{O}_2$ ) in tumour/lysosome-related acidic environments ( $\text{pH} \leq 6.5$ ). Complex in Fig. 35(b) displayed remarkable phototoxicity against cancer cells and high selectivity for cancer cells over normal cells. Mechanism studies have shown that complex-mediated PDT in Fig. 35(b) mainly induced caspase- and ROS-dependent apoptotic cell death through lysosomal damage and cathepsin B release. Even if all the complexes localised within the lysosomes, the complex shown in Fig. 35(b) appeared more promising for tracking lysosomal integrity during PDT, providing a reliable and convenient method for *in situ* monitoring of treatment outcomes and therapeutic effects. Stimuli-responsive iridium complexes with longer absorption/emission wavelengths or larger multi-photon absorption cross-sections were likely to be more valuable for the image-guided therapy of deep-seated tumours. Overall, this work provided new insight into the design of multifunctional theranostic phosphorescent metal complexes as intelligent targeted PDT agents that can enhance tumour selectivity and monitor the therapeutic outcome simultaneously [43,44]. Later, the same research group designed new cyclometalated Ir(III) complexes incorporating benzimidazole derivatives as ancillary ligands, which demonstrated dual anticancer activities as both effective photosensitizers (PSs) and metastasis inhibitors [44]. The studied Ir(III) complexes could effectively inhibit several cancerous processes, including cell migration, invasion, colony formation, and angiogenesis.

Guan *et al.* have reported a series of mitochondria-targeting cyclometalated oncosis-inducing cationic Ir(III) complexes with benzothiazole substituted ligands (Fig. 36) and their antitumor cellular

investigation [66]. Oncosis, or “ischemic cell death”, could be referred to a distinct cell-death mechanism, which is a non-apoptotic form of programmed cell death (PCD). It differs from apoptosis in both morphological characteristics and intracellular pathways, and may hold the key to overcoming a significant challenge in cancer therapy – drug-resistance, which often arises from tumours’ intrinsic resistance to apoptosis. All the metal complexes  $[\text{Ir}(\text{ppy})_2(\text{bbtb})]^+$ ,  $[\text{Ir}(\text{DFppy})_2(\text{bbtb})]^+$ ,  $[\text{Ir}(2\text{pq})_2(\text{bbtb})]^+$ , and  $[\text{Ir}(\text{pbt})_2(\text{bbtb})]^+$  possessed two substituted benzothiazole units in the bpy-based N<sup>N</sup> ligand (4,4'-bis(benzothiazole-2-yl)-2,2'-bipyridine (bbtb)) and different common cyclometalating ligands (e.g. ppy, dfppy, pq and pbt). The chemical derivatives were tested against more than 10 cancer cell lines from various body parts including lungs, colon, kidneys, and liver, 10 drug-resistant cancer cell lines as well as two noncancerous cell lines (normal liver cells HL-7702 and normal kidney cells HEK 293). They showed  $\text{IC}_{50}$  values indicating considerable cytotoxicity against various cancer cells and drug-resistant cell lines, with selectivity towards normal cell lines. On the other hand, these Ir(III) complexes were all localised in the mitochondria of A549cisR cells. In contrast to the other typical Ir(III) antitumor agents, the enhanced ROS level was determined not to express the caspase 3/7 activity for the complexes, thus not inducing caspase-dependent apoptosis. In order to probe the origin of oncosis induced by these complexes, the membrane permeability and porin expression were studied in detail. The results confirmed that the Ir(III) complexes activated the oncosis-specific protein porin and calpain in cisplatin-resistant cell line A549R [66].

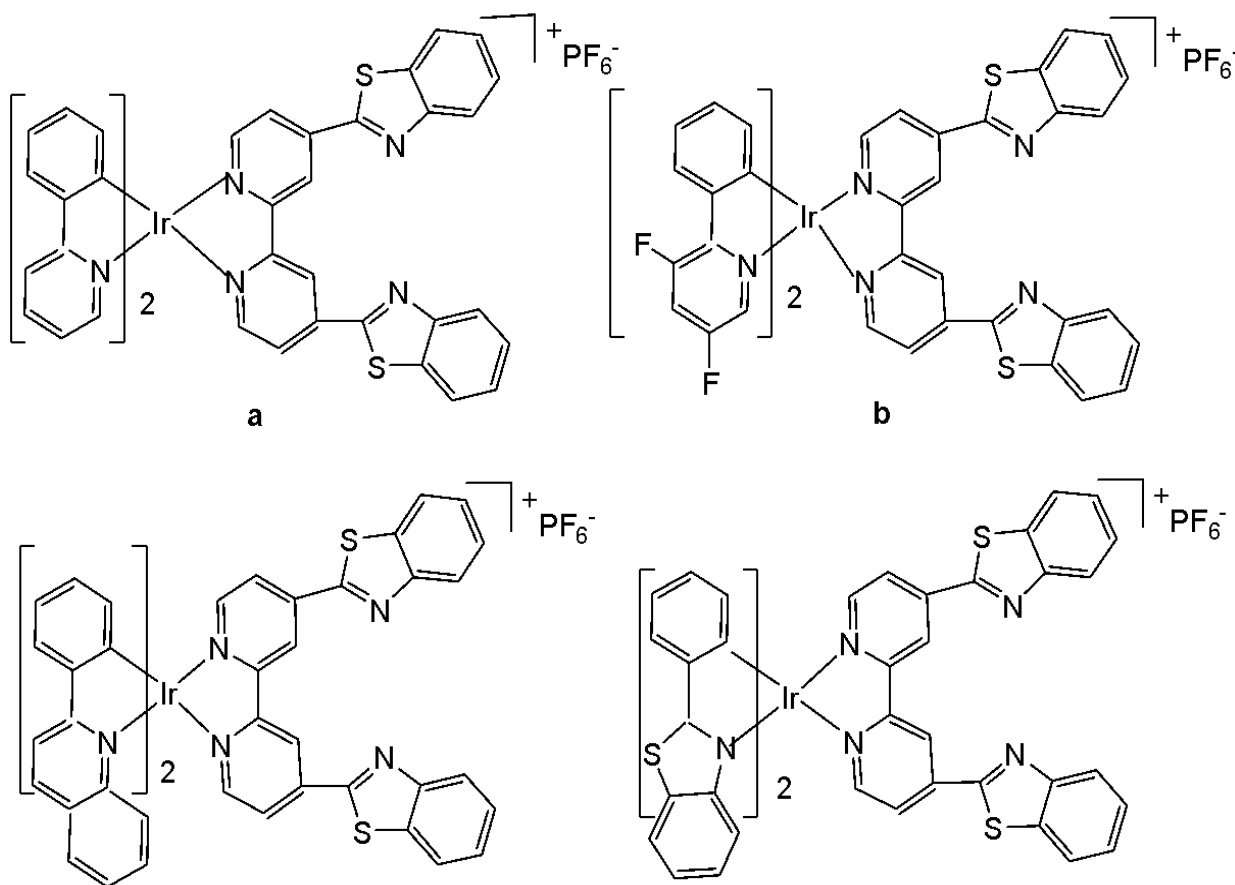
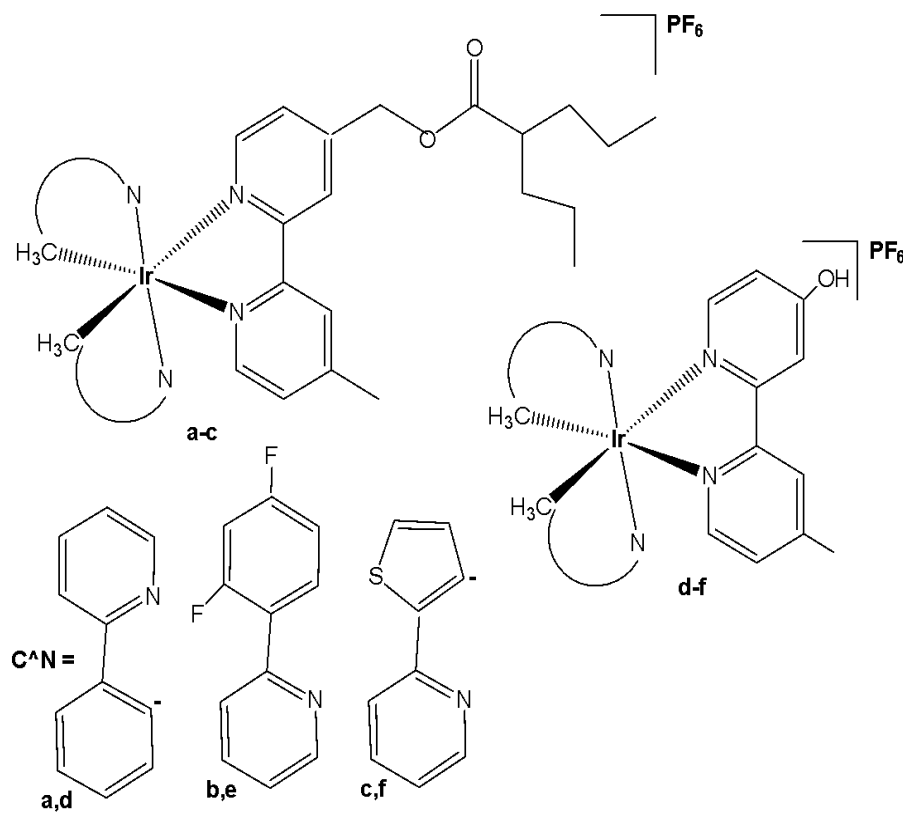


Fig. (36): Ir(III) complexes with benzothiazole substituted ligands.

Ye *et al.* synthesised and reported valproic acid (VPA)-functionalized cyclometalated Ir(III) complexes, Fig. 37(a-f), which exhibited excellent two-photon properties and were highly efficient for live cell imaging [32]. Valproic acid (short-chain, fatty acid) is a histone deacetylase inhibitor (HDACi), which enables cell cycle arrest [83]. By conjugation of valproic acid to Ir(III) complexes

through an ester bond, VPA-functionalized cyclometalated iridium(III) complexes, shown in Fig. 37(a-c) and their analogous complexes Fig. 37(d-f), were designed and synthesised. These complexes displayed excellent two-photon properties, which were favourable for live-cell imaging. The ester bonds in them could be hydrolysed quickly by esterase and display similar inhibition of HDAC activity to VPA. Four groups of entities were used to probe their antiproliferative activity: Ir(III) complexes, hydrolyzed Ir(III) complexes, mixtures of VPA with hydrolyzed Ir(III) complexes, and cisplatin. The order of their antiproliferative efficacy was Fig. 37(a), 37(b), 37(c) > 37(d), 37(e), 37(f). The cytotoxicity studies were determined by MTT assay against human hepatocellular liver carcinoma HepG2, human normal liver cell lines LO2, human cervical carcinoma HeLa and human primary carcinoma A549, with the values for Fig. 37(a) ( $IC_{50} = 1.0 \mu M$ ), for Fig. 37(b) ( $IC_{50} = 0.79 \mu M$ ) and for Fig. 37(c) ( $IC_{50} = 1.3 \mu M$ ), being approximately 70, 89 and 54.5 times more potent than cisplatin against A549R cancer cells. Notably, the VPA-conjugated complexes can overcome cisplatin resistance effectively and are about 54.5–89.7 times more cytotoxic than cisplatin against cisplatin-resistant human lung carcinoma A549R cells. The complexes exhibited 6.6-, 4.4-, and 4.1-fold lower cytotoxicity against LO2 cells, indicating that they possess a certain selectivity toward human tumour cells. Hence, the VPA-conjugation effectively enhanced the anticancer potency of Ir(III) complexes. Mechanistic studies have indicated that iridium(III) complexes, shown in Fig. 37(a-c), penetrated human cervical carcinoma (HeLa) cells quickly and efficiently, accumulated in mitochondria, and induced a series of cell-death-related events mediated by mitochondria. Mechanistic studies of cell death, including ROS level elevation, cell cycle arrest, and caspase-activated apoptosis, indicated that Ir(III) complexes effectively inhibit tumour cell growth [32].



*Fig. (37):* Structures of valproic acid functionalized cyclometalated iridium(III) complexes.

Yuan *et al.* have described iridium complexes (Fig. 38a-c) that target the endoplasmic reticulum, a crucial organelle responsible for protein synthesis, folding, transport, and the maintenance of  $Ca^{2+}$  homeostasis [84]. The synthesis of a series of ER-targeted Ir(III) complexes (Fig. 38a-c) as photodynamic therapy (PDT) photosensitizers, featuring a gradually extended conjugation in the

primary ligand, and the investigation of the relationship between conjugation extent and PDT performance have been conducted. The results have shown that all of the presented complexes could accumulate in the ER and effectively induce cell apoptosis after PDT therapeutics by an ER stress mechanism, and both their singlet oxygen quantum yields and cytotoxicity increased as the conjugation area extended. All complexes showed PDT potency towards different cancer cell lines. Among them, the complex in Fig. 38(b) showed an impressive PI value (94.3) compared to cisplatin against A549 cells with an  $IC_{50}$  down to 0.65  $\mu$ M, acting as an efficient PDT photosensitizer. Studies have shown that post PDT-ER, stress-induced apoptosis accompanied by  $Ca^{2+}$  efflux from the ER occurs, indicating that this complex could be a potential photosensitizer, with apoptosis resulting from severe and prolonged ER stress [84].

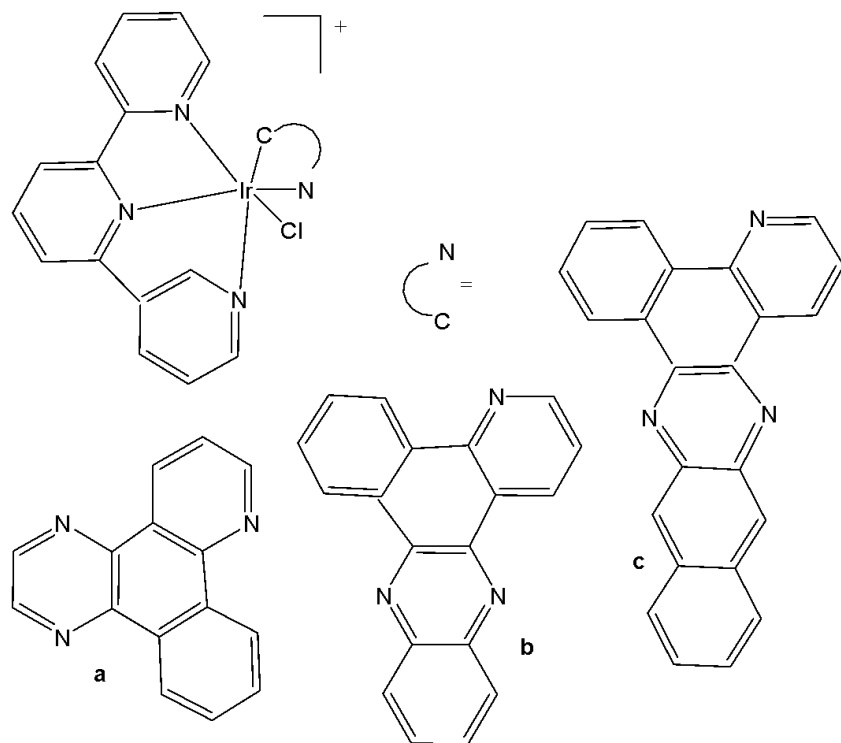
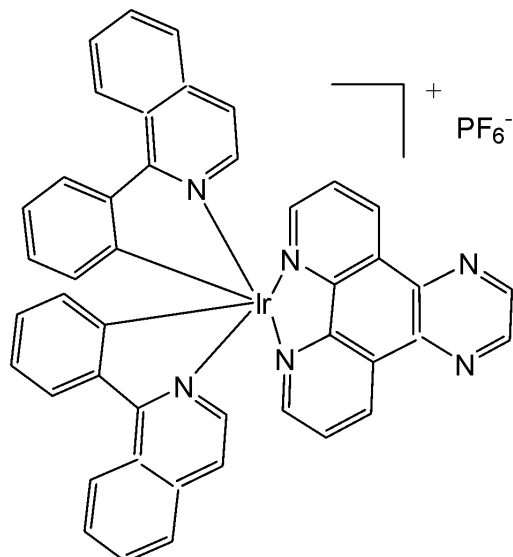


Fig. (38): Structures of terpyridyl ER-targeted Ir(III) complexes.

Zhang *et al.* have obtained novel nanoparticles (NPs) comprising Zr-MOF, a biscyclometalated Ir(III) complex (Fig. 39) and a dual responsive BP-PDM-PG as an antitumor delivery platform [85]. The nanoparticles entered the tumour cells via endocytosis and caused enhanced lysosome escape due to ROS production of the iridium(III) complex. This complex demonstrated efficient PDT, exhibiting red-shifted absorption and emission bands with NIR luminescence, making it highly suitable for real-time cell imaging with an improved signal-to-noise ratio. It also showed good biocompatibility in the dark [85].



*Fig. (39):* Structure of biscyclometalated Ir(III) complex.

The best complementary rational approach to designing Ir(III) complexes with increased activity involves the coordination of ligands that themselves are cytotoxic and that can potentially participate in specific interactions with the biological targets. This approach may also improve the pharmacokinetic properties and bioavailability of the coordinated ligands through factors such as charge modification, enhanced solubility and cellular uptake. The use of the pharmacophore benzimidazole as a ligand has given rise to a wide variety of metal-based compounds that act either as antiangiogenic and/or antitumor agents. The integration of anticancer activity of benzimidazoles into cyclometalated Ir(III) complexes could provide, therefore, an opportunity for the construction of novel theranostic platforms.

It has been reported that biscyclometalated iridium(III) compounds bearing C<sup>N</sup> ligands based on the benzimidazole core were able to photo-potentiate their activity in tumour cells due to a significant enhancement of intracellular ROS [86]. Within the group of Ir(III) organometallic and coordination complexes, the development of small heterocyclic chelating ligands has been carried out successfully to obtain promising metallodrugs with anticancer potency. A series of Ir(III)-based compounds with cyclometalated benzimidazole ligands (Fig. 40) and their cytotoxicity evaluation against epithelial ovarian carcinoma A-2780, A-2780cisR, colon cancer HT-29, breast cancer T-47D cell lines has been reported [87]. Their apoptosis, accumulation, cell cycle arrest, protein binding and DNA binding effects were also discussed. The complexes were synthesised by employing the heterocyclic C<sup>N</sup> ligand 1-butyl-2-phenyl-1H-benzo[d]imidazole-5-carboxylate of methyl. The effects of different substitution (methyl, butyl, benzyl groups) on the benzimidazole nitrogen which modulated the lipophilicity, hydrophilicity and ultimately the cytotoxicity of the metal complexes have been studied. It was found that the phenyl substitution at the C4 position was a determining factor for the SAR analysis. All iridium(III) derivatives of the first series (Fig. 40) were more active than cisplatin towards the A-2780cisR, HT-29 and T-47D lines in the following order Me > Bnz > nBu > cisplatin. The complexes showed high apoptosis, good accumulation and S-phase cell arrest and strongly bonded to HSA at sites I and II and also weakly bonded to DNA at the minor groove.

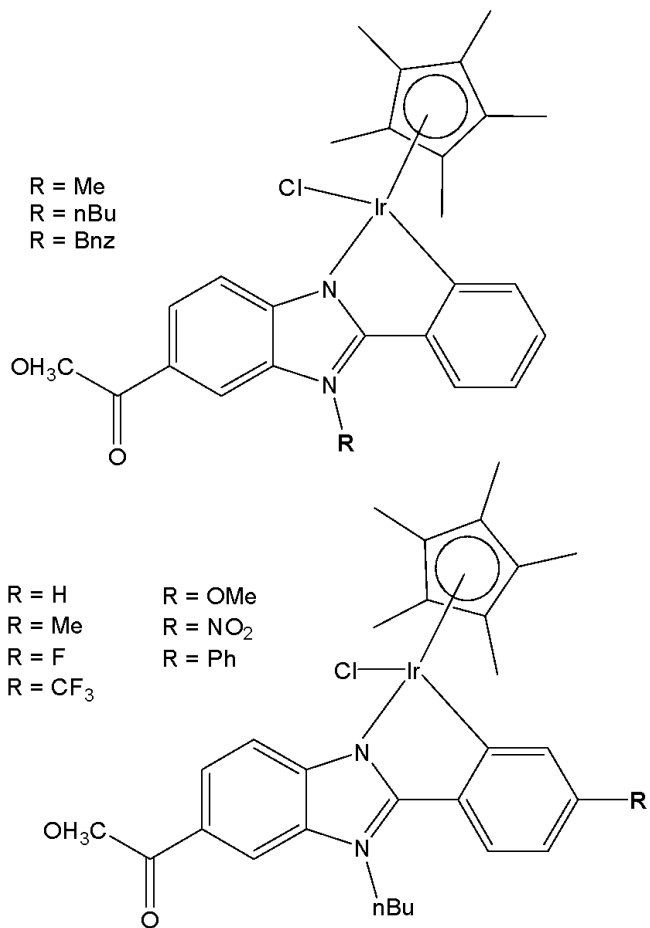


*Fig. (40):* Iridium(III) compounds with cyclometalated benzimidazole ligands.

Another class of various biscyclometalated Ir(III) complexes with imidazole-based ligands of varying alkyl chain length have attracted attention for their stability, biocompatibility, selectivity, and antitumor activity. The attendance of alkyl chains in the ligands of variable size is identified to play a key role in solubility, emission behavior and cell uptake. Some of these derivatives have been alkylated at N1 of the benzimidazole to observe their influence on biological activity. The C<sup>N</sup> ligands 1-nonyl-2-phenyl-1H-benzo[d]imidazole and 1-isopentyl-2-phenyl-1Hbenzo[d]imidazole have been used in the synthesis of octahedral Ir(III) complexes, Fig. 41, [88]. The complexes were found to be luminescent with a moderate emission quantum yield and lifetime in CH<sub>3</sub>CN. The compounds were tested against MCF-7 cancer and MCF-10 normal cell lines. The *in vitro* growth inhibition assay of the complexes with a shorter alkyl chain (complexes of 1-isopentyl-2-phenyl-1Hbenzo[d]imidazole) displayed higher antineoplastic activity (IC<sub>50</sub> < 0.5  $\mu$ M) compared to the complexes with a longer alkyl chain (complexes of 1-nonyl-2-phenyl-1H-benzo[d]imidazole) with IC<sub>50</sub> < 30  $\mu$ M against human breast cancer MCF-7 cells. The flow cytometry assay and fluorescence microscopy analysis suggested that cellular accumulation was primarily responsible for the variation in anticancer activity. Therefore, tuning the anticancer activity and cellular imaging property mediated by the alkyl chain would be of great importance and would be useful in anticancer research. Additionally, some N<sup>N</sup> donating aromatic bidentate ancillary ligands based on 2,2'-bipyridine and 1,10-phenanthroline have also been studied [88]. It has been indicated that there was an obvious relationship between the cellular accumulation and antitumor activity with the size of the alkyl chain existing in the compounds. The alkyl chain variation has allowed not only modulation of antitumor activity, but also of luminescent potential properties.

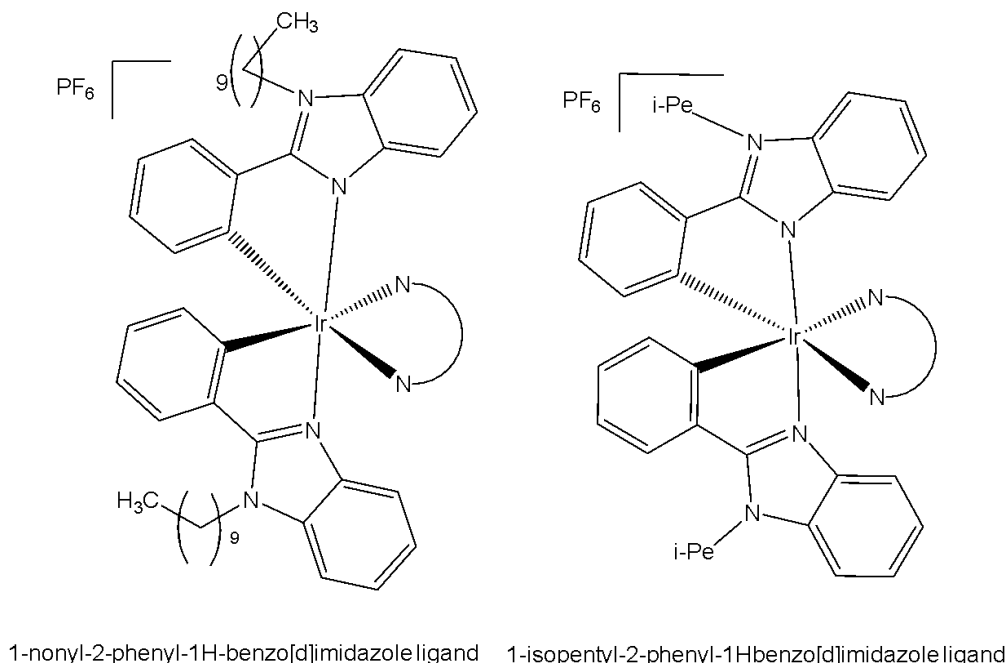


*Fig. (41):* Iridium compounds with two cyclometalated benzimidazole ligands.

Similar to platinum-based drugs, iridium(III) complexes can form adducts with DNA very easily, triggering apoptotic cell death. A series of luminescent biscyclometalated antitumor derivatives of the type  $[\text{Ir}(\text{III})(\text{C}^{\text{N}})^2(\text{N}^{\text{N}})]\text{PF}_6$  of benzimidazole-based  $\text{N}^{\text{N}}$  bidentate ligands with ester and n-butyl groups for their functionalization in C5 and N1 positions have been reported [89]. The complexes had distorted octahedral structures. Two of the  $\text{N}^{\text{N}}$  ligands were attached with a methyl ester as a handle for further chemical functionalization in the future. Different substituents in the ligands have allowed to improve the lipophilic properties of iridium(III) complexes. Iridium(III) complexes with functionalized ligands 2-(pyridine-2-yl)-1H-benzo[d]imidazole, 1-butyl-2-(pyridine-2-yl)-1H-benzo[d]imidazole-5-carboxylate of methyl and 1-butyl-2-(quinoline-2-yl)-1H-benzo[d]imidazole-5-carboxylate of methyl have been synthesised, Fig. 42, [89]. The cytotoxicity tests have been performed with the malignant A-2780, A-2780cisR, MCF-7(ER+) and MDAMB-231 cell lines, as well as the benign BGM cell line. These complexes have exhibited low  $\text{IC}_{50}$  values in the nanomolar order against the ovarian and breast cancer cell lines, some of them being 100 times more active than cisplatin in MDAMB-231. The least active were the iridium(III) complexes with 2-(pyridine-2-yl)-1H-benzo[d]imidazole ligand, because of the lesser lipophilicity of the ligand. Almost all of the compounds have shown low cytotoxicity against normal BGM cells. The bioimaging experiment was performed based on red-emitting complexes and A2780 cells, and it was found that the complexes were predominantly localized in actin cortex, which was a protein-based modulator for cell membrane and cell surface behaviors, as shown by confocal luminescence microscopy. This discovery could open the door to a new large family of drug bioconjugates with diverse and simultaneous functions. In addition, the authors proposed that the higher hydrophobicity probably accounted for their higher anticancer potency against the cancer cells. On the other hand, the ICP-MS analysis of metal contents in nuclear DNA and total cellular RNA in MCF-7 cells revealed the high antineoplastic potency was not associated with the nucleic acids binding, according to the investigation of the metal levels in nuclear DNA and total cellular RNA in MCF-7 cells.

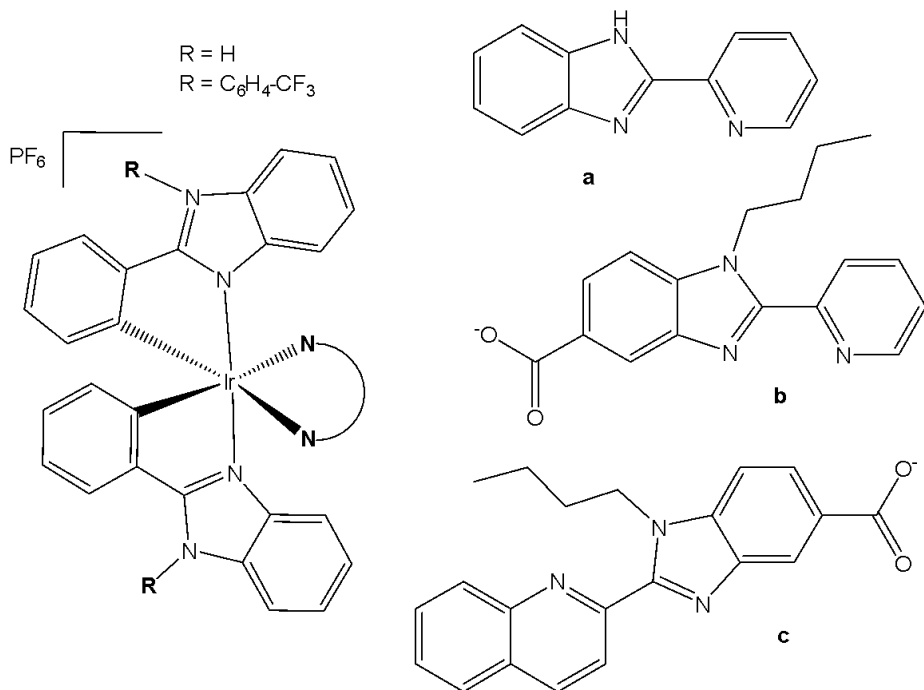
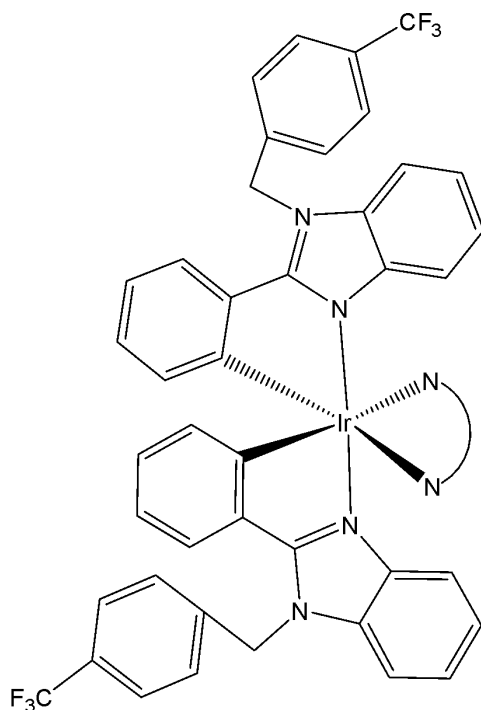


Fig. (42): Iridium compounds with one functionalized 2-(pyridine-2-yl)-1H-benzo[d]heteroazole ligand and N<sup>+</sup>C bidentate co-ligands.

Bicycometalated iridium(III) compounds have displayed good potential as PDT candidates in the treatment of different types of cancer, as shown above. A series of kinetically inert bis-cyclometalated octahedral [Ir(III)(C<sup>+</sup>N)<sub>2</sub>(N<sup>+</sup>N)]PF<sub>6</sub> compounds of 2-phenyl-1-(4-(trifluoromethyl) benzyl)-1H-benzo[d]imidazole (C<sup>+</sup>N) and a second highly aromatic N<sup>+</sup>N donor ligands based on 1,10-phenanthroline, dipyrdo[3,2-*d*:2',3'-*f*]quinoxaline, dipyrdo[3,2-*a*:2',3'-*c*]phenazine, benzo[*i*]dipyrdo[3,2-*a*:2',3'-*c*]phenazine, and dipyrdo[3,2-*a*:2',3'-*c*]phenazine-10,11-imidazolone. The effect of the degree of  $\pi$  conjugation of the polypyridyl ligand on the toxicity in cancer cells has been investigated. The cytotoxic activity of the compounds was evaluated against A-2780, A-2780cisR, HeLa, and MCF-7 tumour cell lines, as well as against the healthy MCF-10A cell line. The less lipophilic compounds with 1,10-phenanthroline and dipyrdo[3,2-*d*:2',3'-*f*]quinoxaline have exhibited an activity greater than that of cisplatin in the tested A2780, HeLa, and MCF-7 tumour cells and showed the lowest level of cellular accumulation. The complexes displayed the capability to overcome acquired and inherent resistance to conventional cisplatin (in A2780cisR and MCF-7 cells, respectively). The results have suggested that a greater cytotoxic potency and less lipophilicity were promoted by decreasing the size of the auxiliary N<sup>+</sup>N ligand. The authors have demonstrated that the Ir(III) complexes, unlike clinically used platinum antitumour drugs, do not kill cells through the DNA damage response. Instead, they killed cells by inhibiting protein translation by targeting preferentially the endoplasmic reticulum. The obtained findings have also revealed that the toxic effect of the Ir(III) complexes could be significantly potentiated by irradiation with visible light (by more than two orders of magnitude). The photo-potentiation of the studied Ir(III) complexes could be attributed to a marked increase ( $\approx$ 10–30-fold) in intracellular reactive oxygen species. Together, these data highlighted the functional diversity of anticancer metal-based drugs and the usefulness of a mechanism-based rationale for selecting candidate agents that are effective against chemo-resistant tumours for further preclinical testing. All compounds have overcome the resistance to cisplatin and have exhibited greater selectivity than cisplatin towards malignant cells with regard to benign ones [90].



*Fig. (43):* Iridium compound with two cyclometalated 2-phenyl-1-(4-(trifluoromethyl)benzyl)-1H-benzo[d]imidazole ligands.

Somatostatin receptor-targeted luminescent iridium(III) biscyclometalated complexes and their hypothetical application as targeted theranostics have been reported [91]. A new series of antitumor complexes  $[\text{Ir}(\text{III})(\text{C}^{\wedge}\text{N})_2(-\text{N}^{\wedge}\text{N})]\text{PF}_6$  (Fig. 44), featuring highly distorted octahedral geometries, have been employed as octreotide peptide-based tumor-targeting vectors to investigate their potential as theranostic agents [91]. In the studied highly cytotoxic and luminescent Ir(III) complexes, the  $\text{C}^{\wedge}\text{N}$  ligand 1-phenylpyrazole was conjugated with  $\text{N}^{\wedge}\text{N}$  ligands, 1-butyl-2-pyridyl- benzimidazole-5-carboxylate derivatives. Their cytotoxic effects against HeLa and MDA-MB-231 cells have been investigated. Methyl-substituted derivative has displayed higher antiproliferative activity, and it has been found that visible light irradiation led to a slight enhancement in  $\text{IC}_{50}$  values. The attachment of the Ir(III) complex to octreotide (OCT) was designed through the formation of an amide bond between a carboxylic function in the benzimidazole diimine ligand and the N-terminal end of the peptide sequence. Besides octreotide, the authors have also selected a dicarba analogue, since the replacement of the disulfide bond by a  $\text{CH}_2-\text{CH}_2$  linkage increased stability in the reductive cellular environment without significantly altering the binding affinity for somatostatin receptors. Conjugation of Ir(III) derivative ( $\text{R} = \text{H}$ ) with the peptide moieties octreotide (OCT-S or OCT- $\text{CH}_2$ ) correlated with its accumulation since peptide vehicles were non-cytotoxic and the cytotoxicity was increased in all cases upon visible light irradiation and ROS production was confirmed [91].

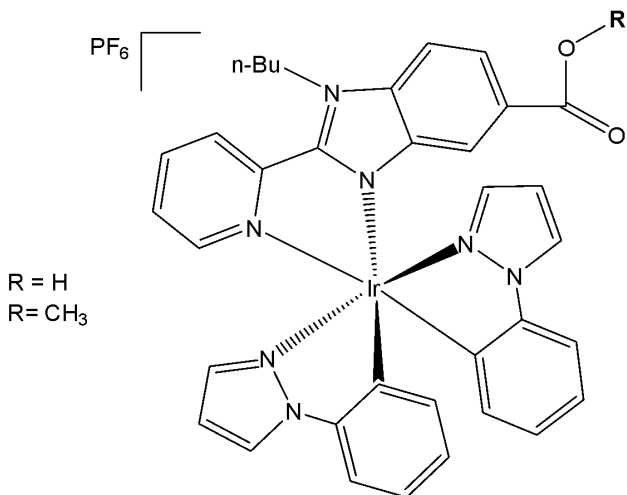


Fig. (44): Iridium compounds conjugated with octreotide peptides.

#### IV. OTHER IRIDIUM(III) COMPLEXES

##### 4.1. Cyclopentadienyl Iridium Complexes

The half-sandwiched organo-iridium cyclopentadienyl anticancer complexes with cyclometalating agents and a chloride as a monodentate ligand are the most popular. Only some specific representatives of them are presented in this review. Hartinger *et al.* have reported that unstable dithio- and diselenobenzoquinones could be trapped by coordination to an  $[(\eta^5\text{-C}_5\text{Me}_5)\text{Ir}]$  moiety thus resulting iridium complexes with anticancer activity, comparable to cisplatin [92]. The  $\{\text{Cp}^*\text{Ir}\}$  fragment ( $\text{Cp}^* =$  pentamethylcyclopentadienyl) is a stabilizing entity for isolation of reactive intermediates, often used for the synthesis of successful organometallic linkers to construct functional coordination assemblies. Quinones play an important role in scavenging of reactive oxygen species, in electron transport in the respiratory chain and photosynthesis. Their potential uses as anticancer drugs and central components of antibiotics have been investigated [93,94]. In contrast to benzoquinone, only a few quinones with heavier chalcogen elements have been reported, due to their inherent instability. The biological action of quinones is often linked to their electron-transfer rates and redox behavior. The replacement of the oxygen atoms in quinone by the heavier chalcogen atoms, sulfur or selenium, leads to highly reactive intermediates with functional groups  $\text{C}=\text{E}$  ( $\text{E} = \text{S}, \text{Se}$ ) [95]. It is noteworthy, that selenium is an essential dietary component for many living systems, and there is increasing evidence for the efficacy of certain forms of selenium as cancer-chemopreventive compounds.

In order to increase the stability of chalcogen-benzoquinone species, the  $[(\eta^5\text{-C}_5\text{Me}_5)\text{Ir}]$  fragment has been introduced to the reactive dithio- and diseleno-benzoquinone species, leading to the isolation of the iridium complexes  $[\text{Ir}(\eta^4\text{-C}_6\text{H}_4\text{E}_2)(\eta^5\text{-C}_5\text{Me}_5)]$ , Fig. 45(a–c), [92,95]. The first stable  $\eta^4$ -diseleno-p-benzoquinone complex,  $[\text{Cp}^*\text{Ir}(\eta^4\text{-C}_6\text{H}_4\text{Se}_2)]$ , has been isolated by Amouri *et al.* [95]. The X-ray structure confirmed the coordination of the elusive diselenobenzoquinone intermediate. The structure of diseleno-iridium complex (Fig. 45c) clearly showed that the  $\text{Cp}^*\text{Ir}$  moiety coordinated to only four diene carbons of the  $\pi$ -selenoquinone ligand. Inspection of the crystal packing in the complex (Fig. 45c) showed that the individual diselenoquinone molecules exhibited  $\pi$ – $\pi$  interactions between the  $\eta^5\text{-}\{\text{Cp}^*\text{Ir}\}$  moiety and the  $\text{Se}=\text{C}$  unsaturated bonds in the  $\eta^4\text{-}(\text{SeC}_6\text{H}_4\text{Se})$  unit of another selenoquinone complex, thus providing a one-dimensional supramolecular chain along  $a$  axis. Spectroscopic and structural data supported stabilization of the complex by metal-to-ligand  $\pi$ -backbonding.

The anticancer activity of this complex was compared to the related O and S analogues. The dithiobenzoquinone complexes, Fig. 45(a–c), have shown moderate cytotoxic activity toward A2780 cells, whereas the diselenobenzoquinone complex in Fig. 45(c), which contained the trapped unstable p-diselenobenzoquinone moiety, with  $IC_{50} = 5 \mu\text{M}$ , was as active as cisplatin ( $IC_{50} = 3 \mu\text{M}$ ), although its mode of action is probably quite distinct. Indeed, the high cytotoxicity of the diselenobenzoquinone complex in Fig. 45(c) illustrates the role of selenium as an important element to combat cancer, and paves the way for the preparation of other functionalized selenoquinone metal complexes with medicinal properties. Modest cytotoxicity ( $IC_{50} = 49 \mu\text{M}$  and  $154 \mu\text{M}$ ) was established for the  $\text{Cp}^*\text{Ir}(\text{III})$  complexes of o- and p-dithiobenzoquinone. Nevertheless, these sandwich complexes, Fig. 45(a–c), [92,95], were found to be highly potent towards A2780 cells, in striking contrast to its inactive p-benzoquinone Ir(III) analogue. Contrary to other iridium anticancer drugs described above, which were hypothesized to act by DNA targeting, the benzoquinone complexes acted in a mechanism similar to that of menadione. Although the mode of action of the benzoquinone complexes was not investigated, it seems probable that rapid release of Se or Se-containing metabolites will be responsible for the potency of the p-diselenobenzoquinone complex.

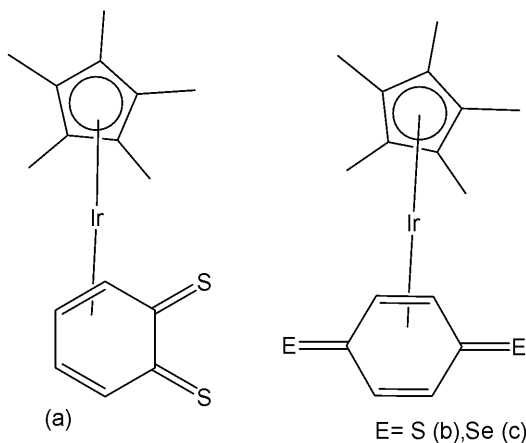


*Fig. (45):* Iridium compounds of dithio- and diselenobenzoquinones.

The low-spin  $5d^6$  organo-iridium complexes with N,N-chelating agents and a chloride anion have been found to be highly unstable toward aquation but inactive as antineoplastic agents [96,97]. The cyclometalated complexes  $[\text{Ir}(\text{N}^{\text{A}}\text{C})(\eta^5\text{-C}_5\text{Me}_5)\text{Cl}]$  with  $\text{C}^{\text{A}}\text{N}$  ligands, such as 2-phenylpyridine, 2-(p-tolyl)pyridine, 2-phenylquinoline, 2-(2,4-difluorophenyl)pyridine, Fig. 46(d–g), have shown high activity toward A2780 human ovarian cancer cells with  $IC_{50}$  values ranging from 2.5 to  $10.8 \mu\text{M}$ , which are comparable to that of cisplatin ( $1.2 \mu\text{M}$ ) [96]. The  $\text{N}^{\text{A}}\text{O}$  complex  $[\text{Ir}(\text{N}^{\text{A}}\text{O})(\eta^5\text{-C}_5\text{Me}_5)\text{Cl}]$  with 1,2-naphthoquinone-1-oximato ligand (Fig. 46h) exhibited much higher cytotoxicity toward HUVEC, HeLa, and HL60 cancer cell lines compared to cisplatin [98]. The remarkable cytotoxicity of this complex has been attributed to necrotic cell death. The  $\text{N}^{\text{A}}\text{O}$  complex  $[\text{Ir}(\text{N}^{\text{A}}\text{O})(\eta^5\text{-C}_5\text{Me}_5)\text{Cl}]$  with quinolin-8-ol (Fig. 46i) was not only cytotoxic toward SK-Mel, SNB-19, and C-32 cancer cells, but also active against Gram-positive bacteria including *M. luteus*, *S. aureus*, *E. faecalis*, and *S. epidermidis* [99]. The use of extended planar diimine ligands allowed the synthesis of organometallic complexes with the formula  $[\text{Ir}(\text{N}^{\text{A}}\text{N})(\eta^5\text{-C}_5\text{Me}_5)\text{Cl}]^+$ , Fig. 46(j–l), to initially intercalate into the base pairs of double-stranded DNA, which was followed by substitution of the labile chloride ligands by the N7 atom of purine bases [100,101]. Complexes were potent cytotoxic agents towards the human cancer cell lines MCF-7 and HT-29 and the *in vitro* cytotoxicity of the chlorido complexes was dependent on the size of the polypyridyl ligands. The dipyridophenazine (dppz) complex in Fig. 46k exhibited high cytotoxicity toward MCF-7 and HT-29 cells with  $IC_{50}$  values 2.3 and  $7.4 \mu\text{M}$ , respectively, similar to those of cisplatin (2.3 and  $7.0 \mu\text{M}$ , respectively).

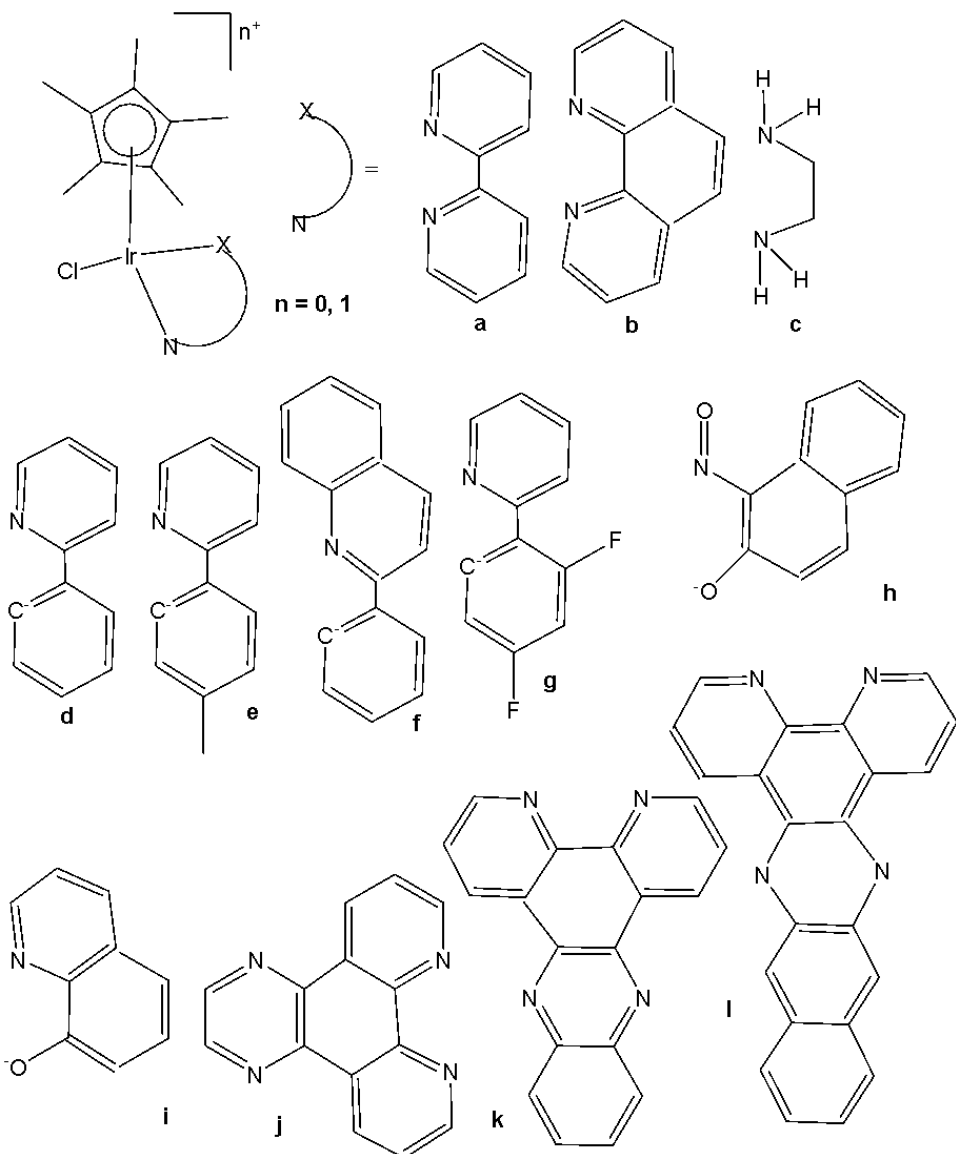
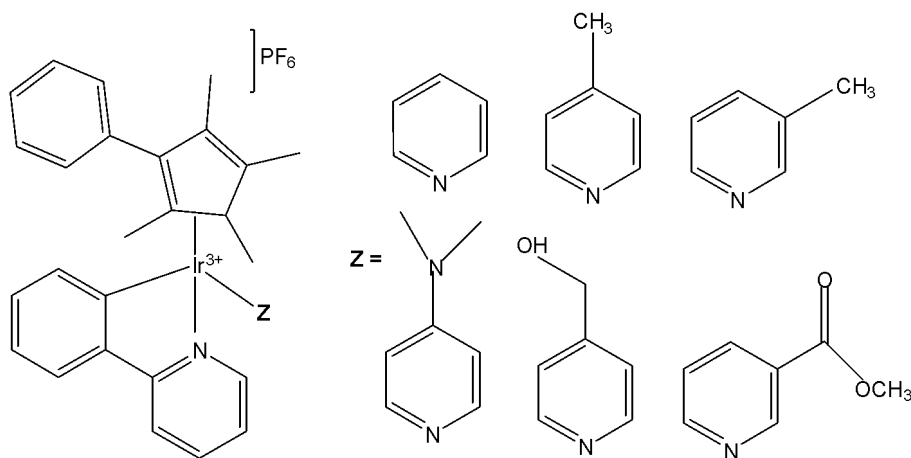


Fig. (46): Cyclopentadienyl iridium complexes with  $N^N$ ,  $N^C$  and  $N^O$  cyclometalating ligands.

The obtained results of the activity of cyclopentadienyl iridium complexes with pyridine derivatives encouraged many scientific groups to explore the activity of complexes containing different  $N^N$ ,  $N^C$  and  $N^O$  cyclometalating ligands. These half-sandwiched cyclopentadienyl iridium(III) complexes contained  $Cp^{xph}$  ( $Cp^{xph} = C_5Me_4C_6H_5$  or tetramethyl-(phenyl)cyclopentadienyl) and  $C^N$ -bound 2-phenylpyridine (phpy) as the cyclopentadienyl and chelating ligands, and various pyridine derivatives as monodentate ligands  $Z$  (Fig. 47) [102]. The half-sandwich Ir(III) coordination compounds of the type  $[(\eta^5-Cp^{xph})Ir(\text{phpy})Z]\text{PF}_6$ , where  $Z = \text{pyridine or its derivatives}$ , have been synthesised and characterized. Their antiproliferative activity toward A2780 human ovarian, A549 lung, and MCF-7 breast cancer cells has been investigated. All the complexes displayed high potency toward the tested human cancer cells, comparable and higher than that of cisplatin, thus being potent anticancer agents according to their *in vitro* studies. The antineoplastic activity could be adjusted by varying the pyridine-based ligands. The  $IC_{50}$  values of the complexes were less than that of cisplatin suggesting that all these complexes were highly active. The complex containing a 4-dimethylamine substituent on pyridine with  $IC_{50}$  value  $0.20\ \mu\text{M}$  towards MCF-7 cell line was the most active (4–5 times more potent than cisplatin) with sub-micromolar activity in a wide range of cancer cell lines, particularly against leukemia, CNS cancer, colon cancer, and breast cancer [102]. In general,

complexes containing electron withdrawing groups on pyridine ring have shown less anticancer activity compared to complexes with electron donating groups. The antiproliferative investigations have shown that N,N-dimethylpyridin-4-amine (electron-donating) demonstrated an increased activity in the cell growth inhibition. Meanwhile, the high cytotoxicity of the complexes was attributed to the promotion of generation of intracellular ROS and the resultant collapse of mitochondrial membrane potential.



*Fig. (47):* Ir(III) tetramethyl-(phenyl)cyclopentadienyl complexes with 2-phenylpyridine

#### 4.2. Other Iridium(III) Complexes

Four cyclometalated iridium(III) complexes, shown in Fig. 48(a-d), with 2,4-diamino1,3,5-triazine derivatives with the general formula  $[\text{Ir}(\text{dfppy})_2(\text{py})_2(\text{L})]^+$ , where dfppy = 2-(2,4-difluorophenyl)pyridine and L = 6-(pyridin-2-yl)-1,3,5-triazine-2,4-diamine, Fig. 48(a); 6-(isoquinolin-1-yl)-1,3,5-triazine-2,4-diamine, Fig. 48(b); 6-(quinolin-2-yl)-1,3,5-triazine-2,4-diamine, Fig. 48(c); 6-(isoquinolin-3-yl)-1,3,5-triazine-2,4-diamine, Fig. 48(d), have been described by Xiong *et al.* [103]. The mitochondria-specific target, cellular uptake and antitumor activity, as well as cell-cycle arrest and apoptosis signaling pathways of the compounds were investigated. The studies were carried out using MTS kit on various cancer cell lines which included MCF-7, NCI-H460, HePG2, Bel-7402, HCT-116, HeLa, A549 and cisplatin resistant cell line A5649R. The cytotoxicity results revealed that the complex 17(a) had activity comparable with cisplatin whereas the complexes in Fig. 48(b) and Fig. 48(c) showed higher cytotoxicity. Interestingly, the complex in Fig. 48(d) which is the isomer of Fig. 48(b) and Fig. 48(c) showed excellent activity towards many of the tested cell lines. Further studies have shown that the complexes had higher selectivity towards tumour cell lines than normal cell lines which was attributed to the mechanism of entering the cell which was different for both cancer and normal cell lines. The complexes in Fig. 48(a) and Fig. 48(b) showed higher selectivity whereas these in Fig. 48(c) and Fig. 48(d) showed selectivity almost similar to cisplatin. All these complexes could generate reactive oxygen species, and induce apoptosis by mitochondrial dysfunction [103]. As evidenced by ICP-MS, energy-independent pathway was the cellular uptake mechanism for LO2 cells while all the complexes were taken up by A549R cells via energy-dependent pathway. Moreover, the intracellular iridium amounts as well as the distribution of localisation of the complexes in A549R were similar.

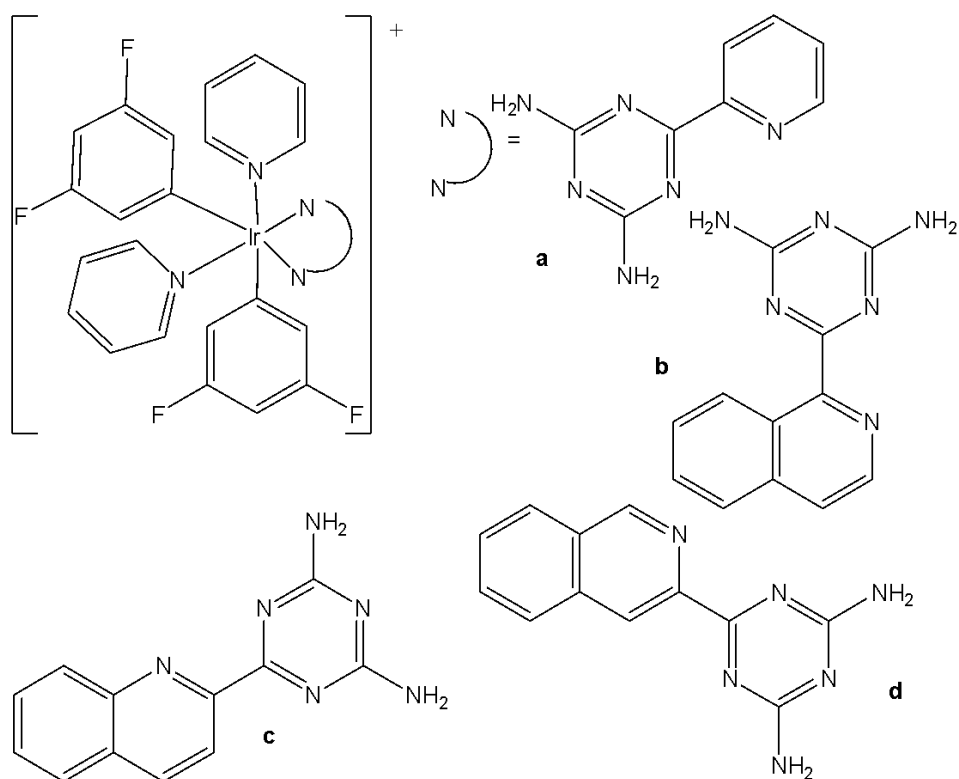


*Fig. (48):* Structures of Ir(III) complexes  $[\text{Ir}(\text{dfppy})_2(\text{py})_2(\text{L})]^+$ .

A range of substitutionally inert metal complexes, bearing unprotected maleimide moieties, have been specifically designed as structural analogues of known organic anticancer drugs or as topographically suitable substrates for enzyme active sites [104,105]. In the absence of redox activity, their mechanism of action must be based on non-covalent interactions such as p-stacking (intercalation) or hydrogen bonding to target molecules. Chemically inert noncytotoxic metal complexes are promising scaffolds for targeting enzyme active sites, which may allow them to serve as enzyme inhibitors. Meggers and co-workers have reported phototoxic activity for (diene)Ir(III) complexes, which contain a trans sited chelating pyridocarbazole ligand, originally designed as protein and lipid kinase inhibitors [104]. The studied pyridocarbazole complexes  $[\text{Ir}(\text{pcz})(\text{cod})(\text{X})(\text{Y})]$ , Fig. 49(a–e), bearing different substituents R at the maleimide nitrogen atom, were noncytotoxic and have been shown to inhibit the receptor tyrosine kinase FLT4, which plays an essential role in the maintenance of lymphatic vessels as well as in the development of the embryonic cardiovascular system [104]. The FLT4 inhibition properties were strongly dependent on the ligands X and Y. The dichloro complex in Fig. 49(a) showed the highest activity ( $\text{IC}_{50} = 123 \text{ nM}$ ), and was much more potent than the dimethyl complex in Fig. 49(d) ( $\text{IC}_{50} = 1007 \text{ nM}$ ). Also, the complex in Fig. 49(a) displayed high selectivity for FLT4 among 229 protein kinases. This complex was found to inhibit both angiogenesis in developing zebrafish embryos and cancer cell-induced angiogenesis. It strongly inhibited vessel formation of the zebrafish embryos being affected 3 days postfertilization at a concentration of  $5 \mu\text{M}$ . This bioactivity has been ascribed to FLT4 inhibition, because the complex in Fig. 49(f), having an identical coordination sphere around the iridium(III) center but lacking the protein inhibition ability, did not show any effect on the zebrafish assays because of a methylated maleimide moiety. It has been found that the free maleimide nitrogen atom was essential for being capable of forming two canonical hydrogen bonds with the hinge region of the ATP-binding site of protein kinases.

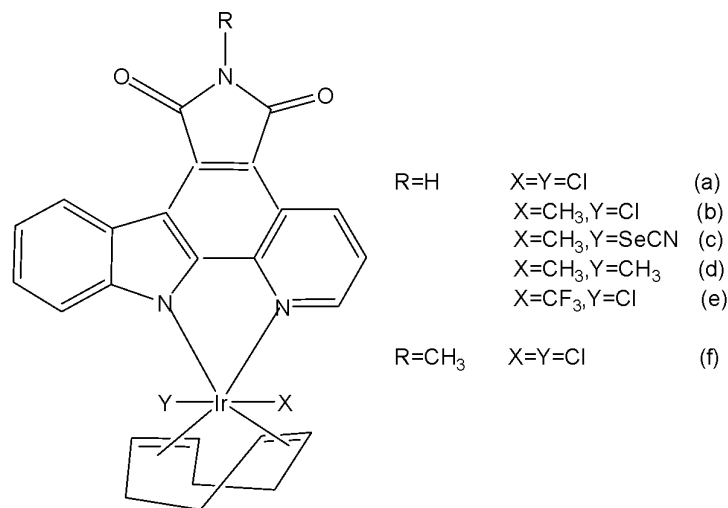


*Fig. (49):* Photocytotoxic (diene)Ir(III) protein kinase inhibitors.

Further studies of the same team have shown that the antiangiogenicity of the complex, shown in Fig. 50, was independent of light [105]. Interestingly, exposure to visible light for 1 h increased its cytotoxicity toward HeLa cells by *ca.* 34-fold and led to significant apoptosis. The investigation of photoreactivity revealed that, in the presence of chloride, visible light induced the substitution of the selenocyanate ligand with a chloride ligand. However, the reason why such ligand substitution led to efficient cellular apoptosis was unknown. This appeared to be the first time that phototoxicity has been observed for iridium complexes. The presence of the strongly labilizing methyl group was particularly beneficial for phototoxic activity and led in the case of the selenocyanate complex to rapid  $\text{SeCN}^-/\text{Cl}^-$  substitution followed by cell apoptosis. Light-dependent antiangiogenic properties were also established for this compound using endothelial cell spheroids embedded in a collagen matrix [105,106].

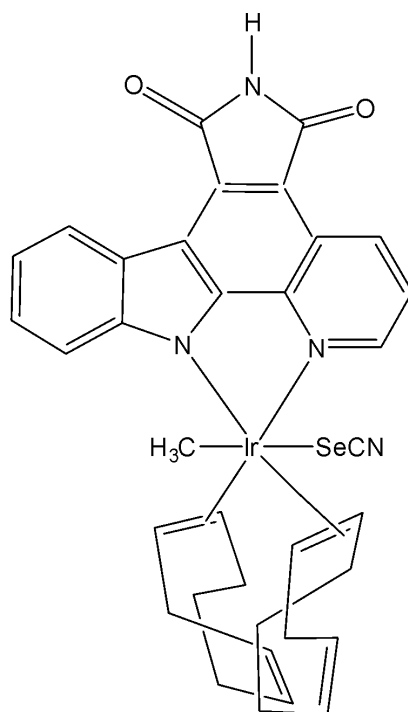


*Fig. (50):* Photocytotoxic (diene)Ir(III) complex with selenocyanate ligand.

Neutral metal complexes with 8-quinolinethiolate ligands displayed variable anticancer activity [107]. Most of them were very cytotoxic toward human fibrosarcoma HT-1080 and mouse hepatoma MG-22A cells. Among the 8-quinolinethiolate complexes  $[M(N^S)_n]$  with different transition metals, the iridium(III) complex  $[Ir(N^S)_3]$ , Fig. 51(a), displayed the highest activity against human fibrosarcoma HT-1080, mouse hepatoma MG-22A, and mouse melanoma B-16 cells [107]. However, this complex was also highly cytotoxic toward NIH 3T3 normal mouse embryo fibroblasts, limiting its potential as an antineoplastic drug. It has been found that the nature of the substituent, its position in the quinoline ring, and the nature of the metal significantly affected the antitumor activity and toxicity of metal complexes of 8-quinolinethiolates. Interestingly, the introduction of a methyl group to the 4-position of the quinoline ring of these complexes significantly increased the selectivity of their cytotoxic activity. The iridium(III) 4-methyl-8-quinolinethiolate complex  $[Ir(N^S)_3]$  in Fig. 51(b) was about 40 times more cytotoxic toward HT-1080 and MG-22A cancer cells than to 3T3 normal cells [108,109]. Systematic studies of the complexes with methyl- and methoxy-substituted 8-quinolinethiolate ligands revealed that complexes with high cytotoxicity substantially induced nitric oxide formation in the cells. The most cytotoxic towards human fibrosarcoma HT-1080 and mouse hepatoma MG-22A tumour cells was the iridium(III) 6-methoxy-8-quinolinethiolate complex, however it was highly toxic towards normal mouse embryonic NIH 3T3 fibroblasts. The iridium(III) 5-methyl-8-quinolinethiolate complex was somewhat less active to MG-22A cells but showed quite good selectivity because of its markedly lower toxicity. The iridium(III) 8-quinolineselenolate complexes  $[Ir(N^Se)_3]$ , Fig. 51(c–f), have shown analogous substituent-dependent cytotoxicity and selectivity [110,111]. The greatest selectivity in cytotoxic activity was noted for iridium(III) 4-methyl-8-quinolineselenolate complex. The cytotoxicity of the complexes was also found to be closely related to their ability to generate nitric oxide.

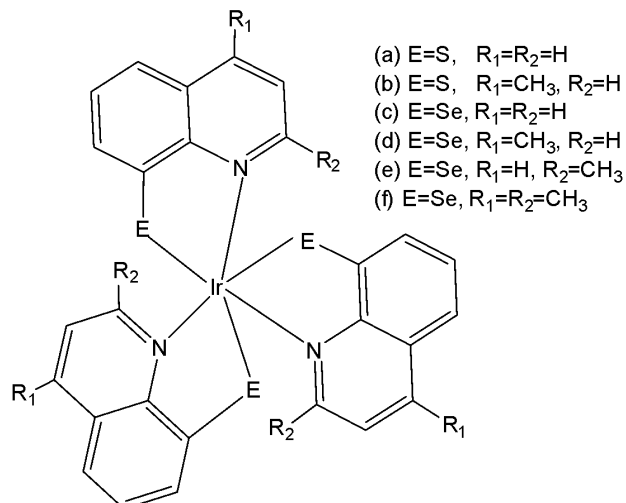


**Fig. (51):** Iridium(III) 8-quinolinethiolate and 8-quinolineselenolate complexes.

Recently, Conesa *et al.* have synthesised the iridium(III) half-sandwich complex with the formula  $[Ir(\eta^5k^1-C_5Me_4CH_2py)(2\text{-phenylpyridine})]PF_6$ , Fig. 52, where  $C_4Me_4CH_2py = 2\text{-}((2,3,4,5\text{-tetramethylcyclopenta-1,3-dien-1-yl)methyl)pyridine}$ , which was extraordinarily potent in a number of cancer cell lines [112]. The extraordinary feature of the structure of the complex resided on bearing a metal center sheltered by two chelate rings, one of which stabilized the metals' coordination sphere which helped to control the iridium reactivity. Thus, the metal was less eager to react with nucleophiles, it was preserved from detoxification, reaching with the biological targets more efficiently. The complex has been tested against A2780, HCT 116, MCF-7 cells and the results indicated that the complex, Fig. 52, had high sub-micromolar potency towards all human cancer cell lines with  $IC_{50}$  values between 0.11–0.82  $\mu\text{M}$ , which means 85, 77, 25 and 15 times more potent than clinically used cisplatin in the tested MCF7, MDAMB231, HCT116 and A2780 cells, respectively. The complex

$[\text{Ir}(\eta^5\text{k}^1\text{-C}_5\text{Me}_4\text{CH}_2\text{py})(2\text{-phenylpyridine})]\text{PF}_6^-$  exclusively and effectively accumulated in the mitochondria of the human breast cancer MCF7 cell line, proven by cryo-3D correlative imaging method, which can be applied to a number of biochemical processes for specific elemental localisation within the native cellular landscape [112]. Furthermore, unique information is obtained toward the intracellular events at the essential metal level triggered by metallodrug exposure of cancer cells.

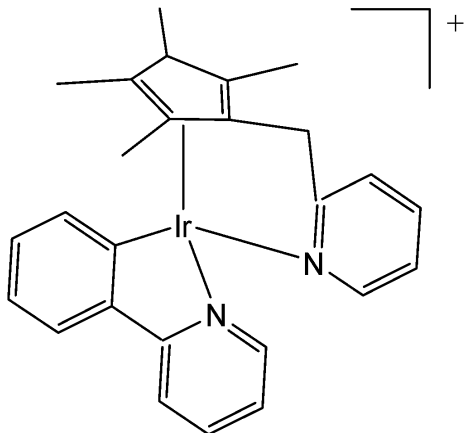


Fig. (52): Structure of Iridium(III) complex  $[\text{Ir}(\eta^5\text{k}^1\text{-C}_5\text{Me}_4\text{CH}_2\text{py})(2\text{-phenylpyridine})]\text{PF}_6^-$ .

Wang *et al.* have synthesised and reported a clickable iridium hydride complex, presented in Fig. 53, [113]. The cytotoxicity and production of reactive oxygen species study in A2780 and MCF-7 cancer cells indicated a potent anticancer activity of the iridium hydride complex towards A2780 cells with  $\text{IC}_{50} = 0.98 \mu\text{M}$  and towards MCF-7 cells with  $\text{IC}_{50} = 4.46 \mu\text{M}$ , which was three times better value compared to cisplatin. The ICP-MS analysis and the cellular imaging suggested the accumulation of the iridium hydride complex in the nucleus and cytoplasm. Further label-free quantitative proteomic analysis indicated that the ECM–receptor interaction pathway was activated by the complex. The analysis of down-regulated proteins suggested that the complex affected cellular DNA transcription, post-translational glycosyl modification, and redox homeostasis. Besides, the complex also damaged several crucial proteins and enzymes in the mitochondria and nucleus, associated to cellular metabolism and DNA replication, leading to the disorder of the cellular processes. These results provided a new approach to mechanism studies of metallodrugs combining click chemistry and proteomic analysis [113].

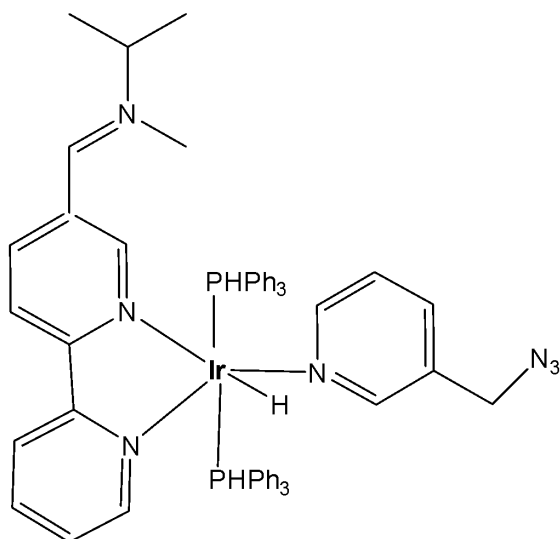


Fig. (53): Structure of iridium hydride complex.

## V. CONCLUSION

The application of cyclometalated iridium(III) complexes as potential antitumor agents and cellular imaging probes has been extensively explored and reported. Although many known iridium(III) complexes are chemically inert, their cytotoxic activity can be enhanced by increasing the lability of the iridium–ligand bonds or by improving lipophilicity, which promotes cellular uptake. Numerous studies have demonstrated that the cytotoxic activity of these complexes depends on efficient cellular internalization, reactive oxygen species (ROS) generation, and cell cycle arrest—mechanisms that often differ from those induced by clinically used metal-based drugs. However, establishing a complete structure–activity relationship remains challenging.

It is noteworthy that most reported iridium(III) complexes exhibit  $IC_{50}$  values below 100  $\mu\text{M}$  and show good selectivity and tolerance toward healthy cells. Their anticancer mechanisms are distinct from those of platinum-based drugs, offering cytotoxicity even against cisplatin-resistant cancer cell lines.

A significant strategy to enhance the biological activity of iridium(III) organometallic complexes involves incorporating organic ligands with known biological properties to design new complexes with improved therapeutic potential. The introduction of specific substituents into ligands can yield better activity and selectivity, novel mechanisms of action, and modified pharmacokinetic profiles. Furthermore, ligand functionalization enables organelle-targeted delivery—such as to lysosomes, mitochondria, nuclei, or subnuclear structures—broadening their biological applicability.

Unique structural and emissive characteristics, including structural complexity, tunable reactivity, diverse ligand substitution kinetics, redox versatility, high cellular uptake, and distinct spectroscopic features, make cyclometalated iridium(III) complexes promising scaffolds for modulation, sensing, and imaging of biological processes. These attributes contribute to the development of multifunctional reagents with broad biological and therapeutic applications.

Overall, the reviewed findings emphasize that this field of anticancer drug discovery warrants continued and systematic investigation to establish alternative classes of effective chemotherapeutic and theranostic agents. Nonetheless, challenges such as low aqueous solubility, off-target phototoxicity, limited *in vivo* stability, and difficulties in large-scale synthesis still impede clinical translation. It is expected that this review will serve as valuable guidance for the further development and rational design of these promising iridium-based anticancer candidates.

### *Authors' Contributions*

The author confirms sole responsibility for the following: study conception and design, data collection, analysis and interpretation of results, and manuscript preparation.

### *Consent For Publication*

Not applicable.

### *Conflict Of Interest*

The author declares no conflict of interest, financial or otherwise.

### *Funding*

None.

## ACKNOWLEDGEMENTS

The financial support received by the European Union-Next Generation EU, through the National Recovery and Resilience Plan of the Republic of Bulgaria, project No. BGRRP-2.004-0004-Co1 is greatly acknowledged.

## REFERENCES

1. Todorov, L.; Kostova, I. Recent Trends in the Development of Novel Metal-Based Antineoplastic Drugs. *Molecules*, **2023**, *28*(4), 1959.
2. Kostova, I. Rational Design and Synthesis of Bioactive Molecules. *Int. J. Mol. Sci.*, **2024**, *25*(18), 9927.
3. Kostova, I. Survey of Main Group Metals and Metalloids in Cancer Treatment. *Inorganics*, **2024**, *12*, 29.
4. Kostova, I. Rational Design of Metal-Based Pharmacologically Active Compounds. *Inorganics*, **2024**, *12*, 335.
5. Kostova I. Ruthenium Complexes as Anticancer Agents. *Curr. Med. Chem.*, **2006**, *13*(9), 1085-1107.
6. Jahromi, E.Z.; Divsalar, A.; Saboury, A.A.; Khaleghizadeh, S.; Mansouri-Torshizi, H.; Kostova I. Palladium complexes: new candidates for anti-cancer drugs. *J. Iran. Chem. Soc.*, **2016**, *13*(5), 967-989.
7. Kostova I. Platinum Complexes as Anticancer Agents, *Recent Pat. Rev. Anti -Canc. Drug Disc.*, **2006**, *1*(1), 1-22.
8. Shahlaei, M.; Asl, S. M.; Derakhshani, A.; Kurek, L.; Karges, J.; Macgregor, R.; Kostova, I.; Saboury A.A. Platinum-Based Drugs in Cancer Treatment: Expanding Horizons and Overcoming Resistance. *J. Mol. Struct.*, **2024**, *1301*, 137366.
9. Kostova, I. *Biological and Medical Significance of Chemical Elements*, Bentham Science Publishers, **2023**.
10. Ma, D. L.; Wu, C.; Wu, K. J.; Leung, C. H. Iridium (III) complexes targeting apoptotic cell death in cancer cells. *Molecules*, **2019**, *24*(15), 2739.
11. Cao, J. J.; Zheng, Y.; Wu, X. W.; Tan, C. P.; Chen, M. H.; Wu, N.; Mao, Z. W. Anticancer cyclometalated iridium(III) complexes with planar ligands: mitochondrial DNA damage and metabolism disturbance. *J. Med. Chem.*, **2019**, *62*, 3311–3322.
12. Kostova, I. Cytotoxic Organometallic Iridium(III) Complexes. *Molecules*, **2025**, *30*, 801.
13. Tan, C. P.; Zhong, Y. M.; Ji, L. N.; Mao, Z. W. Phosphorescent metal complexes as theranostic anticancer agents: combining imaging and therapy in a single molecule. *Chem. Sci.*, **2021**, *12*(7), 2357-2367.
14. Szymaszek, P.; Tyszka-Czochara, M.; Ortyl, J. Iridium (III) complexes as novel theranostic small molecules for medical diagnostics, precise imaging at a single cell level and targeted anticancer therapy. *Eur. J. Med. Chem.*, **2024**, 116648.
15. Liu, Z.; Salassa, L.; Habtemariam, A.; Pizarro, A. M.; Clarkson, G. J.; Sadler, P. J. Contrasting reactivity and cancer cell cytotoxicity of isoelectronic organometallic iridium(III) complexes. *Inorg. Chem.*, **2011**, *50*, 5777-5783.
16. Dörr, M.; Meggers, E. Metal complexes as structural templates for targeting proteins. *Curr. Opin. Chem. Biol.*, **2014**, *19*, 76-81.
17. Lo, K.K.W. Luminescent rhenium(I) and iridium(III) polypyridine complexes as biological probes, imaging reagents, and photocytotoxic agents. *ACC Chem. Res.*, **2015**, *48*, 2985-2995.
18. Ruiz, J.; Rodríguez, V.; Cutillas, N.; Samper, K. G.; Capdevila, M.; Palacios, O.; Espinosa, A. Novel C,N-chelate rhodium(III) and iridium(III) antitumor complexes incorporating a lipophilic steroid-like conjugate and their interaction with DNA. *Dalton Trans.*, **2012**, *41*, 12847-12856.
19. Li, T.Y.; Wu, J.; Wu, Z.G.; Zheng, Y.X.; Zuo, J.L.; Pan, Y. Rational Design of Phosphorescent Iridium(III) Complexes for Emission Color Tunability and Their Applications in OLEDs. *Coord. Chem. Rev.*, **2018**, *374*, 55–92.
20. Liu, Z.; Li, J.J.; Ge, X.X.; Zhang, S.; Xu, Z.; Gao, W. Design, Synthesis, and Evaluation of Phosphorescent Ir(III)Complexes with Anticancer Activity. *J. Inorg. Biochem.*, **2019**, *197*, 110703.

21. Anjong, T. F.; Kim, G.; Jang, H. Y.; Yoon, J.; Kim, J. Diiridium (iii) complexes: luminescent probes and sensors for G-quadruplex DNA and endoplasmic reticulum imaging. *New J. Chem.*, **2017**, *41*(1), 377-386.
22. Tso, K.K.S.; Lo, K.K.W. Strategic applications of luminescent iridium (III) complexes as biomolecular probes, cellular imaging reagents, and photodynamic therapeutics. *Iridium (III) in optoelectronic and photonics applications*, **2017**, 415-477.
23. Baschieri, A.; Muzzioli, S.; Fiorini, V.; Matteucci, E.; Massi, M.; Sambri, L.; Stagni, S. Introducing a new family of biotinylated Ir (III)-pyridyltriazole lumophores: Synthesis, photophysics, and preliminary study of avidin-binding properties. *Organometallics*, **2014**, *33*(21), 6154-6164.
24. Zamora, A.; Vigueras, G.; Rodríguez, V.; Santana, M. D.; Ruiz, J. Cyclometalated iridium (III) luminescent complexes in therapy and phototherapy. *Coord. Chem. Rev.*, **2018**, *360*, 34-76.
25. Qin, W. W.; Pan, Z. Y.; Cai, D. H.; Li, Y.; He, L. Cyclometalated iridium(iii) complexes for mitochondria-targeted combined chemo-photodynamic therapy. *Dalton Trans.*, **49**, *2020*, 3562-3569.
26. Liu, X.; Hao, H.; Ge, X.; He, X.; Liu, Y.; Wang, Y.; Liu, Z. Triphenylamine-appended cyclometalated iridium(III) complexes: preparation, photophysical properties and application in biology/luminescence imaging. *J. Inorg. Biochem.*, **2019**, *199*, 110757.
27. Xiang, H.; Chen, H.; Tham, H. P.; Phua, S. Z. F.; Liu, J. G.; Zhao, Y. Cyclometalated iridium(III)-complex-based micelles for glutathione-responsive targeted chemotherapy and photodynamic therapy. *ACS Appl. Mater. Interfaces*, **2017**, *9*, 27553-27562.
28. Meksawangwong, S.; Gohil, B.; Punyain, W.; Pal, R.; Kielar, F. Synthesis and investigation of a tris-cyclometalated iridium complex bearing a single quaternary ammonium group. *Inorg. Chim. Acta*, **2019**, *497*, 119066.
29. Song, X. D.; Chen, B. B.; He, S. F.; Pan, N. L.; Liao, J. X.; Chen, J. X.; Sun, J. Guanidine-modified cyclometalated iridium(III) complexes for mitochondria-targeted imaging and photodynamic therapy. *Eur. J. Med. Chem.*, **2019**, *179*, 26-37.
30. Ye, R. R.; Tan, C. P.; Ji, L. N.; Mao, Z. W. Coumarin-appended phosphorescent cyclometalated iridium(iii) complexes as mitochondria-targeted theranostic anticancer agents. *Dalton Trans.*, **2016**, *45*, 13042-13051.
31. Hisamatsu, Y.; Suzuki, N.; Masum, A. A.; Shibuya, A.; Abe, R.; Sato, A.; Aoki, S. Cationic amphiphilic tris-cyclometalated iridium(III) complexes induce cancer cell death via interaction with Ca<sup>2+</sup>-calmodulin complex. *Bioconjug. Chem.*, **2016**, *28*, 507-523.
32. Ye, R. R.; Cao, J. J.; Tan, C. P.; Ji, L. N.; Mao, Z. W. Valproic acid-functionalized cyclometalated iridium(III) complexes as mitochondria-targeting anticancer agents. *Chemistry*, **2017**, *23*, 15166-15176.
33. Steunenberg, P.; Ruggi, A.; van den Berg, N. S.; Buckle, T.; Kuil, J.; van Leeuwen, F. W.; Velders, A. H. Phosphorescence imaging of living cells with amino acid-functionalized tris (2-phenylpyridine) iridium (III) complexes. *Inorg. Chem.*, **2012**, *51*, 2105.
34. Berkers, C. R.; van Leeuwen, F. W.; Groothuis, T. A.; Peperzak, V.; van Tilburg, E. W.; Borst, J.; Ovaa, H. Profiling proteasome activity in tissue with fluorescent probes. *Mol. Pharmac.*, **2007**, *4*(5), 739-748.
35. Moromizato, S.; Hisamatsu, Y.; Suzuki, T.; Matsuo, Y.; Abe, R.; Aoki, S. Design and synthesis of a luminescent cyclometalated iridium (III) complex having N, N-diethylamino group that stains acidic intracellular organelles and induces cell death by photoirradiation. *Inorg. Chem.*, **2012**, *51*(23), 12697-12706.
36. Nakagawa, A.; Hisamatsu, Y.; Moromizato, S.; Kohno, M.; Aoki, S. Synthesis and photochemical properties of pH responsive tris-cyclometalated iridium (III) complexes that contain a pyridine ring on the 2-phenylpyridine ligand. *Inorg. Chem.*, **2014**, *53*(1), 409-422.

37. Qiu, K.; Huang, H.; Liu, B.; Liu, Y.; Huang, Z.; Chen, Y.; Chao, H. Long-term lysosomes tracking with a water-soluble two-photon phosphorescent iridium (III) complex. *ACS Appl. Mater. Interfaces*, **2016**, 8(20), 12702-12710.
38. Lv, W.; Zhang, Z.; Zhang, K. Y.; Yang, H.; Liu, S.; Xu, A.; Huang, W. A mitochondria-targeted photosensitizer showing improved photodynamic therapy effects under hypoxia. *Angew. Chem. Int. Ed.*, **2016**, 55, 9947-9951.
39. Chen, M. H.; Wang, F. X.; Cao, J. J.; Tan, C. P.; Ji, L. N.; Mao, Z. W. Light-Up mitophagy in live cells with dual-functional theranostic phosphorescent iridium(III) complexes. *ACS Appl. Mater. Interfaces*, **2017**, 9, 13304-13314.
40. Liu, J.; Jin, C.; Yuan, B.; Liu, X.; Chen, Y.; Ji, L.; Chao, H. Selectively lighting up two photon photodynamic activity in mitochondria with AIE-active iridium(III) complexes. *Chem. Commun.*, **2017**, 53, 2052-2055.
41. Jin, C.; Liu, J.; Chen, Y.; Guan, R.; Ouyang, C.; Zhu, Y.; Chao, H. Cyclometalated iridium(III) complexes as AIE phosphorescent probes for real-time monitoring of mitophagy in living cells. *Sci. Rep.*, **2016**, 6, 22039.
42. He, L.; Tan, C. P.; Ye, R. R.; Zhao, Y. Z.; Liu, Y. H.; Zhao, Q.; Mao, Z. W. Theranostic iridium(III) complexes as one- and two-photon phosphorescent trackers to monitor autophagic lysosomes. *Angew. Chem. Int. Ed.*, **2014**, 53, 12137-12141.
43. He, L.; Li, Y.; Tan, C. P.; Ye, R. R.; Chen, M. H.; Cao, J. J.; Mao, Z. W. Cyclometalated iridium(III) complexes as lysosome-targeted photodynamic anticancer and real-time tracking agents. *Chem. Sci.*, **2015**, 6, 5409-5418.
44. Wang, F. X.; Chen, M. H.; Lin, Y. N.; Zhang, H.; Tan, C. P.; Ji, L. N.; Mao, Z. W. Dual functions of cyclometalated iridium(III) complexes: anti-metastasis and lysosome-damaged photodynamic therapy. *ACS Appl. Mater. Interfaces*, **2017**, 9, 42471-42481.
45. Cao, R.; Jia, J.; Ma, X.; Zhou, M.; Fei, H. Membrane localized iridium(III) complex induces endoplasmic reticulum stress and mitochondria-mediated apoptosis in human cancer cells. *J. Med. Chem.*, **2013**, 56, 3636-3644.
46. Mandal, S.; Poria, D. K.; Ghosh, R.; Ray, P. S.; Gupta, P. Development of a cyclometalated iridium complex with specific intramolecular hydrogen-bonding that acts as a fluorescent marker for the endoplasmic reticulum and causes photoinduced cell death. *Dalton Trans.*, **2014**, 43, 17463-17474.
47. Tian, X.; Zhu, Y.; Zhang, M.; Luo, L.; Wu, J.; Zhou, H.; Tian, Y. Localization matters: a nuclear targeting two-photon absorption iridium complex in photodynamic therapy. *Chem. Commun.*, **2017**, 53, 3303-3306.
48. Li, C.; Yu, M.; Sun, Y.; Wu, Y.; Huang, C.; Li, F. A nonemissive iridium(III) complex that specifically lights-up the nuclei of living cells. *J. Am. Chem. Soc.*, **2011**, 133, 11231-11239.
49. Wu, N.; Cao, J. J.; Wu, X. W.; Tan, C. P.; Ji, L. N.; Mao, Z. W. Iridium(III) complexes with five-membered heterocyclic ligands for combined photodynamic therapy and photoactivated chemotherapy. *Dalton Trans.*, **2017**, 46, 13482-13491.
50. Cao, J. J.; Tan, C. P.; Chen, M. H.; Wu, N.; Yao, D. Y.; Liu, X. G.; Mao, Z. W. Targeting cancer cell metabolism with mitochondria-immobilized phosphorescent cyclometalated iridium(III) complexes. *Chem. Sci.*, **2017**, 8, 631-640.
51. Zhang, W. Y.; Du, F.; He, M.; Bai, L.; Gu, Y. Y.; Yang, L. L.; Liu, Y. J. Studies of anticancer activity *in vitro* and *in vivo* of iridium(III) polypyridyl complexes-loaded liposomes as drug delivery system. *Eur. J. Med. Chem.*, **2019**, 178, 390-400.
52. Venkatesh, V.; Berrocal-Martin, R.; Wedge, C. J.; Romero-Canelón, I.; Sanchez-Cano, C.; Song, J. I.; Sadler, P. J. Mitochondria-targeted spin-labelled luminescent iridium anticancer complexes. *Chem. Sci.*, **2017**, 8, 8271-8278.

53. He, L.; Zhang, M. F.; Pan, Z. Y.; Wang, K. N.; Zhao, Z. J.; Li, Y.; Mao, Z. W. A mitochondria-targeted iridium(III)-based photoacid generator induces dualmode photodynamic damage within cancer cells. *Commun. Chem.*, **2019**, *55*(70), 10472–10475.
54. McKenzie, L. K.; Sazanovich, I. V.; Baggaley, E.; Bonneau, M.; Guerchais, V.; Williams, J. G.; Bryant, H. E. Metal complexes for two-photon photodynamic therapy: A cyclometalated iridium complex induces twophoton photosensitization of cancer cells under near-IR light. *Chem. Eur. J.*, **2017**, *23*(2), 234–238.
55. Murphy, L.; Congreve, A.; Pålsson, L. O.; Williams, J. G. The time domain in co-stained cell imaging: time-resolved emission imaging microscopy using a protonatable luminescent iridium complex. *Chem. Commun. (Camb.)*, **2010**, *46*, 8743–8745.
56. Wang, M. M.; Xue, X. L.; Sheng, X. X.; Su, Y.; Kong, Y. Q.; Qian, Y.; Liu, H. K. Unveiling the anti-cancer mechanism for half-sandwich and cyclometalated Ir(III)-based complexes with functionalized  $\alpha$ -lipoic acid. *RSC Adv.*, **2020**, *10*, 5392–5398.
57. Pérez-Arnaiz, C.; Acuña, M. I.; Bustos, N.; Echevarría, I.; Martínez-Alonso, M.; Espino, G.; Domínguez, F. Thiabendazole-based Rh(III) and Ir(III) biscyclometalated complexes with mitochondria-targeted anticancer activity and metal-sensitive photodynamic activity. *Eur. J. Med. Chem.*, **2018**, *157*, 279–293.
58. Thomas, S. J.; Balónová, B.; Cinatl Jr, J.; Wass, M. N.; Serpell, C. J.; Blight, B. A.; Michaelis, M. Thiourea and guanidine compounds and their iridium complexes in drug-resistant cancer cell lines: Structure-activity relationships and direct luminescent. *ChemMedChem*, **2020**, *15*(4), 349–353.
59. Zhao, J.; Sun, S.; Li, X.; Zhang, W.; Gou, S. Enhancing photodynamic therapy efficacy of upconversion-based nanoparticles conjugated with a long-lived triplet excited state iridium(III)-naphthalimide complex: toward highly enhanced hypoxia-inducible factor-1. *ACS Appl. Bio Mater.*, **2019**, *3*, 252–262.
60. Xue, F.; Lu, Y.; Zhou, Z.; Shi, M.; Yan, Y.; Yang, H.; Yang, S. Two in one: luminescence imaging and 730 nm continuous wave laser driven photodynamic therapy of iridium complexes. *Organometallics*, **2015**, *34*(1), 73–77.
61. Hong, X. L.; Zhou, Y. H.; Zeng, C. C.; Wu, X. C.; Liu, Y. J. Apoptosis *in vitro* in PC-12 cells induced by an organometallic Ir(III) complex through a ROS-mediated mitochondrial pathway. *J. Organomet. Chem.*, **2017**, *846*, 312–320.
62. Liang, Z. H.; Wan, D.; Yi, Q. Y.; Zhang, W. Y.; Liu, Y. J. A cyclometalated iridium(III) complex induces apoptosis and autophagy through inhibition of the PI3K/AKT/mTOR pathway. *Trans. Met. Chem.*, **2018**, *43*, 243–257.
63. Wang, B.; Liang, Y.; Dong, H.; Tan, T.; Zhan, B.; Cheng, J.; Cheng, S. H. A luminescent cyclometalated iridium (III) complex accumulates in mitochondria and induces mitochondrial shortening by conjugation to specific protein targets. *ChemBioChem*, **2012**, *13*(18), 2729–2737.
64. Lo, K. K. W.; Leung, S. K.; Pan, C. Y. Luminescent iridium (III) arylbenzothiazole complexes: Photophysics, electrochemistry, bioconjugation, and cellular uptake. *Inorg. Chim. Acta*, **2012**, *380*, 343–349.
65. Kuang, S.; Liao, X.; Zhang, X.; Rees, T. W.; Guan, R.; Xiong, K.; Chao, H. FerriIridium: A Lysosome-targeting iron(III)-activated iridium(III) prodrug for chemotherapy in gastric cancer cells. *Angew. Chem. Int. Ed.*, **2020**, *59*, 3315–3321.
66. Guan, R.; Chen, Y.; Zeng, L.; Rees, T. W.; Jin, C.; Huang, J.; Chao, H. Oncosis-inducing cyclometalated iridium(III) complexes. *Chem. Sci.*, **2018**, *9*, 5183–5190.
67. Yi, S.; Lu, Z.; Zhang, J.; Wang, J.; Xie, Z.; Hou, L. Amphiphilic gemini iridium(III) complex as a mitochondria-targeted theranostic agent for tumor imaging and photodynamic therapy. *ACS Appl. Mater. Interfaces*, **2019**, *11*, 15276–15289.

68. Wang, F. X.; Chen, M. H.; Hu, X. Y.; Ye, R. R.; Tan, C. P.; Ji, L. N.; Mao, Z. W. Ester-modified cyclometalated iridium (III) complexes as mitochondria-targeting anticancer agents. *Sci. Rep.*, **2016**, *6*, 38954.
69. Martínez-Alonso, M.; Busto, N.; Aguirre, L. D.; Berlanga, L.; Carrión, M. C.; Cuevas, J. V.; Espino, G. Strong influence of the ancillary ligand over the photodynamic anticancer properties of neutral biscyclometalated Ir(III) complexes bearing 2-benzoazole-phenolates. *Chem. Eur. J.*, **2018**, *24*(66), 17523–17537.
70. Ho, P. Y.; Ho, C. L.; Wong, W. Y. Recent advances of iridium (III) metallophosphors for health-related applications. *Coord. Chem. Rev.*, **2020**, *413*, 213267.
71. Wu, K. J.; Ho, S. H.; Dong, J. Y.; Fu, L.; Wang, S. P.; Liu, H.; Ma, D. L. Aliphatic group-tethered iridium complex as a theranostic agent against malignant melanoma metastasis. *ACS Appl. Bio Mater.*, **2020**, *3*, 2017–2027.
72. Sun, L.; Chen, Y.; Kuang, S.; Li, G.; Guan, R.; Liu, J.; Chao, H. Iridium (III) anthraquinone complexes as two-photon phosphorescence probes for mitochondria imaging and tracking under hypoxia. *Chem. - A Eur. J.*, **2016**, *22*, 8955–8965.
73. Wendlandt, A. E.; Stahl, S. S. Quinone-catalyzed selective oxidation of organic molecules. *Angew. Chem. Int. Ed.*, **2015**, *54*(49), 14638–14658.
74. Liu, Z.; Deeth, R. J.; Butler, J. S.; Habtemariam, A.; Newton, M. E.; Sadler, P. J. Reduction of quinones by NADH catalyzed by organoiridium complexes. *Angew. Chem. Int. Ed.*, **2013**, *52*(15), 4194.
75. Du, F.; Bai, L.; He, M.; Zhang, W. Y.; Gu, Y. Y.; Yin, H.; Liu, Y. J. Design, synthesis and biological evaluation of iridium(III) complexes as potential antitumor agents. *J. Inorg. Biochem.*, **2019**, *201*, 110822.
76. Lo, K. K. W.; Lee, P. K.; Lau, J. S. Y. Synthesis, characterization, and properties of luminescent organoiridium (III) polypyridine complexes appended with an alkyl chain and their interactions with lipid bilayers, surfactants, and living cells. *Organometallics*, **2008**, *27*(13), 2998–3006.
77. Lau, J. S.-Y.; Lee, P.-K.; Tsang, K. H.-K.; Ng, C. H.-C.; Lam, Y.-W.; Cheng, S.-H.; Lo, K. K.-W. Luminescent cyclometalated iridium(III) polypyridine indole complexes—synthesis, photophysics, electrochemistry, protein-binding properties, cytotoxicity, and cellular uptake. *Inorg. Chem.*, **2009**, *48*, 708–718.
78. Leung, S. K.; Kwok, K. Y.; Zhang, K. Y.; Lo, K. K. W. Design of luminescent biotinylation reagents derived from cyclometalated iridium (III) and rhodium (III) bis (pyridylbenzaldehyde) complexes. *Inorg. Chem.*, **2010**, *49*(11), 4984–4995.
79. Chen, H.; Ge, C.; Cao, H.; Zhang, X.; Zhang, L.; Jiang, L.; Zhang, Q. Isomeric Ir(III) complexes for tracking mitochondrial pH fluctuations and inducing mitochondrial dysfunction during photodynamic therapy. *Dalton Trans.*, **2019**, *48*, 17200–17209.
80. Yang, X. H.; Zhang, Q.; Dou, S. B.; Xiao, L.; Jia, X. L.; Yang, R. L.; Niu, Z. G. Synthesis, properties, DFT calculations, and cytotoxic activity of phosphorescent iridium(III) complexes with heteroatom ancillary ligands. *J. Coord. Chem.*, **2020**, *73*(14), 2004–2014.
81. Zhang, W. Y.; Yi, Q. Y.; Wang, Y. J.; Du, F.; He, M.; Tang, B.; Huang, H. L. Photoinduced anticancer activity studies of iridium(III) complexes targeting mitochondria and tubules. *Eur. J. Med. Chem.*, **2018**, *151*, 568–584.
82. He, L.; Liao, S. Y.; Tan, C. P.; Lu, Y. Y.; Xu, C. X.; Ji, L. N.; Mao, Z. W. Cyclometalated iridium (III)- $\beta$ -carboline complexes as potent autophagy-inducing agents. *Chem. Commun.*, **2014**, *50*(42), 5611–5614.
83. Kaiser, M.; Zavrski, I.; Sterz, J.; Jakob, C.; Fleissner, C.; Kloetzel, P. M.; Heider, U. The effects of the histone deacetylase inhibitor valproic acid on cell cycle, growth suppression and apoptosis in multiple myeloma. *Haematologica*, **2006**, *91*(2), 248–251.

84. Yuan, B.; Liu, J.; Guan, R.; Jin, C.; Ji, L.; Chao, H. Endoplasmic reticulum targeted cyclometalated iridium(iii) complexes as efficient photodynamic therapy photosensitizers. *Dalton Trans.*, **2019**, *48*, 6408–6415.
85. Zhang, Y.; Fu, H.; Chen, S.; Liu, B.; Sun, W.; Gao, H. Construction of an iridium(iii)-complex-loaded MOF nanoplatform mediated with a dual-responsive polycationic polymer for photodynamic therapy and cell imaging. *Chem. Commun.*, **2020**, *56*, 762–765.
86. Novohradsky, V.; Vigueras, G.; Pracharova, J.; Cutillas, N.; Janiak, C.; Kostrhunova, H.; Kasparkova, J. Molecular superoxide radical photogeneration in cancer cells by dipyridophenazine iridium(III) complexes. *Inorg. Chem. Front.*, **2019**, *6*(9), 2500–2513.
87. Yellol, G. S.; Donaire, A.; Yellol, J. G.; Vasylyeva, V.; Janiak, C.; Ruiz, J. On the antitumor properties of novel cyclometalated benzimidazole Ru(II), Ir(III) and Rh(III) complexes. *Chem. Commun.*, **2013**, *49*(98), 11533–11535.
88. Laha, P.; De, U.; Chandra, F.; Dehury, N.; Khullar, S.; Kim, H. S.; Patra, S. Alkyl chainmodified cyclometalated iridium complexes as tunable anticancer and imaging agents. *Dalton Trans.*, **2018**, *47*(44), 15873–15881.
89. Yellol, J.; Pérez, S. A.; Yellol, G.; Zajac, J.; Donaire, A.; Vigueras, G.; Ruiz, J. Highly potent extranuclear-targeted luminescent iridium(III) antitumor agents containing benzimidazole based ligands with a handle for functionalization. *Chem. Commun.*, **2016**, *52*(98), 14165–14168.
90. Pracharova, J.; Vigueras, G.; Novohradsky, V.; Cutillas, N.; Janiak, C.; Kostrhunova, H.; Brabec, V. Exploring the effect of polypyridyl ligands on the anticancer activity of phosphorescent iridium (III) complexes: From proteosynthesis inhibitors to photodynamic therapy agents. *Chem. Eur. J.*, **2018**, *24*(18), 4607–4619.
91. Novohradsky, V.; Zamora, A.; Gandioso, A.; Brabec, V.; Ruiz, J.; Marchán, V. Somatostatin receptor-targeted organometallic iridium(III) complexes as novel theranostic agents. *Chem. Commun.*, **2017**, *53*(40), 5523–5526.
92. Hartinger, C. G. Trapping Unstable Benzoquinone Analogues by Coordination to a  $[(\eta\text{-C}_5\text{Me}_5)\text{Ir}]$  Fragment and the Anticancer Activity of the Resulting Complexes. *Angew. Chem. Int. Ed.*, **2010**, *45*(49), 8304–8305.
93. Steinberg-Yfrach, G.; Liddell, P. A.; Hung, S. C.; Moore, A. L.; Gust, D.; Moore, T. A. Conversion of light energy to proton potential in liposomes by artificial photosynthetic reaction centres. *Nature*, **1997**, *385*(6613), 239–241.
94. Larsen, P. L.; Clarke, C. F. Extension of life-span in *Caenorhabditis elegans* by a diet lacking coenzyme Q. *Science*, **2002**, *295*(5552), 120–123.
95. Amouri, H.; Moussa, J.; Renfrew, A. K.; Dyson, P. J.; Rager, M. N.; Chamoreau, L. M. Discovery, structure, and anticancer activity of an iridium complex of diselenobenzoquinone. *Angew. Chem. Int. Ed.*, **2010**, *49*(41), 7530–7533.
96. Liu, Z.; Habtemariam, A.; Pizarro, A. M.; Clarkson, G. J.; Sadler, P. J. Organometallic iridium (III) cyclopentadienyl anticancer complexes containing C, N-chelating ligands. *Organometallics*, **2011**, *30*(17), 4702–4710.
97. Millett, A. J.; Habtemariam, A.; Romero-Canelón, I.; Clarkson, G. J.; Sadler, P. J. Contrasting anticancer activity of half-sandwich iridium (III) complexes bearing functionally diverse 2-phenylpyridine ligands. *Organometallics*, **2015**, *34*(11), 2683–2694.
98. Wirth, S.; Rohbogner, C. J.; Cieslak, M.; Kazmierczak-Baranska, J.; Donevski, S.; Nawrot, B.; Lorenz, I. P. Rhodium (III) and iridium (III) complexes with 1, 2-naphthoquinone-1-oximate as a bidentate ligand: synthesis, structure, and biological activity. *JBIC J. Biol. Inorg. Chem.*, **2010**, *15*, 429–440.
99. Śliwińska, U.; Pruchnik, F. P.; Ułaszewski, S.; Latocha, M.; Nawrocka-Musiał, D. Properties of  $\eta\text{5-pentamethylcyclopentadienyl}$  rhodium (III) and iridium (III) complexes with quinolin-8-ol and their cytostatic activity. *Polyhedron*, **2010**, *29*(6), 1653–1659.

100. Schäfer, S.; Ott, I.; Gust, R.; Sheldrick, W. S. Influence of the Polypyridyl (pp) Ligand Size on the DNA Binding Properties, Cytotoxicity and Cellular Uptake of Organoruthenium (II) Complexes of the Type  $[(\eta_6\text{-C}_6\text{Me}_6)\text{ Ru (L)(pp)}]^{n+}$  [L= Cl, n= 1; L=(NH<sub>2</sub>)<sub>2</sub>CS, n= 2]. *Eur. J. Inorg. Chem.*, **2007**, 3034-3046.
101. Schäfer, S.; Sheldrick, W. S. Coligand tuning of the DNA binding properties of half-sandwich organometallic intercalators: Influence of polypyridyl (pp) and monodentate ligands (L= Cl, (NH<sub>2</sub>)<sub>2</sub>CS, (NMe<sub>2</sub>)<sub>2</sub>CS) on the intercalation of ( $\eta_5$ -pentamethylcyclopentadienyl)-iridium (III)-dipyridoquinoxaline and-dipyridophenazine complexes. *J. Organomet. Chem.*, **2007**, 692(6), 1300-1309.
102. Liu, Z.; Romero-Canelón, I.; Habtemariam, A.; Clarkson, G. J.; Sadler, P. J. Potent half-sandwich iridium (III) anticancer complexes containing C<sup>4</sup>N-chelated and pyridine ligands. *Organometallics*, **2014**, 33(19), 5324-5333.
103. Xiong, K.; Chen, Y.; Ouyang, C.; Guan, R. L.; Ji, L. N.; Chao, H. Cyclometalated iridium(III) complexes as mitochondria-targeted anticancer agents. *Biochimie*, **2016**, 125, 186-194.
104. Wilbuer, A.; Vlecken, D. H.; Schmitz, D. J.; Kräling, K.; Harms, K.; Bagowski, C. P.; Meggers, E. Iridium complex with antiangiogenic properties. *Angew. Chem. Int. Ed.*, **2010**, 49(22), 3839-3842.
105. Kastl, A.; Wilbuer, A.; Merkel, A. L.; Feng, L.; Di Fazio, P.; Ocker, M.; Meggers, E. Dual anticancer activity in a single compound: visible-light-induced apoptosis by an antiangiogenic iridium complex. *Chem. Commun.*, **2012**, 48(13), 1863-1865.
106. Lo, K. K. W.; Zhang, K. Y. Iridium(III) complexes as therapeutic and bioimaging reagents for cellular applications. *RSC Adv.*, **2012**, 2, 12069-12083.
107. Lukevics, E.; Shestakova, I.; Domracheva, I.; Nesterova, A.; Zaruma, D.; Ashaks, J. Cytotoxicity of metal 8-quinolinethiolates. *Chem. Heteroc. Comp.*, **2006**, 42, 761-764.
108. Lukevics, E.; Shestakova, I.; Domracheva, I.; Yashchenko, E.; Zaruma, D.; Ashaks, J. Synthesis and cytotoxicity of metal 4-methyl-8-quinolinethiolates. *Chem. Heteroc. Comp.*, **2007**, 43, 634-636.
109. Lukevics, E.; Zaruma, D.; Ashaks, J.; Shestakova, I.; Domracheva, I.; Gulbe, A.; Bridane, V. Synthesis and cytotoxicity of methyl-and methoxy-substituted metal 8-quinolinethiolates. *Chem. Heteroc. Comp.*, **2008**, 44, 559-564.
110. Ashaks, J.; Bankovsky, Y.; Zaruma, D.; Shestakova, I.; Domracheva, I.; Nesterova, A.; Lukevics, E. Synthesis of quinoline-8-selenol, its complex compounds with metals and their cytotoxic activity. *Chem. Heteroc. Comp.*, **2004**, 40, 776-780.
111. Lukevics, E.; Zaruma, D.; Ashaks, J.; Shestakova, I.; Domracheva, I.; Bridane, V.; Yashchenko, E. Synthesis and cytotoxicity of methyl-substituted 8-quinolineselenolates of ruthenium, rhodium, osmium, and iridium. *Chem. Heteroc. Comp.*, **2009**, 45, 182-187.
112. Conesa, J. J.; Carrasco, A. C.; Rodríguez-Fanjul, V.; Yang, Y.; Carrascosa, J. L.; Cloetens, P.; Pizarro, A. M. Unambiguous intracellular localization and quantification of a potent iridium anticancer compound by correlative 3D cryo X-ray imaging. *Angew. Chem. Int. Ed.*, **2020**, 59, 1270-1278.
113. Wang, X.; Zhang, J.; Zhao, X.; Wei, W.; Zhao, J. Imaging and proteomic study of a clickable iridium complex. *Metallomics*, **2019**, 11, 1344-1352.